

# **Thermal Degradation Study of IM7/DMBZ-15 High Temperature Composite by TGA/FTIR**

by  
Melvin P. Nadler  
*Research Department*

**SEPTEMBER 2003**

**NAVAL AIR WARFARE CENTER WEAPONS DIVISION  
CHINA LAKE, CA 93555-6100**

Approved for public release; distribution is  
unlimited.

**20040224 060**

# Naval Air Warfare Center Weapons Division

---

## FOREWORD

The research described in this report was performed at the Naval Air Warfare Center Weapons Division during fiscal years 2001 and 2002. The goal was to understand the chemical mechanisms of decomposition of IM-7/DMBZ-15 carbon fiber epoxy structural composite under high heating rate conditions, with an overall objective of reducing or eliminating catastrophic delamination at high temperature. This work was funded by the NAVAIR 6.1 ILIR program that in turn, is supported by the Office of Naval Research.

This report was reviewed for technical accuracy by Lawrence H. Merwin.

Approved by  
C. F. MARKARIAN, *Head*  
*Research Department*  
12 August 2003

Under authority of  
D. J. VENLET  
RDML, U.S. Navy  
*Commander*

Released for publication by  
K. HIGGINS  
*Director for Research and Engineering*

## NAWCWD Technical Publication 8568

Published by ..... Technical Information Division  
Collation..... Cover, 26 leaves  
First printing ..... 29 paper

REPORT DOCUMENTATION PAGE			Form Approved OMB No. 0704-0188	
Public reporting burden for this collection of information is estimated to average 1 hour per response, including the time for reviewing instructions, searching existing data sources, gathering and maintaining the data needed, and completing and reviewing the collection of information. Send comments regarding this burden estimate or any other aspect of this collection of information, including suggestions for reducing this burden, to Washington Headquarters Services, Directorate for Information Operations and Reports, 1215 Jefferson Davis Highway, Suite 1204, Arlington, VA 22202-4302, and to the Office of Management and Budget, Paperwork Reduction Project (0704-0188), Washington, D.C. 20503.				
1. AGENCY USE ONLY (Leave Blank)		2. REPORT DATE  September 2003		3. REPORT TYPE AND DATES COVERED  October 2000 – September 2002; Final
4. TITLE AND SUBTITLE Thermal Degradation Study of IM7/DMBZ-15 High Temperature Composite by TGA/FTIR (U)			5. FUNDING NUMBERS  PE 06011 52N	
6. AUTHOR(S) Melvin P. Nadler				
7. PERFORMING ORGANIZATION NAME(S) AND ADDRESS(ES) Naval Air Warfare Center Weapons Division China Lake, CA 93555-6100			8. PERFORMING ORGANIZATION REPORT NUMBER  NAWCWD TP 8568	
9. SPONSORING/MONITORING AGENCY NAME(S) AND ADDRESS(ES)			10. SPONSORING/MONITORING AGENCY REPORT NUMBER	
11. SUPPLEMENTARY NOTES				
12a. DISTRIBUTION/AVAILABILITY STATEMENT Approved for public release; distribution is unlimited.			12b. DISTRIBUTION CODE	
13. ABSTRACT (Maximum 200 words)  See reverse.				
14. SUBJECT TERMS Attenuated total reflectance Composite Delamination Degradation FTIR Graphite fiber			15. NUMBER OF PAGES  50	
			16. PRICE CODE	
17. SECURITY CLASSIFICATION OF REPORT  UNCLASSIFIED		18. SECURITY CLASSIFICATION OF ABSTRACT  UNCLASSIFIED	19. SECURITY CLASSIFICATION OF THIS PAGE  UNCLASSIFIED	20. LIMITATION OF ABSTRACT  UL

(U) High temperature graphite composites such as IM7/8552 epoxy, IM7/5250 BMI, and IM7/DMBZ-15 polyimide show blistering and/or "catastrophic" delamination when rapidly heated to temperatures above the glass transition temperature ( $T_g$ ). Reusable Launch Vehicle (RLV) or other high-speed applications of high temperature composites require "good" mechanical properties at a high heating rate and a moderate duration above the  $T_g$ . Thermogravimetric analysis/Fourier transform infrared (TGA/FTIR) and single pass "Thunderdome" attenuated total reflectance (TD ATR)/FTIR small-scale laboratory methods are used to study and model the thermal degradation, gaseous products, and kinetics of high temperature composites during rapid heating and moderate duration near and above- $T_g$ . Results are shown for the thermal degradation of IM7/DMBZ-15 graphite composite and DMBZ-15 polyimide resin ( $T_g = 414^\circ\text{C}$ ) as a function of three heating rates (150, 100, and  $50^\circ\text{C}/\text{min}$ ) and five isothermal temperatures (375, 400, 425, 450, and  $475^\circ\text{C}$ ; in some cases, 500 and  $525^\circ\text{C}$ ), under  $\text{N}_2$  and air. The major gas phase degradation products were identified and quantified ( $\text{H}_2\text{O}$ ,  $\text{CO}_2$ ,  $\text{CO}$ ,  $\text{CH}_4$ ,  $\text{NH}_3$ , and  $\text{MeOH}$ ), and assignments made for some of the intermediates or degradation fragments (aromatic nitrile, aromatic isocyanate, amide polyimide fragment, ...). IM7/DMBZ-15 Composite and DMBZ-15 Resin thermal degradation at high heating rates can be broken down into four regions. Region 1 starts well below- $T_g$  with the evolution of trapped and/or adsorbed gases, such as  $\text{H}_2\text{O}$  or  $\text{CO}_2$ , and a low molecular weight poly(dimethylsiloxane). Region 2, the first kinetic region, is the very rapid evolution of gaseous degradation products or more trapped gases ( $\text{H}_2\text{O}$ ,  $\text{CO}_2$ ,  $\text{CO}$ ,  $\text{CH}_4$ ,  $\text{MeOH}$ , ...) occurring in a narrow temperature (or time) region from just below to slightly above the  $T_g$ . Region 3, the second kinetic region, is from polyimide resin breakdown products and fragments, such as  $\text{NH}_3$ , and an amide resin fragment starting at 435 to  $450^\circ\text{C}$ . Region 4 is the very slow degradation at constant temperature after the initial rapid gas evolution. Water is the major product up to about 435 to  $450^\circ\text{C}$ , where polyimide fragments and products start to dominate. The integrated total initial gas evolution (ppm min/g) in regions 1, 2, and 3 shows a linear increase with temperature for  $\text{H}_2\text{O}$  and  $\text{CO}_2$ , while  $\text{CO}$ ,  $\text{CH}_4$ , and  $\text{NH}_3$  show an exponential rise. Graphite contributes little, if any, products during thermal degradation in  $\text{N}_2$  and air up to  $475^\circ\text{C}$ . The very rapid increase in degradation rate just below- $T_g$  (the start of region 2) corresponds with a TGA weight loss spike and shows the onset of a very rapid hot gas expansion that must be the cause of "catastrophic delamination." Due to oxidation  $\text{CO}$ ,  $\text{CO}_2$ , and to some extent  $\text{H}_2\text{O}$  (for  $T > 425^\circ\text{C}$ ) have higher and increasing concentrations in region 4 in air compared to  $\text{N}_2$ . TD ATR surface spectra of unheated versus heated composite samples show increased surface damage in air compared to  $\text{N}_2$ . This small scale, low cost analysis method should enable prediction of which new composite materials to scale up for high temperature missile, radome, or reentry applications.

## CONTENTS

Acknowledgment .....	1
Introduction.....	3
Experimental Section .....	4
Results.....	5
Heating Rate and Final Isothermal Temperature .....	6
IM7/DMBZ-15 Composite Versus DMBZ-15 Resin.....	9
Unassigned or Non-Quantified Products or Fragments .....	10
TGA Weight Loss Compared to Species Weight Loss .....	11
Composite and Resin Thermal Degradation in Air Versus Nitrogen.....	12
Quantified Species Degradation Rates and Onset of Catastrophic Delamination....	13
IM7/DMBZ-15 Composite Top Surface Heat Damage Using TD ATR Spectra ....	15
Summary .....	16
References.....	18

## ACKNOWLEDGMENT

I would like to thank Roxanne Quintana for her help with the TGA/FTIR air experiments. She has been a great help to me in the final year of my career at NAWCWD. ...

I would also like to thank Frank MacDonald for his advice and the talks we have had on the direction of the high temperature composite program.

This page intentionally left blank.

## INTRODUCTION

Reusable Launch Vehicle (RLV) and other supersonic missile applications of high temperature composites (HTC) require "good" mechanical properties at a high heating rate and moderate duration (10 to 30 minutes) above the glass transition temperature ( $T_g$ ). Currently composite materials are exposed for hundreds of hours to establish a maximum-use temperature without material performance degradation. Missile applications tend to be one-use missions for short duration. The pay-off would be to use lower cost polymer composites to perform for a moderate duration well beyond their  $T_g$ . Oak Ridge National Laboratory and Martin Marietta Energy Systems evaluated mechanical property retention for IM6/3501-6 (carbon fiber/epoxy) composite above the  $T_g$  of 177°C (Reference 1). This work shows compressive strength retention of 40% at 343°C for 30 minutes and 26% at 399°C for 10 minutes, indicating that polymer-based composites can maintain "good" mechanical properties above- $T_g$  for short periods of time (Reference 1). The current approach is to put on an ablating layer that carries no structural loads. Loss of internal missile volume to carry ordnance and increased manufacturing costs are the primary disadvantages of this ablation-based design approach (Reference 2). Flight condition calculations for high-speed vehicles at about Mach 5 and 22-kilometer (km) altitude show heating rates from about 100 to 230°C/minute (min) and a maximum temperature of about 540°C (References 2 and 3). National Aeronautics and Space Administration (NASA) Glenn Research Center, Cleveland, Ohio, developed DMBZ-15 for high temperature applications with a  $T_g = 414^\circ\text{C}$  (References 4 and 5). Thermal degradation, mechanical properties testing, and aging studies on high temperature composites have shown that some polyimides (PMR-15 and IM7/DMBZ-15) have acceptable weight losses after long duration well below- $T_g$ , but also "large" volumes of gases are evolved when heated at high rates to near and above- $T_g$  (References 4 and 6 through 8). Temperature cycling to above- $T_g$  and rapid heating of IM7/8552 Epoxy, IM7/5250 Bismaleimide (BMI) and IM7/DMBZ-15 polyimide composite panels show "catastrophic delamination" and blistering problems (References 2 and 6 through 8). Figure 1 is a scanning electron microscopy (SEM) cross section showing "catastrophic delamination" of an IM7/DMBZ-15 panel after rapid heating to above the  $T_g$  (References 2 and 3). However, IM7/DMBZ-15 can maintain "reasonable" mechanical properties above- $T_g$  for short duration under certain conditions (References 2 and 3). Expansion of gases from moisture and/or degradation under high heating rates is thought to be the cause of the "catastrophic delamination" or blistering. That being said, there are polymer composites that are successfully used at temperature, beyond the material's  $T_g$ . These include dome nose tips that are currently deployed in the Fleet. As an example, the High-Speed Antiradiation Missile (HARM) radome is a quartz/polyimide that is used beyond  $T_g$  for a very short period of time (<1 min; Reference 2). Most of this previous work was performed in a "make it and break it" approach, with little data generated that could be used to extrapolate to a longer time frame or a higher heating rate. A low cost, small scale laboratory study of the thermal degradation of high

temperature composites is needed to obtain a more fundamental understanding of the chemistry, gaseous products, kinetics, and other parameters in order to model large panel behavior.

This report concentrates on IM7/DMBZ-15 high temperature composite using DMBZ-15 polyimide resin developed by NASA Glenn Research Center and IM7 graphite fibers (References 4 and 5). PMR-15 is recognized as the state-of-the-art high temperature resin for long term composite applications at 288°C. However, because of health concerns in the production of the PMR-15, the mutagen methylene dianiline (MDA) was replaced by dimethylbenzidine (DMBZ) in DMBZ-15 (References 4 and 5). PMR-15 and DMBZ-15 have similar mechanical and thermal properties (References 4 and 5). DMBZ-15 should make a good high temperature resin for composites exposed to high heating rates and moderate duration above-T<sub>g</sub> required for RLV or other high speed missile applications. The main goals of this study are to obtain: (1) an improved understanding of the thermal degradation mechanism, chemistry and kinetics; (2) the species, concentrations, and source of the "large" volume of gases evolved; (3) improved prediction of the useful temperature range, duration at temperature, heating rate range, and onset of "catastrophic delamination;" (4) solutions for modification of the polymer resin to eliminate "catastrophic" delamination, blistering, or other problems; and (5) a model of the small scale thermal degradation data that can predict large composite panel thermal and mechanical properties and can determine which new high temperature composite materials to scale up for high speed missile, radome, and reentry applications.

## EXPERIMENTAL SECTION

The first 2 years of this study were concentrated on the thermal degradation of IM7/DMBZ-15 graphite composite and DMBZ-15 cured resin under N<sub>2</sub> and air atmosphere. DMBZ-15 resin panels (15- by 15- by 0.2-centimeter (cm) thick) from Kathy Chuang of NASA Glenn Research Center were cut into 7-millimeter (mm) diameter discs for the thermogravimetric analysis/Fourier transform infrared (TGA/FTIR) studies (75 to 82 milligrams (mg)). IM7/DMBZ-15 graphite polyimide composite panels (30- by 30- by 0.3-cm-thick) fabricated at the Naval Air Warfare Center Weapons Division (NAWCWD), China Lake, California, and NASA Glenn Research Center were also cut into 7-mm-diameter discs (138 to 154 mg). A TA Instruments Model 2050 Thermogravimetric Analyzer (TGA) with a quartz furnace and platinum (Pt) pan was used to heat and weigh the composite and resin sample discs. In order to simulate high speed flight conditions, temperature programs of 150, 100, and 50°C/min heating rate to isothermal temperatures of 375, 400, 425, 450, and 475°C (in some experiments, 500 and 525°C) for 35 to 40 minutes were used to heat the composite and resin samples. The TGA microbalance was purged with a N<sub>2</sub> (or air) flow of 80 cubic centimeters (cc)/min and the furnace with 40 cc/min (total flow of 120 cc/min). The furnace N<sub>2</sub> (or air) flowed over the sample disc in the Pt pan and then into a 48-inch heated transfer line and finally into the heated double pass (20-cm pathlength) FTIR gas cell of a ThermoNicolet TGA/FTIR interface. The TGA/FTIR interface fit into the



sample compartment of a ThermoNicolet Nexus 870 FTIR and heated the transfer line and FTIR gas cell to a constant 225°C (see Figure 2). FTIR spectra versus time were collected using the ThermoNicolet Series software by signal averaging 16 sample spectra (4.62-second (s) scan time at mirror velocity = 3.1647 cm/s) every 10 seconds (referenced to a 128-scan N<sub>2</sub> or air cell background) at 4 cm<sup>-1</sup> resolution. The composite or resin sample temperature and weight loss versus time from the TGA were converted to ASCII format and stored with the ThermoNicolet Series file of spectra versus time of gases in the FTIR cell. There is a 10- to 19-second delay from the TGA time scale to the FTIR spectra time due to the low N<sub>2</sub> or air flow rate, 48-inch transfer line, and FTIR collection time. Quantitative gas concentrations in parts per million (ppm) were obtained with the Infrared Analysis, Inc., QASoft database of gas-phase reference spectra and ThermoNicolet QuantPad software. Reference spectra for H<sub>2</sub>O, CO<sub>2</sub>, CO, CH<sub>4</sub>, NH<sub>3</sub>, and methanol (MeOH) at 2 cm<sup>-1</sup> resolution were converted to 4 cm<sup>-1</sup> resolution by changing the data spacing to 2 cm<sup>-1</sup>. The QuantPad method developed is "composite tga-ftir gases.qnt." Series file spectral data are converted to ppm versus time for each of the gases in the QuantPad method at the cell conditions of T = 225°C and P = 700 mm Hg. Some intermediate species and degradation fragments are not in the QASoft database and therefore could not be quantified. However, absorbance versus time profiles are obtained for the non-quantified species from the Series files using Macro "composite series profiles abs6.mac." Finally, species concentration (ppm) and absorbance profiles for each Series file run are stored as x-y CSV files and read in Microsoft Excel for plotting and data manipulation.

FTIR spectra from the top exposed surface of the heated and unheated composite sample discs were obtained using a ThermoSpectra-Tech "Thunderdome" attenuated total reflectance (TD ATR) accessory with a single pass spherical Ge ATR crystal. TD ATR spectra with a Ge crystal have a penetration depth of about 0.5 to 2 micrometers (μm) and should show oxidation or degradation of the sample surface.

## RESULTS

Figure 3 shows evolved gas species in ppm (in N<sub>2</sub> flow), other intermediates or products in absorbance units, and the TGA temperature (°C) and % weight loss x 100 versus run time in minutes for a typical below-T<sub>g</sub> TGA/FTIR IM7/DMBZ-15 composite thermal degradation experiment at a heating rate (R) of 100°C/min to an isothermal temperature (ISO) of 375°C for 16 minutes (35 minutes total). Water evolution shows the following sequence of events: initial observation at about 80°C, reaches a maximum (MAX) of 3,140 ppm at 292°C, another rise starts at 390°C or from 6.0 to 6.4 minutes to a second maximum of 1,220 ppm (386°C), a weak shoulder at 7.4 to 8.2 minutes, and finally a region of very slow degradation during constant temperature (Figure 3). The initial water peak (MAX = 3,140 ppm) observed well below T<sub>g</sub> must be from adsorbed and/or trapped water; while the second weaker peak (MAX = 2,120 ppm) starting slightly below T<sub>g</sub> is from DMBZ-15 degradation (first kinetic region) and/or more trapped water (Figure 3). A low molecular weight material with an absorbance peak at 1,076 cm<sup>-1</sup> starts

evolving at only 65°C, reaches a maximum at 165°C, and disappears at about 5 minutes (Figure 3). The A(1,076) peak is from dimethylsiloxane (DMS), a low molecular weight mold release or system impurity. The estimated MAX DMS concentration is <2 ppm (determined using octamethylcyclotetrasiloxane (OMCTS) as a reference). Carbon dioxide starts evolving well below-T<sub>g</sub> at about 3 minutes (220°C), increases to a broad maximum of 410 ppm at about 385°C, followed by a slow drop-off to the very slow degradation region at ISO (Figure 3). Note that CO<sub>2</sub> shows a sharp rate increase at about 392°C that correlates with the start of the first kinetic and/or trapped H<sub>2</sub>O region (Figure 3). Water (MAX = 3,140 ppm) is the major quantified degradation product observed in Figure 2, followed by carbon dioxide (MAX = 410 ppm), carbon monoxide (MAX = 42 ppm), methane (MAX = 11 ppm), and finally methanol (MeOH MAX = 5 ppm). Several other unassigned or non-quantified peaks are observed in Figure 3 at 895, 2,913, and 1,176 cm<sup>-1</sup> from composite degradation fragments, intermediates, or other products.

Figure 4 shows TGA/FTIR results for a typical above-T<sub>g</sub> IM7/DMBZ-15 composite thermal degradation experiment at the same heating rate (R = 100°C/min) as Figure 3 but at an ISO of 475°C. The thermal degradation products in Figure 4 are the same as those in the lower isothermal temperature run in Figure 3 except for the addition of ammonia, A(950), A(2,311), and an amide carbonyl peak at 1,708 cm<sup>-1</sup>. The ISO = 475°C run in Figure 4 shows that H<sub>2</sub>O (MAX = 8,830 ppm), CO<sub>2</sub> (MAX = 1,560 ppm), CH<sub>4</sub> (MAX = 1,490 ppm), CO (MAX = 1,330 ppm), and MeOH (MAX = 30 ppm) concentrations and other product absorbance values are higher than those in the ISO = 375°C run in Figure 3. The initial H<sub>2</sub>O loss for the ISO = 375 and 475°C runs must be from surface and/or adsorbed water because they both start well below-T<sub>g</sub> (80 to 90°C) and reach the same maximum of 3,155 ± 15 ppm at 292 ± 2°C (Figures 3 and 4). Water then shows a sharp rise at 422°C (5.2 minutes) to a shoulder at 465°C (5.7 minutes) and maximum of 8,830 ppm at 490°C (6.75 minutes), and finally after about 10 minutes, the very slow degradation at ISO. The first kinetic and/or trapped gas region for H<sub>2</sub>O appears to be the shoulder at 465°C, followed by a dominant second degradation region that peaks at 490°C (Figure 4). NH<sub>3</sub> and the 1,708 cm<sup>-1</sup> peak both start in the second degradation region near the CO and CH<sub>4</sub> maximum. The 1,708 cm<sup>-1</sup> carbonyl peak must be due to an amide fragment from scission of the polyimide ring, because it correlates with the growth of an -NH stretch peak at 3,370 cm<sup>-1</sup> (not shown in Figure 4).

More detail on the effect of heating rate, final temperature, duration at temperature, N<sub>2</sub> versus air, and other parameters on the IM7/DMBZ-15 composite and DMBZ-15 resin thermal degradation chemistry, kinetics, species profiles, and onset of catastrophic delamination is given in the following sections.

## HEATING RATE AND FINAL ISOTHERMAL TEMPERATURE

Figures 5 through 10 show the IM7/DMBZ-15 composite degradation quantified species profiles for H<sub>2</sub>O, CO<sub>2</sub>, CO, CH<sub>4</sub>, MeOH, and NH<sub>3</sub> in ppm/initial composite sample weight in grams (ppm/g) at ISO = 375, 400, 425, 450, and 475°C; R = 150, 100, and 50°C/min; and in N<sub>2</sub> atmosphere. In general, the species concentration increases as

ISO increases from 375 to 475°C (Figures 5 through 10). Each species concentration decreases and their initial observation times are delayed as R decreases from 150, 100, to 50°C/min (Figures 5 through 10). Figures 11 through 16 show the unassigned or non-quantified species peak height profiles for peaks at 895, 1,176, 2,311, 950, 1,708, and 2,913  $\text{cm}^{-1}$  in absorbance units (A) at ISO = 375, 400, 425, 450, and 475°C; R = 150, 100, and 50°C/min; and in  $\text{N}_2$  atmosphere. Four regions of gas evolution can be identified for composite thermal degradation (Figures 3 through 16):

1. Loss of adsorbed, trapped, and low molecular weight species well below-Tg
  - a.  $\text{H}_2\text{O}$  at high ppm/g and trace of DMS ( $\text{A}(1,076 \text{ cm}^{-1})$ ) at  $<90^\circ\text{C}$
  - b.  $\text{CO}_2$  at low ppm/g starting about  $220^\circ\text{C}$
  - c.  $\text{A}(895)$  and  $\text{A}(2,913)$  starting at about  $300^\circ\text{C}$
2. Just below to slightly above-Tg a very rapid loss of gases from degradation and possibly more trapped gases (first kinetic region)
3. Second kinetic region starting at about 425 to  $450^\circ\text{C}$  that includes resin degradation fragments (for example,  $\text{NH}_3$  and the  $1,708 \text{ cm}^{-1}$  amide fragment)
4. Finally, after the initial rapid gas evolution, a very slow degradation rate for moderate duration at constant temperature

The initial rapid evolution of species from thermal degradation (and possibly more trapped gases) in the first and second kinetic regions is in the following order of time (or temperature):

1.  $\text{H}_2\text{O}$  and  $\text{CO}_2$  (MeOH varies)
2.  $\text{CO}$  (MeOH varies)
3.  $\text{CH}_4$ ,  $\text{A}(2,311)$ ,  $\text{A}(1,176)$ , and  $\text{A}(950)$
4.  $\text{A}(1,708)$  and  $\text{NH}_3$

The onset time or initial temperature of species evolution in the kinetic regions varies with heating rate, isothermal temperature, and duration at temperature (Figures 3 through 16). Most of the gas evolution during thermal degradation, under  $\text{N}_2$ , is observed in a narrow region from 1 to 2 minutes to about 10 minutes for  $R = 150^\circ\text{C}/\text{min}$  and  $100^\circ\text{C}/\text{min}$ . However, for  $R = 50^\circ\text{C}/\text{min}$ , 5 to 15 minutes includes most of the initial gas evolution and will maintain a constant 10-minute integration interval for calculation of total gas concentration during maximum gas evolution. A more exact heating rate and temperature dependence can be obtained for the initial rapid gas evolution by integrating each species concentration profile (Figures 5 through 10) from 0 to 10 minutes for  $R = 150$  and  $100^\circ\text{C}/\text{min}$  and 5 to 15 minutes for  $R = 50^\circ\text{C}/\text{min}$ , dividing by sample weight in grams (ppm min/gram) and plotting versus isothermal temperature at the three heating rates. The absorbance versus time profiles (Figures 11 through 16) are plotted as the total absorbance summed over the time interval (0 to 10 minutes for  $R = 150$  and  $100^\circ\text{C}/\text{min}$ ,

and 5 to 15 minutes for  $R = 50^\circ\text{C}/\text{min}$ ) per gram sample versus ISO and R. Figure 17 shows the integrated concentration of  $\text{H}_2\text{O}$  and  $\text{CO}_2$  (ppm min/gram) at maximum gas evolution for IM7/DMBZ-15 composite thermal degradation in  $\text{N}_2$  versus isothermal temperature at all three heating rates. Integrated concentrations for  $\text{CO}$ ,  $\text{CH}_4$ , and  $\text{NH}_3$  (ppm min/g) versus ISO and R are shown in Figure 18. Several interesting observations can be made from Figures 17 and 18:

1.  $\text{CO}$ ,  $\text{CH}_4$ , and  $\text{NH}_3$  all show an exponential increase with ISO, but  $\text{H}_2\text{O}$  and  $\text{CO}_2$  only show a linear increase (375 to  $475^\circ\text{C}$ ).
2.  $\text{H}_2\text{O}$  is the major product, followed by  $\text{CO}_2$  at a much lower (ppm min/g) and has a factor of 6 to 7 higher slope from 375 to  $475^\circ\text{C}$  versus ISO compared to  $\text{CO}_2$ .
3.  $\text{CO}$  and  $\text{CH}_4$  start at lower (0 to 1,000 ppm min/g) compared to  $\text{CO}_2$  (4,000 to 12,000 ppm min/g) at ISO =  $375^\circ\text{C}$ , but at  $475^\circ\text{C}$  they both approach  $\text{CO}_2$  (~30,000 ppm min/g).
4.  $\text{CH}_4$  overtakes  $\text{CO}$  at  $470^\circ\text{C}$  due to a higher exponential rate.
5.  $\text{NH}_3$  is not observed until about 425 to  $435^\circ\text{C}$ , but then increases rapidly.
6.  $\text{CO}_2$  shows only a small change in concentration (except at  $375^\circ\text{C}$ ) with heating rate, while  $\text{H}_2\text{O}$  (maximum change with R [MAX  $\Delta$ ] about 35,000 ppm min/g),  $\text{CO}$  (MAX  $\Delta \sim 7,000$  ppm min/g),  $\text{CH}_4$  (MAX  $\Delta \sim 7,000$  ppm min/g), and  $\text{NH}_3$  (MAX  $\Delta \sim 2,400$  ppm min/g) all show a larger increase in concentration from  $R = 50$  to  $150^\circ\text{C}/\text{min}$ .

Figure 19 shows MeOH (ppm min/g) during maximum gas evolution versus ISO and R (in  $\text{N}_2$ ) for both the composite and resin. The integrated MeOH (ppm min/g) for the composite increases slightly with ISO until about  $425^\circ\text{C}$  and then levels off at a very low concentration (300 to 400 ppm min/g) (Figure 19). Integrated MeOH (ppm min/g) for the resin is about a factor of 10 higher compared to the composite and shows similar trends with ISO but levels off at a higher concentration (3,300 to 4,300 ppm min/g) (Figure 19). Methanol is used as a solvent for preparation of the resin but not for the composite (References 4 and 5). However, the small concentration of methanol observed for the composite may be a degradation product.

The temperature and heating rate dependence will continue into the next section on composite versus resin effects.

## IM7/DMBZ-15 COMPOSITE VERSUS DMBZ-15 RESIN

Figures 20 and 21 show the  $\text{H}_2\text{O}$ ,  $\text{CO}_2$ ,  $\text{CO}$ ,  $\text{CH}_4$ , and  $\text{NH}_3$  integrated concentrations (ppm min/g) during maximum gas evolution versus ISO and R (in  $\text{N}_2$ ) for the DMBZ-15 resin thermal degradation (compare to Figures 17 and 18 for the composite). Note that the composite integrated concentrations are about half those for the resin at the same ISO and R (Figures 17, 18, 20, and 21). A more exact calculation for composite  $\text{H}_2\text{O}$ ,  $\text{CO}_2$ ,  $\text{CO}$ ,  $\text{CH}_4$ , and  $\text{NH}_3$  integrated concentrations divided by those for the resin at the same ISO and R gives an average of  $45 \pm 5\%$ , under most experimental heating conditions. Because the composite is 45% DMBZ-15 resin (References 4 and 5), the graphite fibers must contribute little, if any, products to the composite thermal degradation under  $\text{N}_2$  atmosphere. MeOH evolution, as shown above, is mostly from the solvent used in preparation of the resin, but low concentrations are found in composite degradation. DMS ( $A(1,076 \text{ cm}^{-1})$ ) is observed at very low concentrations ( $<2$  ppm) for most composite and some resin experiments and is probably a mold release, surface impurity, or from the transfer line coating.

The thermal degradation quantified products ( $\text{H}_2\text{O}$ ,  $\text{CO}_2$ ,  $\text{CO}$ ,  $\text{CH}_4$ , and  $\text{NH}_3$ ) show very similar dependences on ISO (375 to  $475^\circ\text{C}$ ) and R (50 to  $150^\circ\text{C}/\text{min}$ ) during maximum gas evolution for both composite and resin except for a factor of about 2.2 higher concentrations for the resin (under most experimental conditions). Most of the degradation kinetics and chemistry for quantified products for both resin and composite are due to the DMBZ-15 resin degradation with little, if any, contribution from the graphite fibers at ISO (375 to  $475^\circ\text{C}$ ), R (50 to  $150^\circ\text{C}/\text{min}$ ), and in  $\text{N}_2$ . The ratio of  $\text{H}_2\text{O}$  to  $\text{CO}_2$  (ppm min/g) slopes for the resin from 375 to  $475^\circ\text{C}$  is 6 to 7 (Figure 22), which is the same as for the composite (Figure 17). Equal  $\text{H}_2\text{O}/\text{CO}_2$  (ppm min/g) versus ISO slope ratios for both resin and composite indicates again that the DMBZ-15 resin mainly determines composite degradation chemistry and kinetics from 375 to  $475^\circ\text{C}$  in  $\text{N}_2$ .

Figure 23 shows  $\text{CO}_2$  (ppm/g) from the thermal degradation of DMBZ-15 resin at  $R = 50^\circ\text{C}/\text{min}$ ,  $\text{ISO} = 375$  to  $475^\circ\text{C}$  in  $\text{N}_2$  for comparison with Figure 6 (right) from the IM7/DMBZ-15 composite. Again observe the approximate factor of 2 greater ppm/g peak values for the resin (Figure 23) compared to the composite (Figure 6 (right)), except for  $\text{ISO} = 375^\circ\text{C}$ . However, more significant is the "smooth" transition from kinetic region 1 to kinetic region 2 as ISO increases from 400 to  $475^\circ\text{C}$  for the resin (Figure 23). Figure 6 (right) for the composite shows a "delay" or increased time at  $400^\circ\text{C}$  before  $\text{CO}_2$  peaks. Figure 22 shows  $\text{H}_2\text{O}$  (ppm/g) evolution from the resin at  $R = 50^\circ\text{C}/\text{min}$ ,  $\text{ISO} = 375$  to  $475^\circ\text{C}$  in  $\text{N}_2$  for comparison with Figure 5 (right) from the composite. The adsorbed and/or trapped  $\text{H}_2\text{O}$  in region 1 for the resin evolves over a longer time interval without a distinct peak at about 5 minutes as observed for the composite (Figures 22 and 5 (right)). Kinetic region 1 for the resin starts at 9 minutes for  $\text{ISO} = 400^\circ\text{C}$  and peaks at 9.5 minutes over a relatively narrow ppm/g range (44,000 to 53,000) for  $\text{ISO} = 400$  to  $475^\circ\text{C}$  ( $\text{H}_2\text{O}$  - Figure 22). Resin kinetic region 2 starts as a weak shoulder at  $\text{ISO} = 425^\circ\text{C}$  and grows to the major peak at  $\text{ISO} = 475^\circ\text{C}$  ( $\text{H}_2\text{O}$  - Figure 22). The transition from kinetic region 1 to 2 is not as clear for the composite in Figure 5 (right). Kinetic region 1

for the resin may be mostly trapped  $\text{H}_2\text{O}$  released slightly below- $T_g$  because the peak concentration only varied from 44,000 to 53,000 ppm/g from 400 to 475°C. Note that at ISO = 375°C for the resin, no sharp rise in  $\text{H}_2\text{O}$  concentration occurs at 9 minutes (Figure 22). Figure 24 for CO (ppm/g) and Figure 25 for  $\text{CH}_4$  (ppm/g) versus time for DMBZ-15 resin at  $R = 50^\circ\text{C}/\text{min}$ , ISO = 400 to 475°C in  $\text{N}_2$  show about a factor of 2 to 3 higher ppm/g peak values at each ISO compared to the corresponding plots for the composite (CO - Figure 7 (right) and  $\text{CH}_4$  - Figure 8 (right)). Kinetic region 1 is not apparent or “hidden” under kinetic region 2 for CO and  $\text{CH}_4$ , except that at ISO = 400°C a “delayed” peak is observed for the composite (CO - Figure 7 (right) and  $\text{CH}_4$  - Figure 8 (right)); otherwise only a sharp rise into a broad dominant kinetic region 2 is observed for both resin (Figures 24 and 25) and composite.

The next section will examine the non-quantified or unassigned species from both resin and composite thermal degradation as a function of ISO and  $R$  in  $\text{N}_2$ .

### UNASSIGNED OR NON-QUANTIFIED PRODUCTS OR FRAGMENTS

Other products include unassigned FTIR peaks, non-quantified species, or possibly  $\text{N}_2$  or  $\text{H}_2$ . The peak at  $1,076\text{ cm}^{-1}$  is a low molecular weight DMS mold release, surface impurity, or transfer line coating at  $<2$  ppm and is not involved in the degradation mechanism. The unassigned peak total  $A(895\text{ cm}^{-1})/\text{g}$  shows a linear dependence on ISO for both composite and resin for all  $R$  under  $\text{N}_2$  (Figure 26). Total  $A(895\text{ cm}^{-1})/\text{g}$  versus ISO for the resin increases 2.5 times faster than for the composite (Figure 26). The total  $A(895\text{ cm}^{-1})/\text{g}$  for the resin also shows a larger increase with  $R$  compared to the composite (Figure 26).  $A(895\text{ cm}^{-1})$  starts below- $T_g$  ( $\sim 300^\circ\text{C}$ ) and shows a distinct kinetic region 1 and 2 for both resin and composite (Figures 3, 4, and 11). Figure 27 shows total  $A(1,176\text{ cm}^{-1})/\text{g}$  versus ISO and  $R$  for composite and resin under  $\text{N}_2$ . Total  $A(1,176\text{ cm}^{-1})/\text{g}$  starts higher for the composite until at about 455 to 475°C, the resin total absorbance becomes higher (Figure 27). The  $A(1,176\text{ cm}^{-1})$  peak for the resin starts in kinetic region 2 at about 425 to 450°C, then increases very rapidly.  $A(1,176\text{ cm}^{-1})$  starts slowly for the composite at 375 to 400°C, then at  $\sim 450^\circ\text{C}$  shows a slight rate increase (Figure 27). The  $2,311\text{ cm}^{-1}$  peak total  $A(2,311\text{ cm}^{-1})/\text{g}$  versus ISO and  $R$  for both composite and resin (in  $\text{N}_2$ ) is shown in Figure 28. Total  $A(2,311\text{ cm}^{-1})/\text{g}$  shows an exponential dependence on ISO for both composite and resin, with the resin growing at a faster rate (Figure 28).  $A(2,311\text{ cm}^{-1})$  starts in kinetic region 2 at about 400 to 425°C for the composite and about 375 to 400°C for the resin (Figures 13 and 28). The  $2,311\text{ cm}^{-1}$  peak is from an aromatic isocyanate or cyanide degradation fragment (note that phenylisocyanate has a peak at  $2,285\text{ cm}^{-1}$  [ThermoNicolet Gas Phase Digital Spectral Library]). Total  $A(950\text{ cm}^{-1})/\text{g}$  versus ISO and  $R$  (in  $\text{N}_2$ ) shows an exponential dependence on ISO for both composite and resin (Figure 29). The  $A(950\text{ cm}^{-1})/\text{g}$  grows only slightly faster for the resin compared to the composite, with the composite values being higher until 405 to 425°C (Figure 29). The  $2,913\text{ cm}^{-1}$  peak is difficult to integrate because  $\text{CH}_4$  and a weak peak at  $2,965\text{ cm}^{-1}$  overlap; but Figure 16 shows that  $A(2,913)$  starts below- $T_g$  at about  $300^\circ\text{C}$ , similar to  $A(895)$  in Figure 11. Most likely the  $2,913\text{ cm}^{-1}$  peak is from an aliphatic and/or aromatic  $-\text{CH}$  stretch from one of the early products.

Figure 30 shows the total  $A(1,708\text{ cm}^{-1})/\text{g}$  versus ISO and R (in  $\text{N}_2$ ) for both composite and resin. Total  $A(1,708\text{ cm}^{-1})/\text{g}$  shows a very sharp rise starting at 435 to 450°C at high heating rate ( $R = 150$  and  $100^\circ\text{C}/\text{min}$ ) for both composite and resin (Figure 30). The total  $A(1,708\text{ cm}^{-1})/\text{g}$  starts at high temperature (435 to 450°C) late in the second kinetic region.  $A(1,708\text{ cm}^{-1})$  must be from an amide carbonyl polyimide degradation fragment that requires scission of the polyimide ring. Note that the amide polyimide degradation fragment condenses on the TGA cell KBr window at 225°C.

Figure 31 shows DMBZ-15 resin potential degradation pathways and products from Reference 5. The peaks at 895, 1,176, and  $950\text{ cm}^{-1}$  require more data before they can be assigned to a specific compound or intermediate. TGA weight loss and calculated weight loss from observed species will be examined in the next section.

### TGA WEIGHT LOSS COMPARED TO SPECIES WEIGHT LOSS

Conversion of the quantified gas concentrations from ppm to  $\mu\text{g}$  allows a comparison of the total quantified evolved gas weight ( $\text{H}_2\text{O}$ ,  $\text{CO}_2$ ,  $\text{CO}$ ,  $\text{CH}_4$ ,  $\text{MeOH}$ , and  $\text{NH}_3$ ) with the TGA weight loss in  $\mu\text{g}$ . Figure 32 shows quantified species in  $\mu\text{g}$  for ISO = 475°C,  $R = 150^\circ\text{C}/\text{min}$  in  $\text{N}_2$ , as well as T ( $^\circ\text{C}$ ) and TGA percent weight loss (%wl). Total  $\mu\text{g}$  versus time of each quantified species are shown in Figure 33 for ISO = 475°C,  $R = 150^\circ\text{C}/\text{min}$  in  $\text{N}_2$  for the composite thermal degradation (same TGA/FTIR parameters as in Figure 32). The total measured weight loss of quantified gases in  $\mu\text{g}$  ( $\text{H}_2\text{O} + \text{CO}_2 + \text{CO} + \text{CH}_4 + \text{MeOH} + \text{NH}_3$ ) compared to the TGA weight loss in  $\mu\text{g}$  is shown for the composite at  $R = 150^\circ\text{C}/\text{min}$  in Figure 34 for ISO = 375°C and in Figure 35 for ISO = 475°C (both in  $\text{N}_2$ ). Total measured weight loss / TGA weight loss decreases from 0.56 at ISO = 375°C to 0.33 at ISO = 475°C for  $R = 150^\circ\text{C}/\text{min}$  in  $\text{N}_2$  at 35 minutes (Figure 36). The remaining fraction (0.44 at 375°C to 0.67 at 475°C) must be from "other products," such as unassigned species, degradation fragments, and possibly  $\text{N}_2$  and/or  $\text{H}_2$ . Therefore the fraction of "other products" increases with isothermal temperature (375 to 475°C) and is  $>0.5$  of the total product weight (quantified gases + other products) starting at about 425°C (Figure 36).

Figures 37 and 38 show TGA %wl after maximum gas evolution for both the composite and resin thermal degradation plotted versus isothermal temperature (ISO = 375 to 475°C) and heating rate ( $R = 50$ , 100, and  $150^\circ\text{C}/\text{min}$ ), respectively. The initial TGA %wl is an exponential function of ISO from 375 to 475°C but an almost linear function of the heating rate from 50 to  $150^\circ\text{C}/\text{min}$  (Figures 37 and 38). Therefore the initial rapid evolution of all products from the thermal degradation of IM7/DMBZ-15 composite and DMBZ-15 resin increases exponentially with the final constant temperature (375 to 475°C), but only shows a linear increase with the initial heating rate (50 to  $150^\circ\text{C}/\text{min}$ ).

The next section will examine the TGA/FTIR results for thermal degradation of IM7/DMBZ-15 composite and DMBZ-15 resin in air. Changes in the thermal degradation chemistry, kinetics, and species profiles with heating rate, final temperature, duration at temperature, and other parameters will be compared for air and N<sub>2</sub>.

## COMPOSITE AND RESIN THERMAL DEGRADATION IN AIR VERSUS NITROGEN

Figures 39 and 40 show the TGA %wl for IM7/DMBZ-15 composite at R = 150°C/min from ISO = 375 to 525°C in N<sub>2</sub> and air, respectively. Note the sharp rise in %wl from 3.5 to 4 minutes that increases in rate as ISO increases (kinetic regions 2 and 3), then rolls over into a region of very slow gain in %wl (region 4) for N<sub>2</sub> atmosphere (Figure 39). Figure 40 (air atmosphere) shows a similar rapid weight loss from 3.5 to about 4 minutes, followed by a rollover to a slow increase in %wl. But starting at about ISO = 450°C and about 35 minutes, the rate of %wl increases slightly until at ISO = 525°C the %wl increase becomes dramatic. Species profiles are shown in Figures 41 and 42 at the same R and ISO as Figures 39 and 40 for N<sub>2</sub> and air atmosphere, respectively. The increased %wl in region 4 is due primarily to CO<sub>2</sub>, CO, and H<sub>2</sub>O from oxidation of the composite (resin) and some of the degradation products (compare Figures 41 and 42). Individual quantitated species profiles (ppm/g) at R = 150°C/min, ISO = 375 to 525°C, and both N<sub>2</sub> and air atmosphere are shown in Figures 43 through 47 for CO<sub>2</sub>, CO, H<sub>2</sub>O, CH<sub>4</sub>, and NH<sub>3</sub>, respectively. Carbon dioxide is higher in region 4 for air compared to N<sub>2</sub> due to oxidation starting at 450°C, but is not higher until about 500°C in kinetic regions 1 and 2 (Figure 43). Carbon monoxide is higher in regions 2, 3, and 4 for air compared to N<sub>2</sub> starting at only 375°C (Figure 44). The increased concentration for CO in region 4 from oxidation in air is not as large as for CO<sub>2</sub> (Figures 43 and 44). Water shows higher concentration in region 4 for air compared to N<sub>2</sub> starting at about 425 to 450°C, and slightly higher peak concentrations in regions 2 and 3 starting at 375°C (Figure 45). Methane shows very little difference between the concentration profiles in air compared to N<sub>2</sub> at R = 150°C/min and ISO = 375 to 525°C (Figure 46). Ammonia shows higher concentrations for N<sub>2</sub> compared to air starting at 475°C in region 4 and starting at 500°C in region 3 (Figure 47). Note that NH<sub>3</sub> is not observed until ISO = 425 to 450°C in region 3 for both air and N<sub>2</sub> atmosphere (Figure 47). Figures 48 and 49 show the integrated concentrations (ppm min/g) for the five quantified species (CO<sub>2</sub>, H<sub>2</sub>O, CO, CH<sub>4</sub>, and NH<sub>3</sub>) during maximum gas evolution (0 to 10 minutes) for composite degradation at R = 150°C/min, ISO = 375 to 525°C, and in N<sub>2</sub> and air. Water starts at about the same integrated concentration for air and N<sub>2</sub> at R = 150°C/min from 375 to 450°C, then increases for air and levels off in N<sub>2</sub> (Figure 48). The composite H<sub>2</sub>O ppm min/g from 375 to 475°C shows a linear dependence with ISO for N<sub>2</sub> (Figure 17 shows linear growth for H<sub>2</sub>O versus ISO at R = 50 to 150°C/min in N<sub>2</sub>) and within experimental error, a close to linear growth in air (Figure 48). The overall composite H<sub>2</sub>O growth, in air, during maximum gas evolution versus ISO fits a third-order polynomial, but errors in the integration from 0 to 10 minutes could allow for about equal values with N<sub>2</sub> from 375 to 475°C. Carbon dioxide integrated concentration from 0 to 10 minutes, versus ISO at R = 150°C/min shows a linear fit from 375 to 475°C for both air and N<sub>2</sub>, and remains



linear in  $N_2$  but increases exponentially in air after 475°C (Figure 48). Figure 49 shows that the CO integrated concentration (ppm min/g) from 0 to 10 minutes at  $R = 150^\circ\text{C}/\text{min}$  versus ISO is uniformly higher for air compared to  $N_2$  until 475°C, where the CO in air continues to grow exponentially but decreases in rate for  $N_2$ . The integrated concentration (ppm min/g) from 0 to 10 minutes at  $R = 150^\circ\text{C}/\text{min}$  for  $CH_4$  is almost identical from 375 to 475°C in air and  $N_2$ , but both start to level off above 475°C with  $CH_4$  in  $N_2$  slightly higher (Figure 49). Figure 49 shows that  $NH_3$  is first observed at about 435°C and grows at the same rate for both air and  $N_2$  until at 470°C, where the rate of growth in air decreases, probably due to oxidation.

Unassigned or non-quantified products or resin fragments total absorbance per gram from 0 to 10 minutes for the composite versus ISO at  $R = 150^\circ\text{C}/\text{min}$  in air and  $N_2$  atmosphere are shown in Figures 50 through 53. The total  $A(895)/g$  increases linearly with ISO from 375 to about 450°C with a slightly higher level in  $N_2$ , then levels off for  $N_2$ , and drops dramatically in air (Figure 50). Figure 51 shows total  $A(1,176)/g$  is the same from 375 to 450°C for air and  $N_2$ , and then grows at a higher rate in  $N_2$  (possibly leveling off at 525°C) compared to air from 475 to 525°C. The species responsible for the peaks at 895 and 1,176  $\text{cm}^{-1}$  appear to oxidize in air above 450°C. Total  $A(950)/g$  is the same from 375 to 450°C in air and  $N_2$ , but grows at a faster rate in air compared to  $N_2$  from 450 to 525°C (Figure 52). Figure 53 shows that total  $A(1,708)/g$  starts at 435 to 445°C for both air and  $N_2$ , then grows rapidly in  $N_2$  (possibly leveling off at 525°C) but at a slower and decreasing rate in air due to oxidation.

The next section will discuss the quantified species degradation rates in ppm/min and the onset of catastrophic delamination for the thermal degradation of IM7/DMBZ-15 composite and DMBZ-15 resin.

## QUANTIFIED SPECIES DEGRADATION RATES AND ONSET OF CATASTROPHIC DELAMINATION

The thermal degradation rate or rate of growth of degradation products in ppm/min is calculated for quantified species using the running 3-point slope of concentration (ppm)/time (minutes). Figures 54 through 56 show the rate of growth of quantified degradation products versus time at  $R = 100^\circ\text{C}/\text{min}$  and  $ISO = 475^\circ\text{C}$  for composite in  $N_2$ , composite in air, and resin in  $N_2$ , respectively. Water shows a very rapid increase in slope or rate of growth starting at 5 minutes (kinetic region 1) from 0 to 10,300 ppm/min in about 0.5 minute;  $CO_2$  rapidly reaches a maximum rate of only 2,000 ppm/min in the same time interval; CO starts at 5.25 minutes growing at a moderate rate to a maximum of 1,260 ppm/min;  $CH_4$  starts at 5.5 minutes (kinetic region 2) growing slowly to a maximum rate of 1,575 ppm/min; and  $NH_3$  starts at 6.2 minutes (late kinetic region 2) and reaches a maximum rate of only 170 ppm/min at 7 minutes (Figure 54). Figure 54 shows that  $H_2O$  starts a second rapid growth in kinetic region 2 at 5.9 minutes but only reached a maximum rate of 5,350 ppm/min, even though most of the  $H_2O$  observed is in kinetic region 2 (see Figure 5 (middle)). The maximum rate of gas evolution from the thermal degradation of the composite is mostly from  $H_2O$  starting below- $T_g$  in kinetic region 1 (under the conditions in Figure 54). Figure 55 shows that  $H_2O$  grows at a

slightly lower rate in air (0 to 9,000 ppm/min in 0.72 minute) compared to N<sub>2</sub> (0 to 10,300 ppm/min in 0.5 minute) (Figure 54). Note in Figure 55 that CO and CO<sub>2</sub> start at the same time and have about the same rate of growth and decrease. Resin thermal degradation in Figure 56 shows H<sub>2</sub>O starts a very rapid growth at 5.04 minutes to a maximum rate of 11,200 ppm/min in just 0.34 minute in kinetic region 1, and then in kinetic region 2 at 5.74 minutes starts a slower growth to a maximum of 7,350 ppm/min in 0.5 minute. Water has the highest rate of growth starting in kinetic region 1 of any composite or resin degradation product in air or N<sub>2</sub> atmosphere.

Figures 57 through 59 show the CO<sub>2</sub> rate of growth for composite thermal degradation in N<sub>2</sub> from ISO = 375 to 475°C at R = 150, 100, and 50°C/min, respectively. The maximum rate of CO<sub>2</sub> growth decreases slightly and the start of evolution moves to longer times for decreasing R at each ISO (Figure 57 through 59). Almost no CO<sub>2</sub> is observed at ISO = 375°C (below-T<sub>g</sub>) and R = 50°C/min in kinetic region 1, and a longer duration at ISO = 400°C is required before maximum rate is reached at 11.5 minutes (Figure 59). Above-T<sub>g</sub> at ISO = 425 to 475°C for R = 50°C/min, the maximum CO<sub>2</sub> rate is reached at about 9.5 minutes (Figure 59). The overshoot in temperature for R = 150 and 100°C/min at ISO = 375 and 400°C (below-T<sub>g</sub>) allows observation of a CO<sub>2</sub> growth rate delayed in time compared to ISO = 425 to 475°C runs (above-T<sub>g</sub>) (Figures 57 and 58). Carbon dioxide has a much lower rate of growth compared to H<sub>2</sub>O (in kinetic region 1), but faster than any other quantified composite or resin degradation product.

What is causing the very high rate of gas evolution below-T<sub>g</sub> (mostly H<sub>2</sub>O) during the thermal degradation of IM7/DMBZ-15 composite or DMBZ-15 resin? Figure 60 shows a TGA plot of weight (%) and temperature (°C) versus time (minutes) for the composite in air at ISO = 375°C and R = 150°C/min. The sharp spike in the weight (%) curve at 3.9 minutes and T = 406°C indicates an extremely rapid weight increase of about 3% (Figure 60). This spike must have been caused by a very rapid release of hot gases that applied a downward force on the composite sample, thereby increasing the weight. The spike in the weight loss curve in Figure 60 is extreme, but several other composite and resin samples showed spikes of lower intensity—but all occurred below the nominal T<sub>g</sub> of the DMBZ-15 resin (414°C (References 4 and 5)). Figure 61 shows the correlation of TGA weight loss spikes with the corresponding total measured gas evolution rates (ppm/min) for the resin at ISO = 400°C in N<sub>2</sub> and R = 150, 100, and 50°C/min. The TGA weight loss spikes occur just before the sharp rise in gas evolution in the FTIR gas cell for the three heating rates (Figure 61). Note that the spike temperatures increase from 390.1, 391.1, to 394.7°C (all below-T<sub>g</sub>) as the heating rate decreases from 150, 100, to 50°C/min (Figure 61). The weight (mg) data in Figure 61 is converted to Thermo Nicolet Series format and only has a time resolution of about 10 seconds (repeat time for the spectral data) compared to 0.01 second for the original TGA data. Therefore, the weight loss spike shown in Figure 61 is not as sharp and has a possible time variation of 0.17 minute compared to the original TGA data. Figure 62 compares the TGA weight loss spike with the H<sub>2</sub>O rate of growth (ppm/min) for resin thermal degradation at 425°C in N<sub>2</sub> and R = 150, 100, and 50°C/min. The weight loss spikes again occur just before the rapid increase in rate for H<sub>2</sub>O evolution, but with a slight lag due to transfer line and

FTIR scan time delays (Figure 62). Spike temperatures again increase from 387.7, 389.5, to 394.9°C (all below- $T_g$ ) as R decreases from 150, 100, to 50°C/min (Figure 62).

The very rapid exponential increase in degradation rate and/or release of trapped gases in the first kinetic region from just below to slightly above- $T_g$  is the onset of an extremely rapid hot gas expansion that causes “catastrophic delamination” and/or blistering. The catastrophic delamination onset temperature increases with decreasing heating rate ( $R = 150$  to 50°C/min) and is usually below the DMBZ-15 polyimide  $T_g$  (414°C). The polyimide resin  $T_g$  may be lowered by formation of water above the critical point, thus allowing the rapid escape of gases below the nominal resin  $T_g$  of 414°C.

### IM7/DMBZ-15 COMPOSITE TOP SURFACE HEAT DAMAGE USING TD ATR SPECTRA

Figures 63 and 64 show TD/ATR top surface spectra of unheated compared to heated (ISO = 375 to 475°C) IM7/DMBZ-15 composite at  $R = 150^\circ\text{C}/\text{min}$  in  $\text{N}_2$  and  $R = 100^\circ\text{C}/\text{min}$  in air, respectively.

The unheated versus heated composite TD ATR spectra in  $\text{N}_2$  atmosphere show the following peak changes (Figure 63):

1. Peak at  $1,491\text{ cm}^{-1}$  decreases in intensity and disappears at  $450^\circ\text{C}$  as  $1,468\text{ cm}^{-1}$  shoulder starts at  $375^\circ\text{C}$  and becomes more intense than  $1,491\text{ cm}^{-1}$  at  $425^\circ\text{C}$ .
2. Broad peak at  $1,367\text{ cm}^{-1}$  shifts to  $1,358\text{ cm}^{-1}$  from unheated to  $475^\circ\text{C}$ .
3. Broad peak at  $1,097\text{ cm}^{-1}$  shifts to  $1,088\text{ cm}^{-1}$  from unheated to  $475^\circ\text{C}$ .
4. Spectral contrast or definition decreases as ISO increases, probably due to increased surface hardness.
5. Out-of-phase  $1,716\text{ cm}^{-1}$  imide carbonyl stretch shows no change from unheated to  $475^\circ\text{C}$ .
6. In-phase  $1,780\text{ cm}^{-1}$  imide carbonyl stretch shifts slightly to  $1,777\text{ cm}^{-1}$  or changes due to increased surface hardness.

The unheated versus heated composite TD ATR spectra in air atmosphere show the following peak changes (Figure 64):

1. Peak at  $1,491\text{ cm}^{-1}$  gone at about  $400^\circ\text{C}$  and peak at  $1,471$  to  $1,469\text{ cm}^{-1}$  dominates at only  $375^\circ\text{C}$ .
2. Broad peak at  $1,367\text{ cm}^{-1}$  shifts to  $1,357\text{ cm}^{-1}$  at  $375^\circ\text{C}$  and continues shifting to  $1,348\text{ cm}^{-1}$  at  $475^\circ\text{C}$ .
3. Broad peak at  $1,097\text{ cm}^{-1}$  shifts to about  $1,090\text{ cm}^{-1}$  from unheated to  $475^\circ\text{C}$ .

4. Spectral contrast is worse at 475°C in air compared to N<sub>2</sub>, and only broad peaks are observed.
5. Out-of-phase 1,716 cm<sup>-1</sup> imide carbonyl stretch shifts to 1,720 cm<sup>-1</sup> at only 375°C and to 1,726 cm<sup>-1</sup> at 475°C.
6. In-phase 1,780 cm<sup>-1</sup> imide carbonyl stretch shifts slightly to 1,777 cm<sup>-1</sup> at 475°C due to increased surface hardness.

Changes from 1,500 to 1,350 cm<sup>-1</sup> show loss of -CH<sub>3</sub>, and shifts in aromatic modes occur at lower temperature in air compared to N<sub>2</sub> for the IM7/DMBZ-15 composite top surface. The out-of-phase 1,716 cm<sup>-1</sup> imide carbonyl stretch remains constant up to 475°C at the composite surface in N<sub>2</sub> but shifts to 1,720 cm<sup>-1</sup> at only 375°C and to 1,726 cm<sup>-1</sup> at 475°C in air. Top surface imide linkages for the composite or resin are "stable" up to about 475°C in N<sub>2</sub> but show significant changes at about 375 to 400°C in air. TGA/FTIR data show that internal imide linkage degradation starts at 435 to 450°C in air or N<sub>2</sub>.

## SUMMARY

In the 2 years of this project, TGA/FTIR and TD ATR were shown to be very useful tools for the study of the thermal degradation of high temperature composites, in particular IM7/DMBZ-15 polyimide. The major gas phase degradation products were identified and quantified (H<sub>2</sub>O, CO<sub>2</sub>, CO, CH<sub>4</sub>, NH<sub>3</sub>, and MeOH) and assignments were made for some of the non-quantified intermediates or degradation fragments. Non-quantified or other products include peaks observed at 895, 1,176, 2,311 (phenyl isocyanate derivative), 2,913 (aromatic or aliphatic -CH fragment), 950, 2,965, 3,370, and 1,708 cm<sup>-1</sup> (amide polyimide fragment) and possibly N<sub>2</sub> and H<sub>2</sub> (Figure 31). Four regions of gas evolution were identified for the resin and composite thermal degradation under N<sub>2</sub> and air atmosphere: (1) loss of surface and trapped H<sub>2</sub>O and CO<sub>2</sub> (also low concentrations of DMS) at well below-T<sub>g</sub>; (2) just below to slightly above-T<sub>g</sub>, a very rapid loss of gases from degradation and more trapped gases (first kinetic region); (3) a second kinetic region starting at 435 to 450°C that includes polymer degradation fragments (such as NH<sub>3</sub> and the 1,708 cm<sup>-1</sup> amide fragment); and (4) a very slow degradation rate for moderate duration at constant temperature. Resin degradation chemistry is of primary concern because it was determined that the graphite fibers do not contribute significant products from 375 to 475°C under N<sub>2</sub> or air. The very rapid exponential increase in degradation rate in the first kinetic region from just below to slightly above-T<sub>g</sub> is the onset of an extremely rapid hot gas expansion that causes "catastrophic delamination" and blistering. The catastrophic delamination onset temperature decreases with increasing heating rate (onset T = 394.7 to 390.1°C for R = 50 to 150°C/min) and is usually below the DMBZ-15 polyimide T<sub>g</sub> (414°C) (Figure 61). The polyimide resin T<sub>g</sub> may be lowered by formation of water above the critical point, thus allowing the rapid escape of gases below the nominal T<sub>g</sub> of 414°C. Water is the major evolved gas and degradation product up to about 435 to 450°C, when polyimide

resin fragments and intermediates start to dominate. The initial rapid evolution of all products (regions 1, 2, and 3) from the thermal degradation of IM7/DMBZ-15 composite and DMBZ-15 resin increases exponentially with the isothermal temperature (375 to 475°C), but only shows a linear increase with the initial heating rate (50 to 150°C/min). Most of the thermal degradation products have similar concentrations in air or N<sub>2</sub> atmosphere (regions 2 and 3), but CO is higher by a factor of 2 to 3 in air for regions 2, 3, and 4. Oxidation, in air, causes CO, CO<sub>2</sub>, and to some extent H<sub>2</sub>O (for T>425°C) to have higher and increasing concentrations in region 4, especially for ISO = 500 and 525°C, compared to N<sub>2</sub>. Under N<sub>2</sub> atmosphere, TD ATR shows that no imide linkages are damaged at the "top" surface of the composite up to 475°C, but in air, surface imide linkages are broken starting at only 375°C. However, TGA/FTIR data show that the imide linkages are stable up to about 435 to 450°C for the interior of the composite in air or N<sub>2</sub>. Surface and edge effects versus interior degradation are important concepts for predicting large panel properties from the small scale data. For example, exterior composite surfaces perpendicular to the fiber direction degrade faster than the top and bottom resin-rich composite surfaces.

Temperature and heating rate limits have been established for IM7/DMBZ-15 graphite composite based on the kinetic data and an improved understanding of the thermal degradation mechanism. Other high temperature composite candidates should be studied using the small scale TGA/FTIR method discussed here in order to obtain temperature, heating rate, duration at temperature, and onset of catastrophic delamination limits to compare with IM7/DMBZ-15. This small scale, low cost analysis method will enable prediction of which new composites to scale up for high temperature missile, radome, or reentry applications.

## REFERENCES

1. Oak Ridge National Laboratory. *Composite Heat Damage. Part 1. Mechanical Testing of IM6/3501-6 Laminates; and Part 2. Nondestructive Evaluation Studies of IM6/3501-6 Laminates*, by B. J. Frame, C. J. Janke, W. A. Simpson, R. E. Ziegler, and H. E. Philpot. Tennessee, ORNL, 1990. (Publication no. ORNL/ATD-33, publication UNCLASSIFIED.)
2. F. MacDonald, K. C. Chuang, P. B. Stickler, and S. Coghill. "Beyond  $T_g$  Characterization of Polymer Matrix Composite Materials for Moderate Duration Applications," *Proc. National Space & Missile Materials Symp.*, 24-28 June 2001, Monterey Conference Center, Monterey, California. (Presentation and proceedings UNCLASSIFIED.)
3. M. P. Nadler and F. MacDonald. "Thermal Degradation Analysis of IM7/DMBZ-15 High Temperature Composite by TGA/FTIR," *Proc. 33<sup>rd</sup> Internat'l SAMPE Technical Conf.*, 5-8 November 2001, Seattle, Washington. (Publication and proceedings UNCLASSIFIED.)
4. K. C. Chuang, K. J. Bowles, D. A. Scheiman, D. S. Papadopoulos, and D. Hardy-Green. "Synthesis and Characterization of a High  $T_g$  Polyimide (DMBZ-15)," *The Internat'l Symp. Polyimides and Other High Temp. Polymers*, 29 November - 1 December 1999, Robert Treat Hotel, Newark, New Jersey. (Publication and proceedings UNCLASSIFIED.)
5. K. C. Chuang, J. E. Waters, and D. Hardy-Green. "A High  $T_g$  Thermosetting Polyimide," *42nd Internat'l SAMPE Symp.*, Vol. 42 (1997). P. 1283. (Publication and proceedings UNCLASSIFIED.)
6. National Aeronautics and Space Administration. "A Study of Elevated Temperature Testing Techniques for the Fatigue Behavior of PMCS: Application to T650-35/AMB21," by A. L. Gyekenyesi, M. G. Castelli, J. R. Ellis, and C. S. Burke. NASA, 1995. (NASA TM-106927, publication UNCLASSIFIED.)
7. McDonnell Douglas Corp. *Mechanical Properties and Thermal Degradation of Advanced Composites Under Rapid Heating*, by L. B. Greszczuk. MDC, 1985. (Report no. DNA-TR-85-71-V2, report UNCLASSIFIED.)
8. National Aeronautics and Space Administration. Comparison of Graphite-Fabric-Reinforced PMR-15 and Avimid N Composites After Long Term Isothermal Aging at Various Temperatures, by K. J. Bowles, L. McCorkle, and L. Ingrahm. NASA. (NASA TM-107529, publication UNCLASSIFIED.)

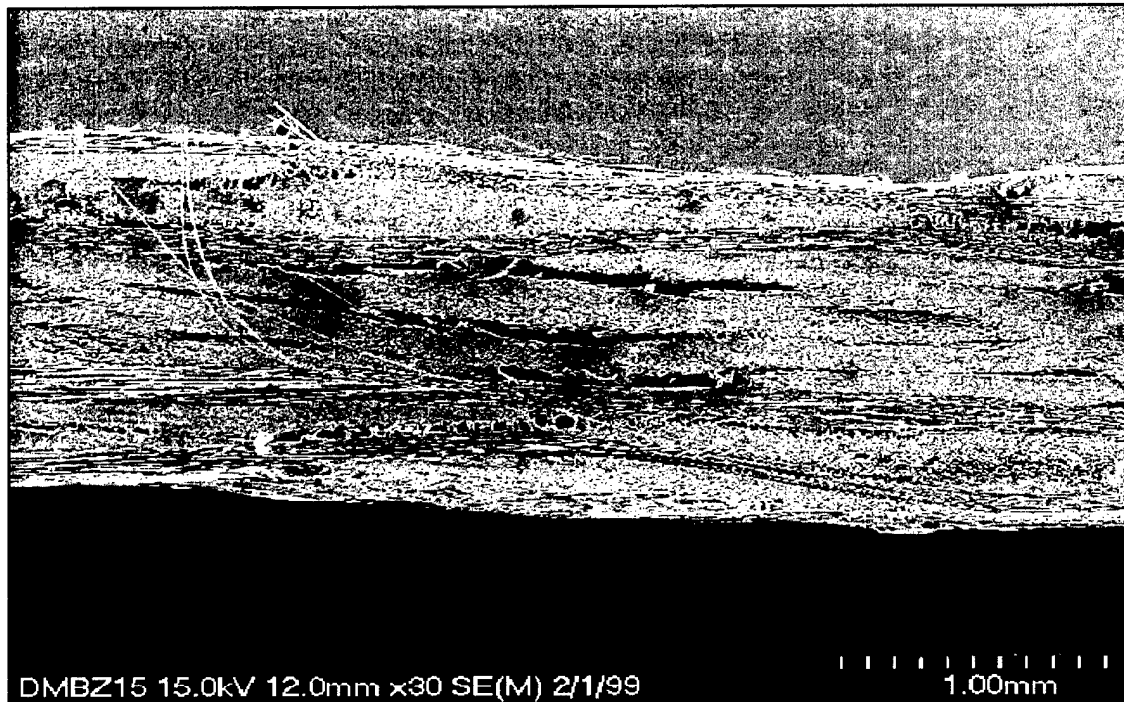


FIGURE 1. SEM (Cross Section) of IM7/DMBZ-15 Composite Panel Catastrophic Delamination After Rapid Heating.

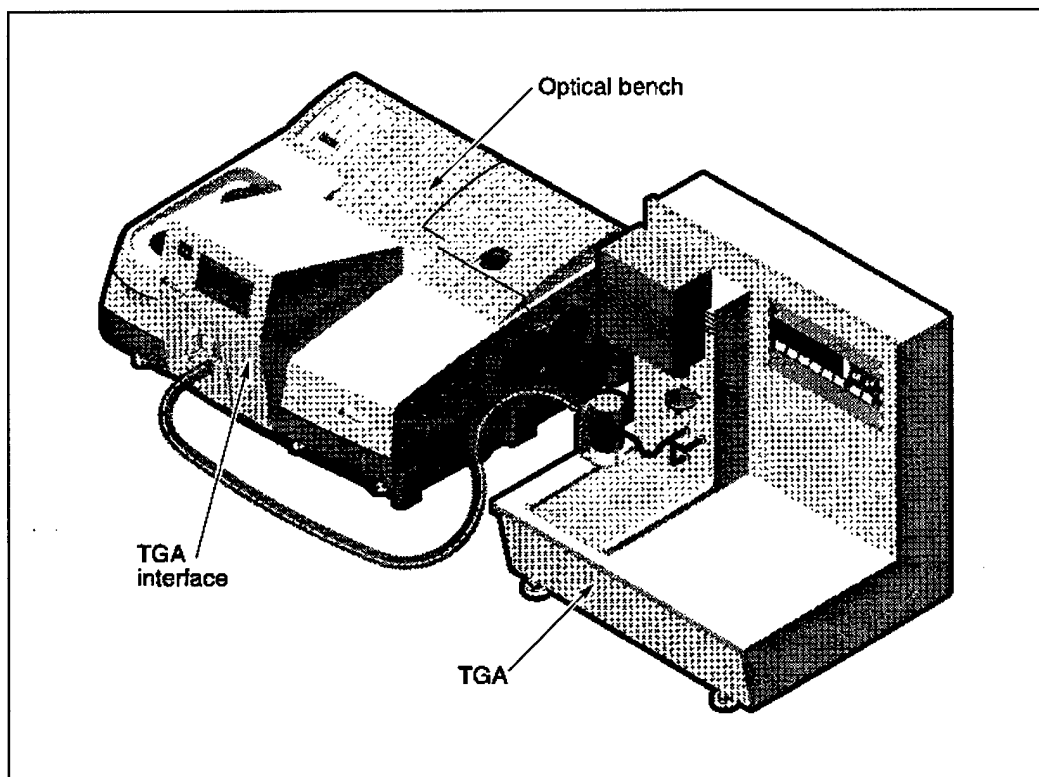


FIGURE 2. TGA/FTIR Setup.

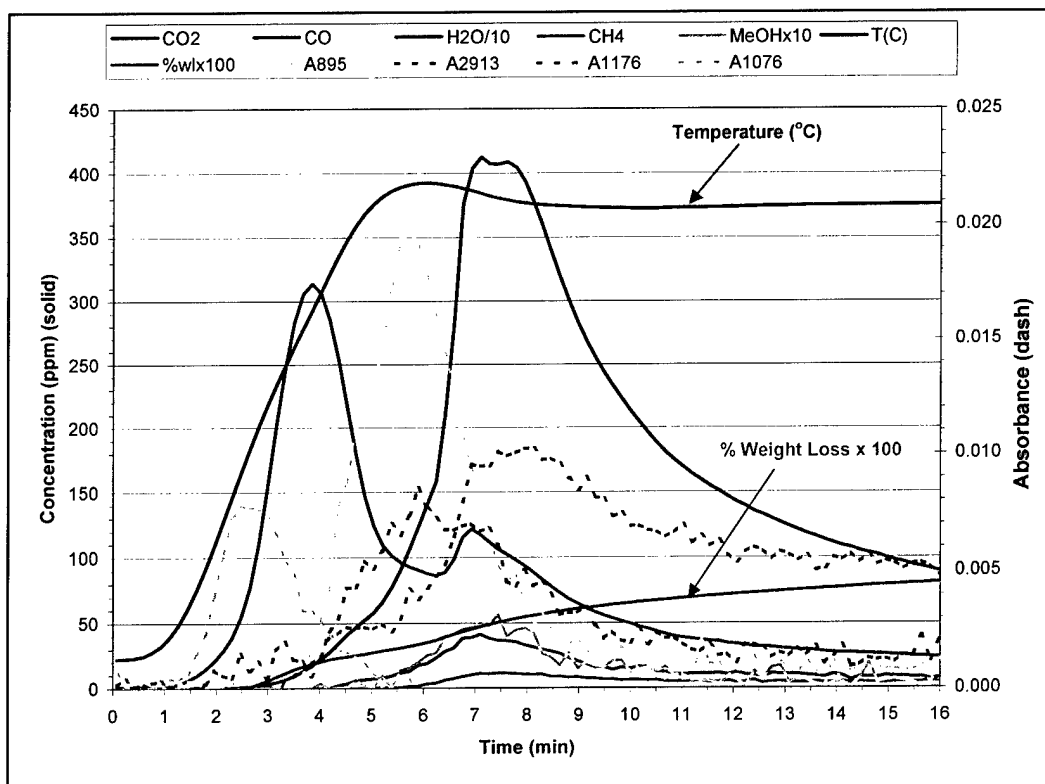


FIGURE 3. TGA/FTIR Results for Below-T<sub>g</sub> Run, R = 100°C/min, ISO = 375°C in N<sub>2</sub>.

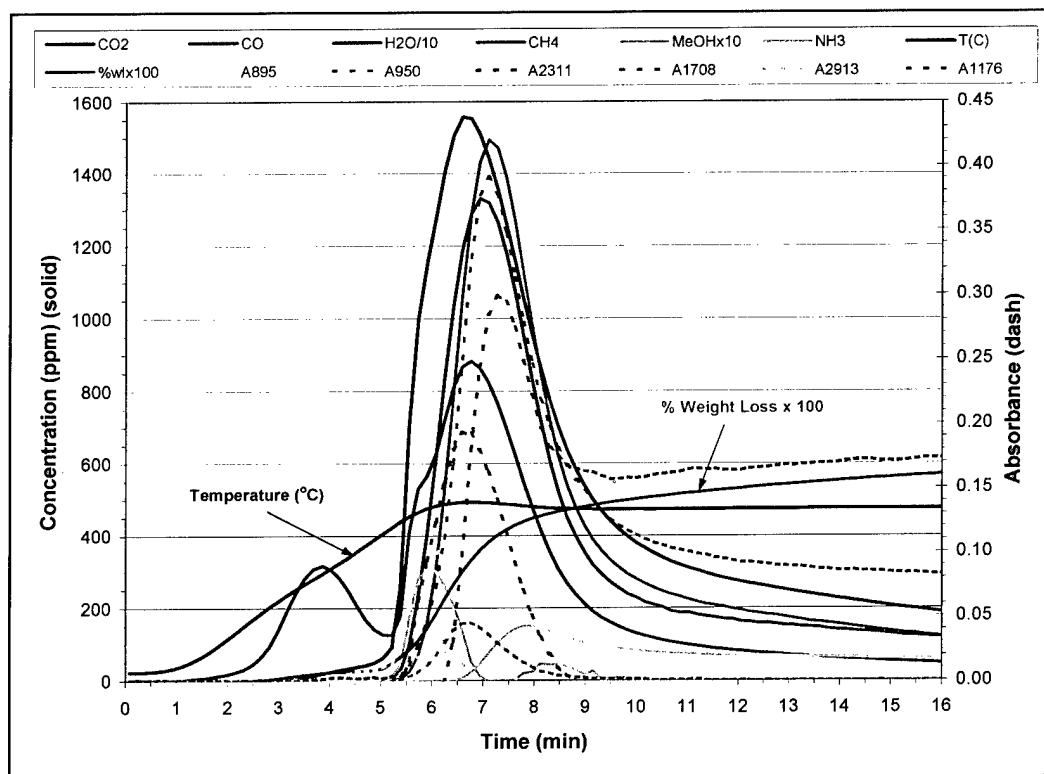


FIGURE 4. TGA/FTIR Results for Above-T<sub>g</sub> Run, R = 100°C/min, ISO = 475°C, in N<sub>2</sub>.



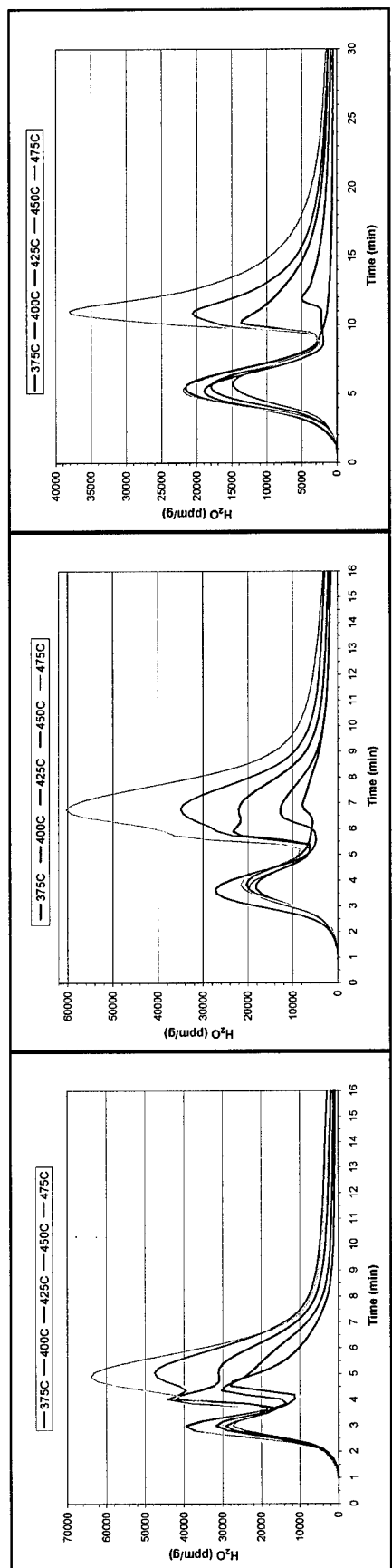


FIGURE 5. H<sub>2</sub>O (ppm/g) From IM7/DMBZ-15 Composite at ISO = 375 to 475°C in N<sub>2</sub>.  
Left R = 150°C/min, Middle R = 100°C/min, and Right R = 50°C/min.

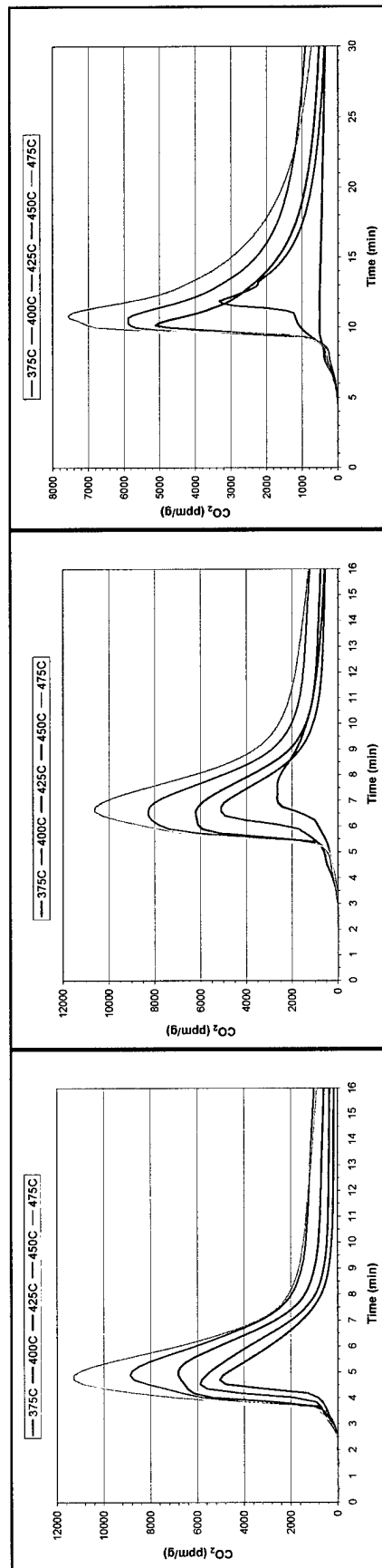


FIGURE 6. CO<sub>2</sub> (ppm/g) From IM7/DMBZ-15 Composite at ISO = 375 to 475°C in N<sub>2</sub>.  
Left R = 150°C/min, Middle R = 100°C/min, and Right R = 50°C/min.

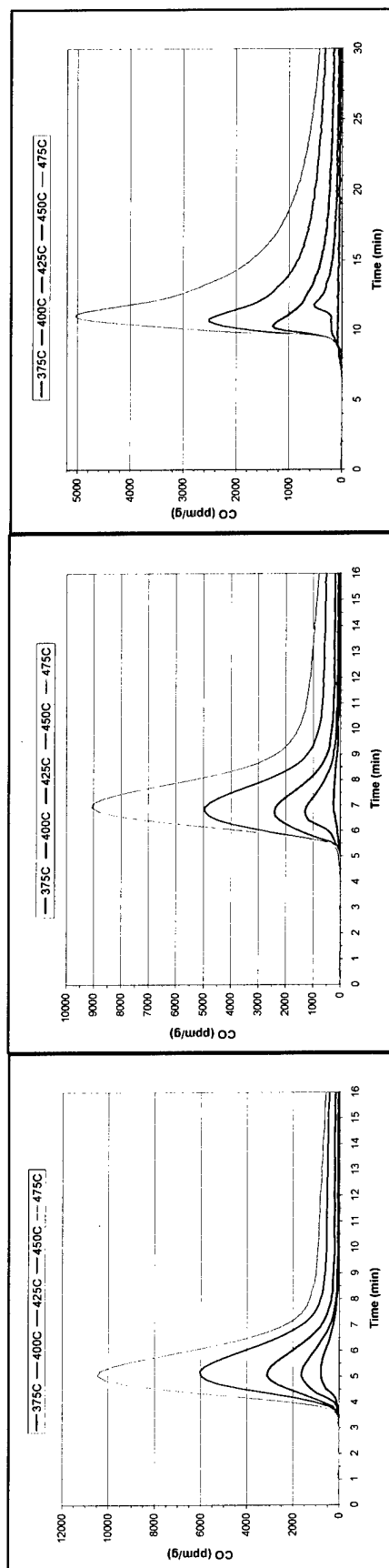


FIGURE 7. CO (ppm/g) From IM7/DMBZ-15 Composite at ISO = 375 to 475°C in N<sub>2</sub>  
 Left R = 150°C/min, Middle R = 100°C/min, and Right R = 50°C/min.

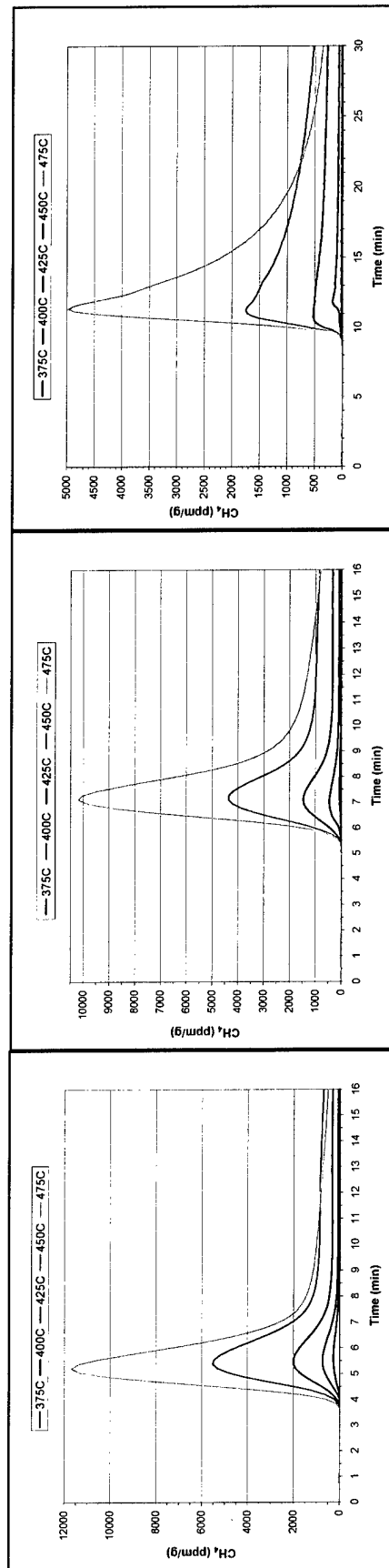


FIGURE 8. CH<sub>4</sub> (ppm/g) From IM7/DMBZ-15 Composite at ISO = 375 to 475°C in N<sub>2</sub>  
 Left R = 150°C/min, Middle R = 100°C/min, and Right R = 50°C/min.

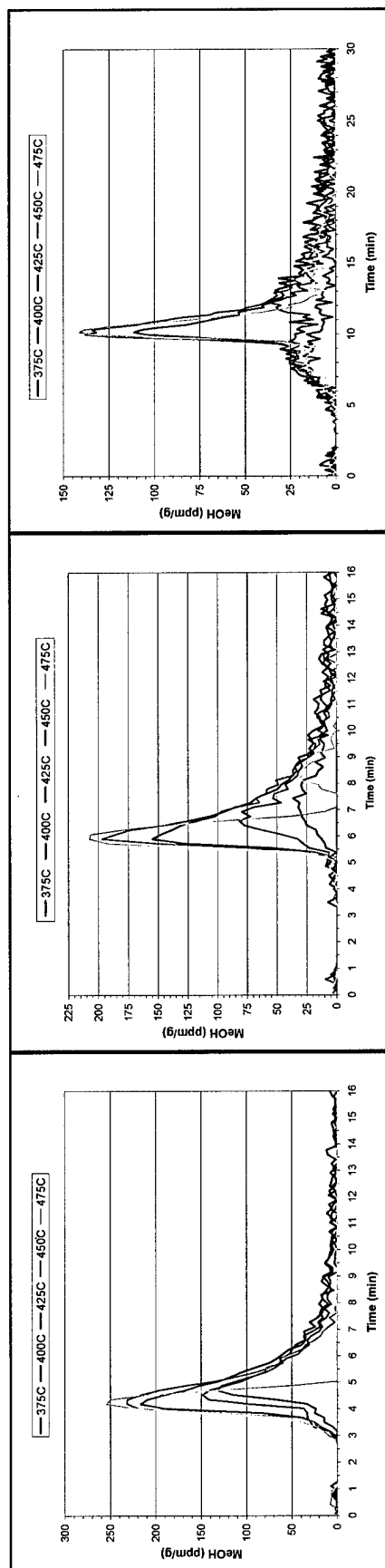


FIGURE 9. MeOH (ppm/g) From IM7/DMBZ-15 Composite at ISO = 375 to 475°C in N<sub>2</sub>.  
Left R = 150°C/min, Middle R = 100°C/min, and Right R = 50°C/min.

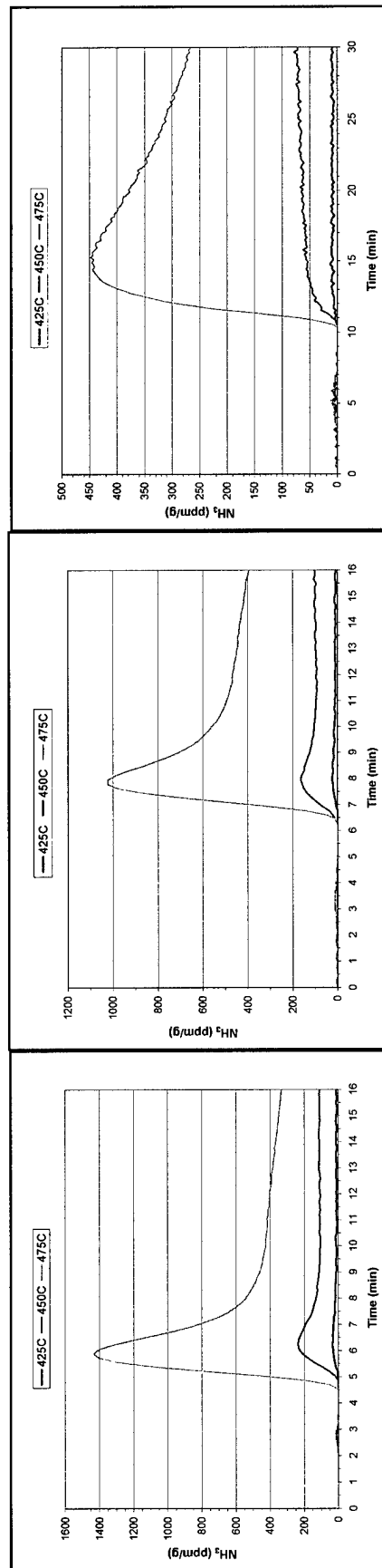


FIGURE 10. NH<sub>3</sub> (ppm/g) From IM7/DMBZ-15 Composite at ISO = 375 to 475°C in N<sub>2</sub>.  
Left R = 150°C/min, Middle R = 100°C/min, and Right R = 50°C/min.

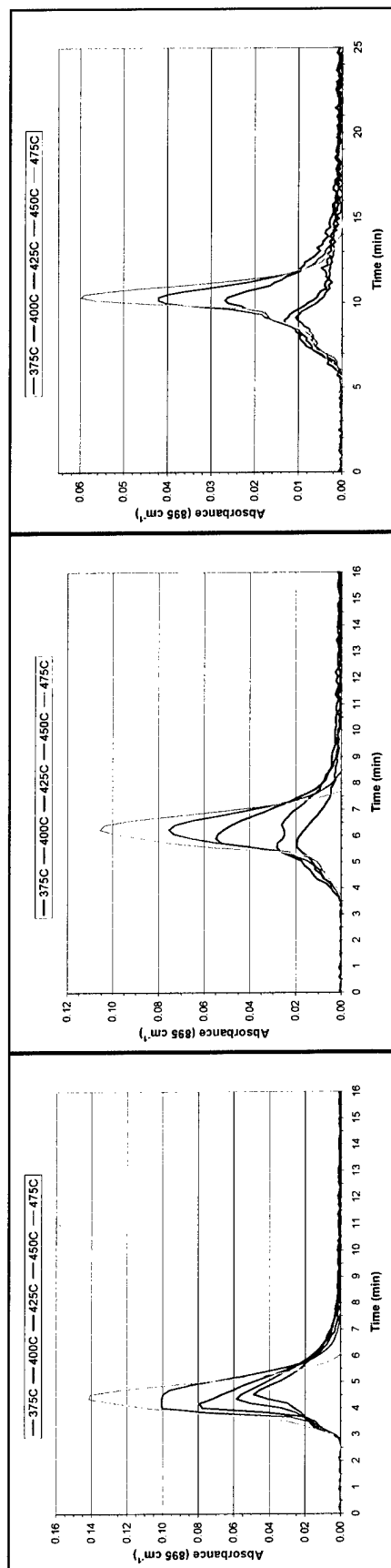


FIGURE 11. A(895  $\text{cm}^{-1}$ ) From IM7/DMBZ-15 Composite at ISO = 375 to 475°C in  $\text{N}_2$ .  
Left R = 150°C/min, Middle R = 100°C/min, and Right R = 50°C/min.

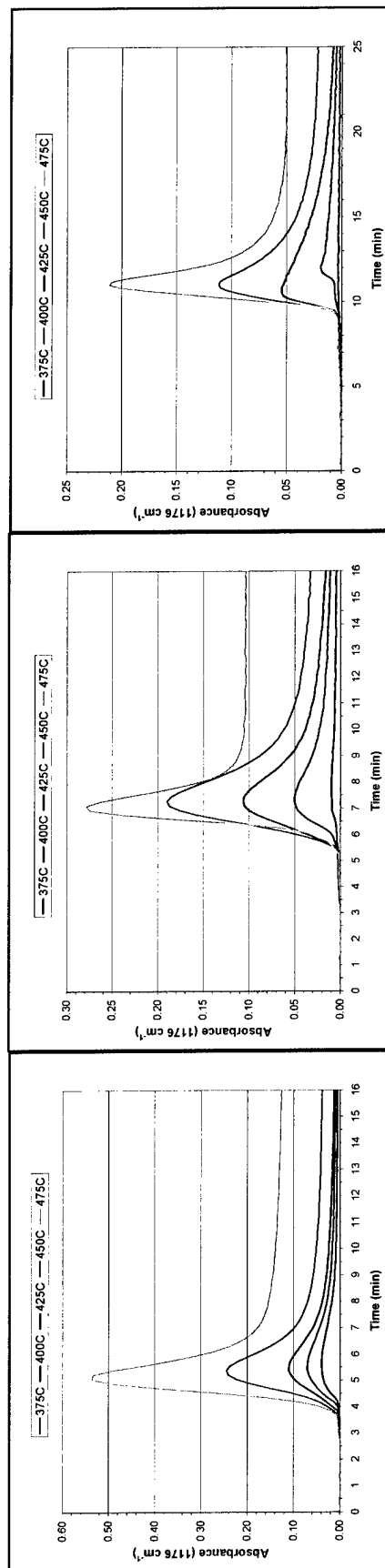


FIGURE 12. A(1,176  $\text{cm}^{-1}$ ) From IM7/DMBZ-15 Composite at ISO = 375 to 475°C in  $\text{N}_2$ .  
Left R = 150°C/min, Middle R = 100°C/min, and Right R = 50°C/min.

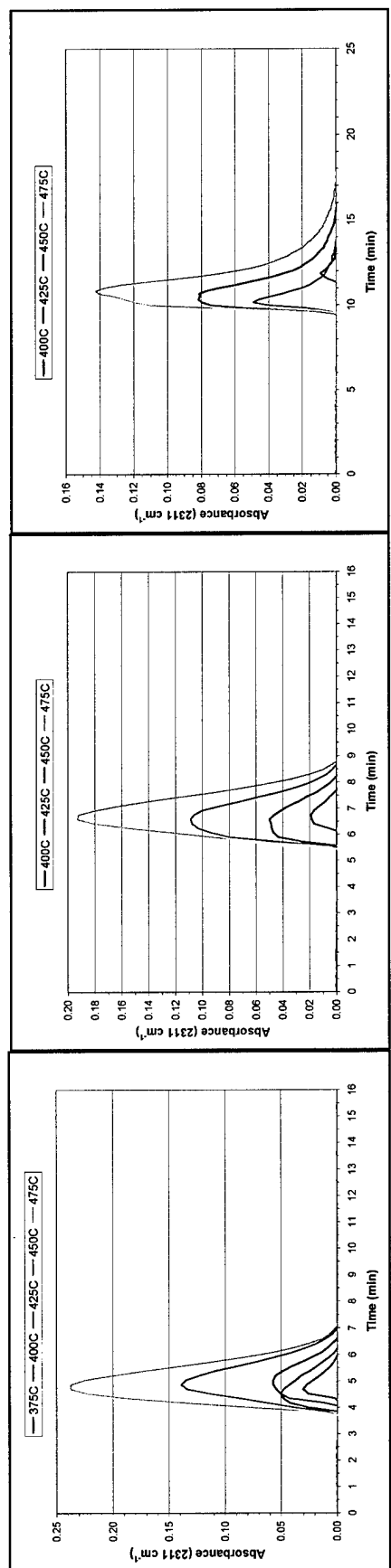


FIGURE 13. A( $2,311\text{ cm}^{-1}$ ) From IM7/DMBZ-15 Composite at ISO = 375 to 475°C in  $\text{N}_2$ .  
Left R = 150°C/min, Middle R = 100°C/min, and Right R = 50°C/min.

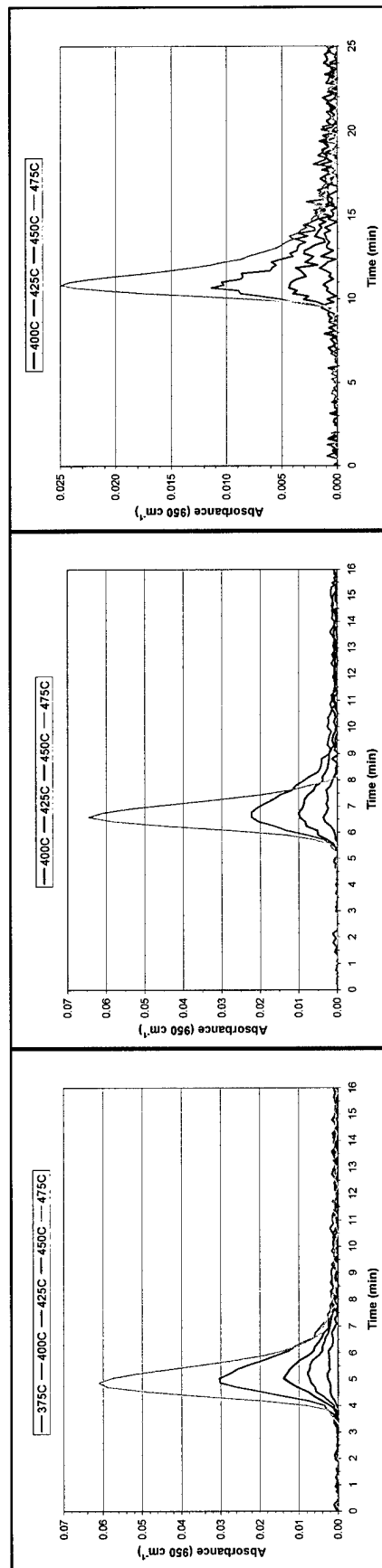


FIGURE 14. A( $950\text{ cm}^{-1}$ ) From IM7/DMBZ-15 Composite at ISO = 375 to 475°C in  $\text{N}_2$ .  
Left R = 150°C/min, Middle R = 100°C/min, and Right R = 50°C/min.

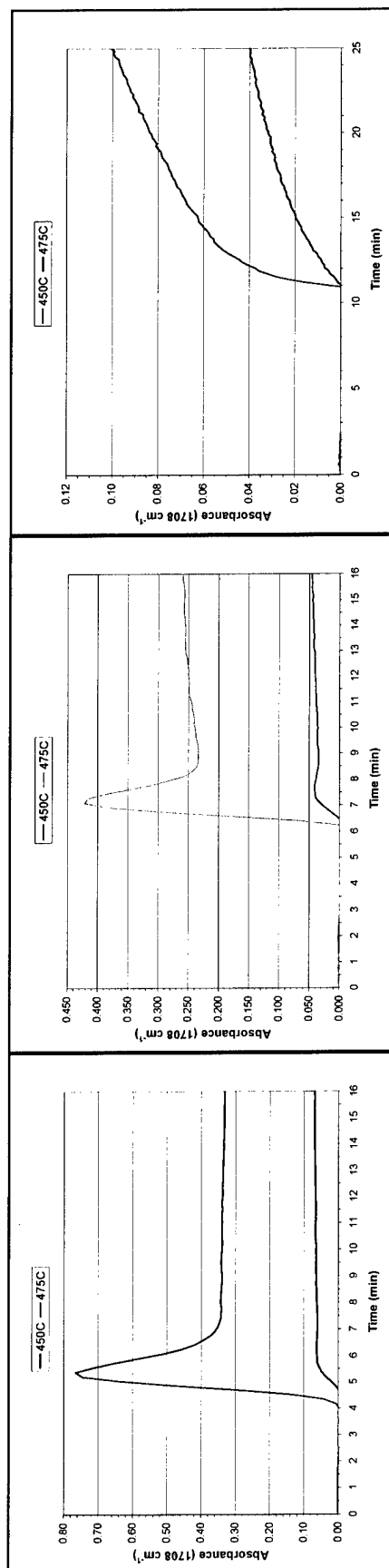


FIGURE 15.  $A(1,708\text{ cm}^{-1})$  From IM7/DMBZ-15 Composite at ISO = 375 to 475°C in  $\text{N}_2$ .  
Left R = 150°C/min, Middle R = 100°C/min, and Right R = 50°C/min.

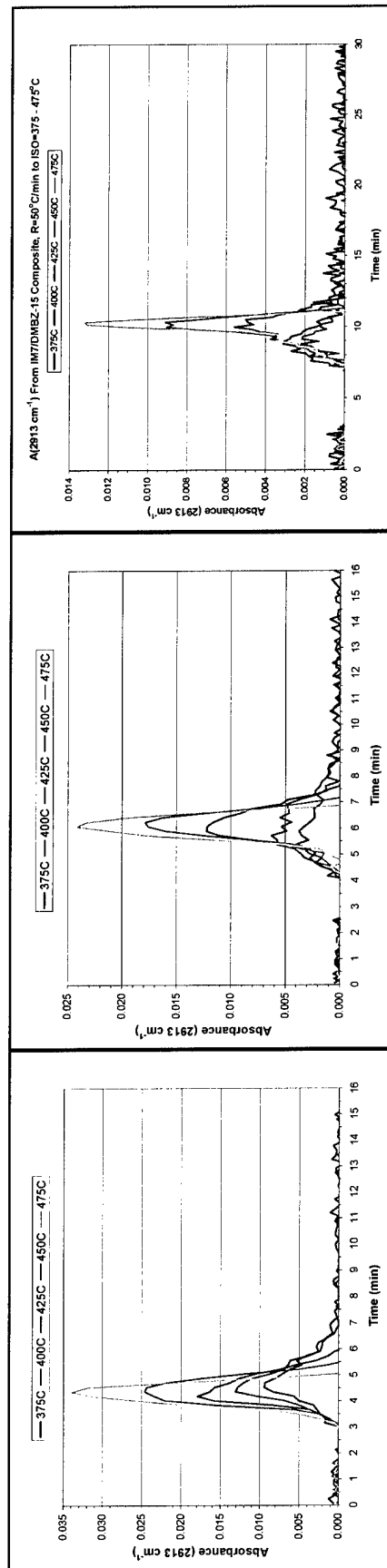


FIGURE 16.  $A(2,913\text{ cm}^{-1})$  From IM7/DMBZ-15 Composite at ISO = 375 to 475°C in  $\text{N}_2$ .  
Left R = 150°C/min, Middle R = 100°C/min, and Right R = 50°C/min.

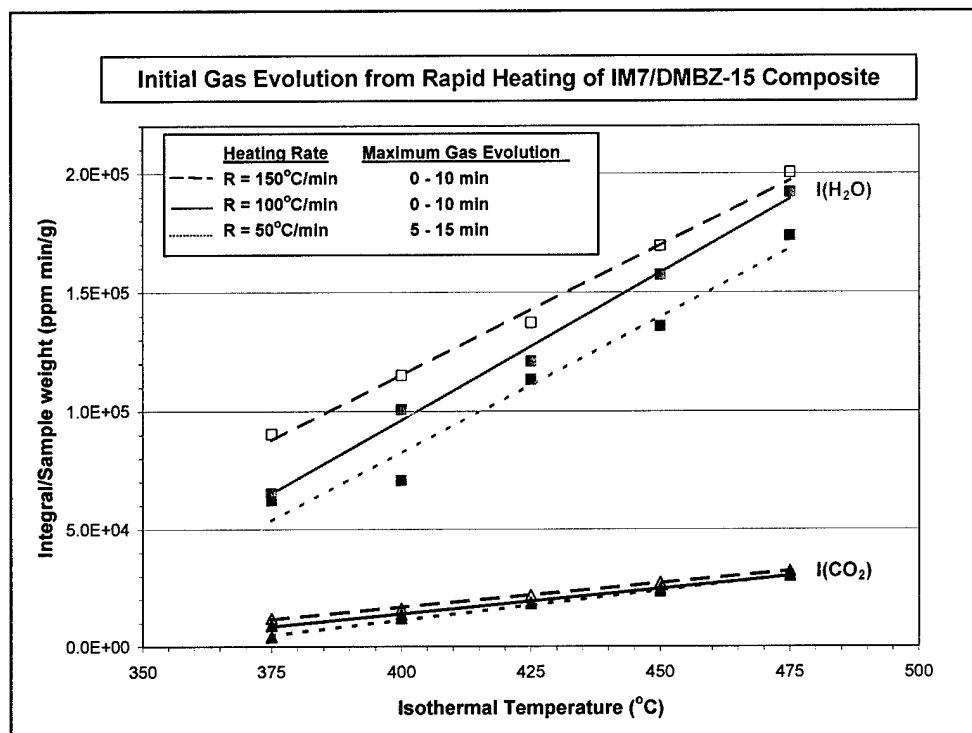


FIGURE 17. Integrated CO<sub>2</sub> and H<sub>2</sub>O (ppm min/g) During Maximum Gas Evolution Versus ISO at R = 150, 100, and 50°C/min for IM7/DMBZ-15 Composite in N<sub>2</sub>.

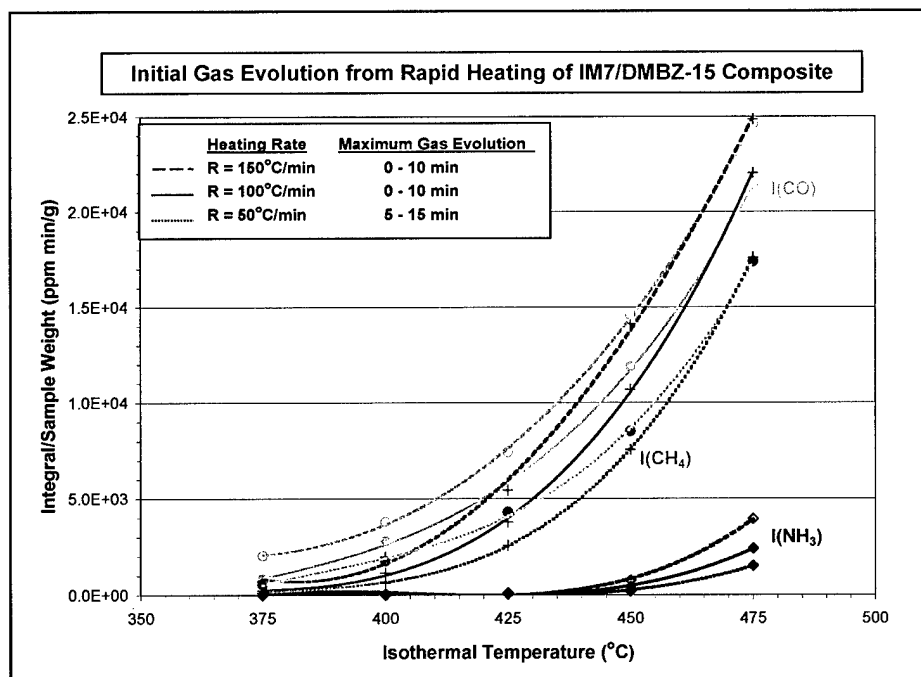


FIGURE 18. Integrated CO, CH<sub>4</sub>, and NH<sub>3</sub> (ppm min/g) During Maximum Gas Evolution Versus ISO at R = 150, 100, and 50°C/min for IM7/DMBZ-15 Composite in N<sub>2</sub>.

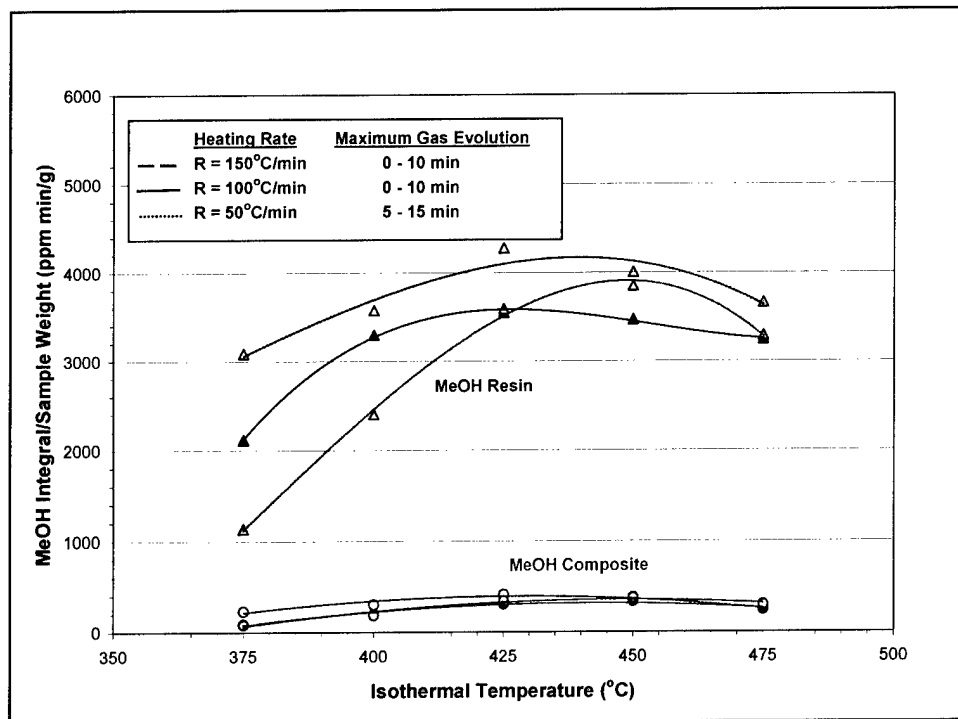


FIGURE 19. MeOH During Maximum Gas Evolution (ppm min/g) for IM7/DMBZ-15 Composite and DMBZ-15 Resin Versus ISO at R = 150, 100, and 50°C/min in N<sub>2</sub>.

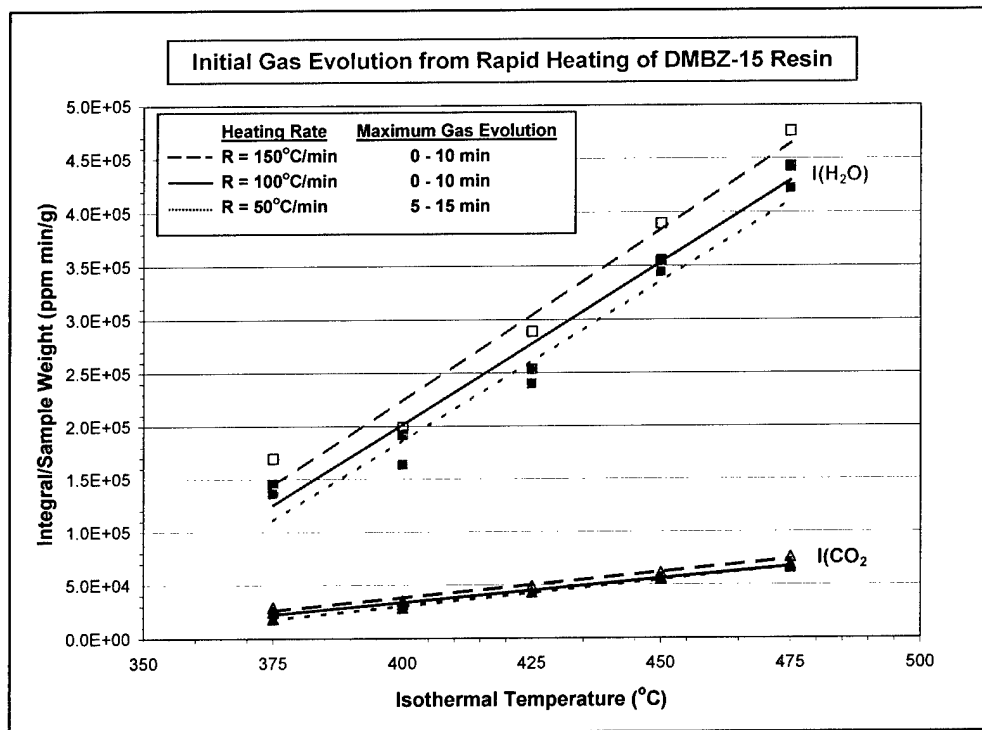


FIGURE 20. H<sub>2</sub>O and CO<sub>2</sub> During Maximum Gas Evolution (ppm min/g) for DMBZ-15 Resin Versus ISO at R = 150, 100, and 50°C/min in N<sub>2</sub>.



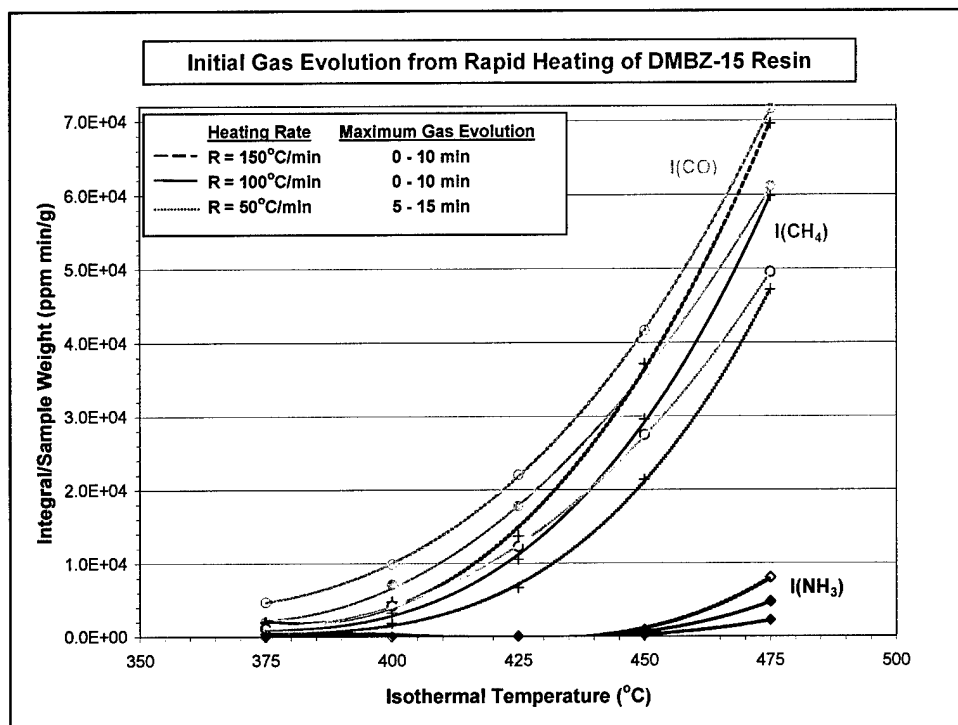


FIGURE 21. CO, CH<sub>4</sub>, and NH<sub>3</sub> (ppm min/g) During Maximum Gas Evolution Versus ISO at R = 150, 100, and 50°C/min for DMBZ-15 Resin in N<sub>2</sub>.

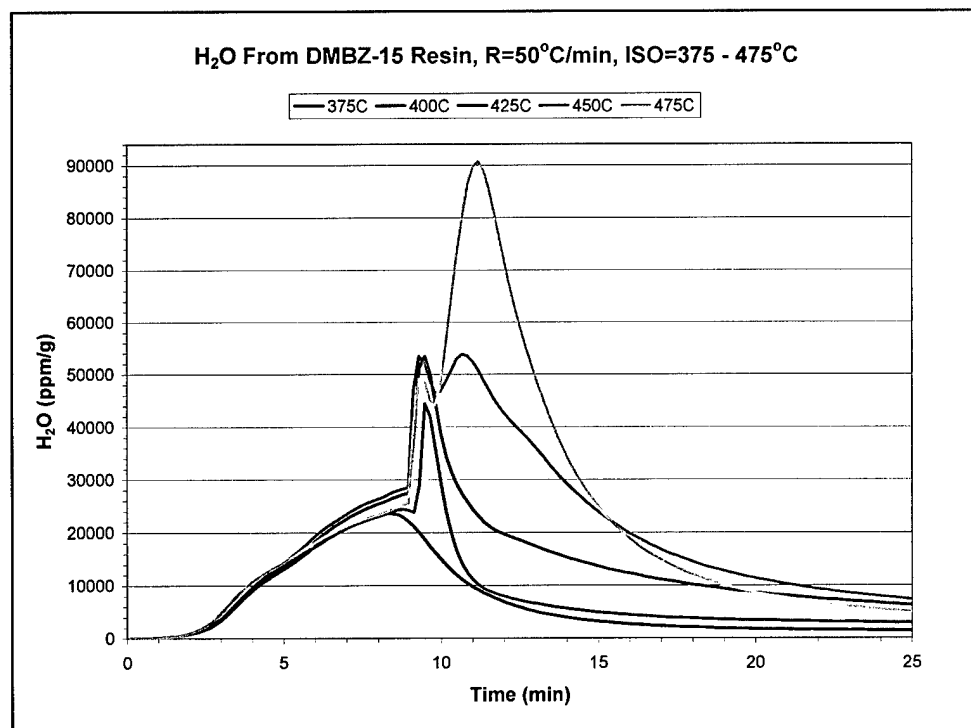


FIGURE 22. H<sub>2</sub>O (ppm/g) From DMBZ-15 Resin at R = 50°C/min, ISO = 375 to 475°C, and in N<sub>2</sub>.

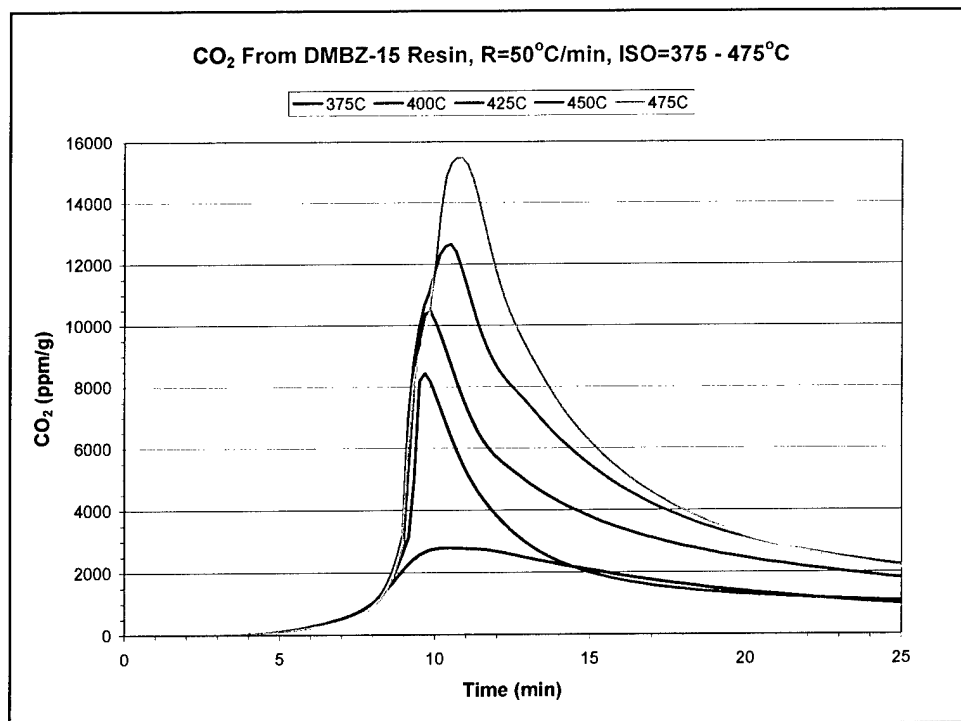


FIGURE 23. CO<sub>2</sub> (ppm/g) From DMBZ-15 Resin at R = 50°C/min, ISO = 375 to 475°C, and in N<sub>2</sub>.

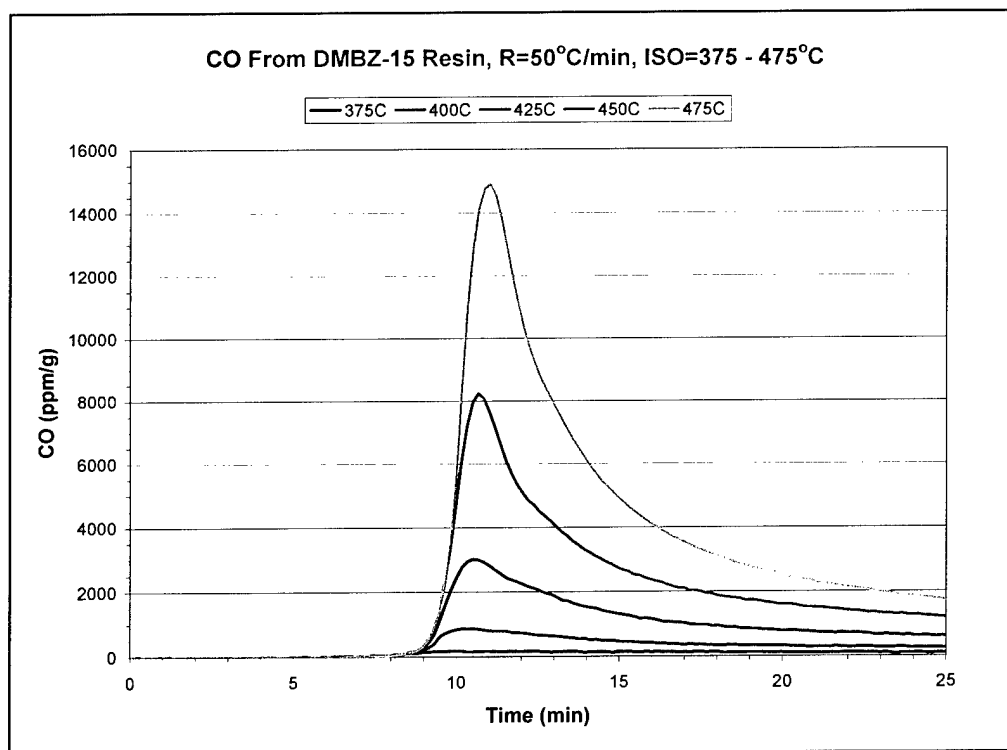


FIGURE 24. CO (ppm/g) From DMBZ-15 Resin at R = 50°C/min, ISO = 375 to 475°C, and in N<sub>2</sub>.

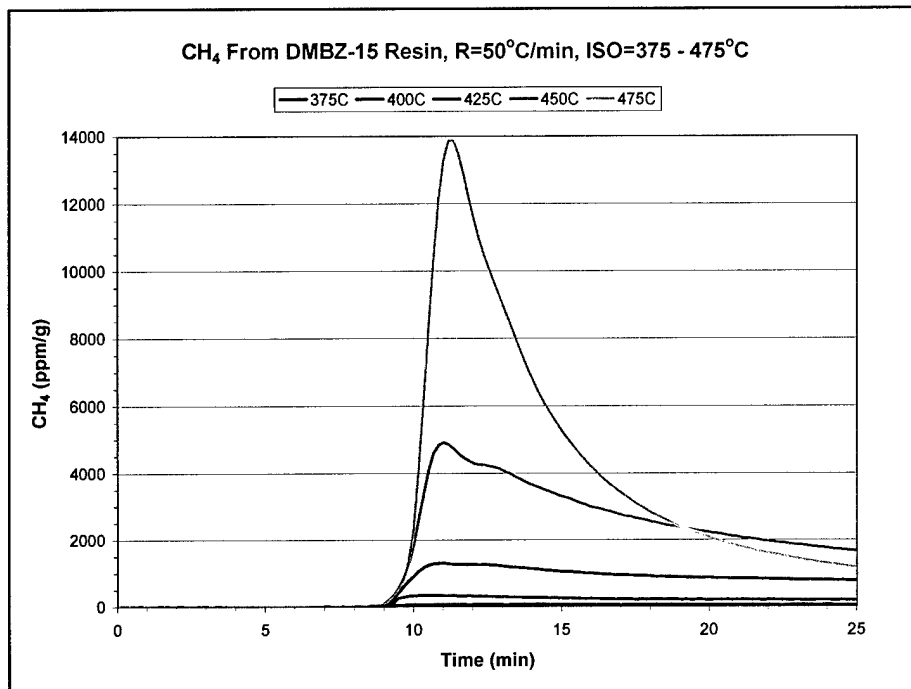


FIGURE 25. CH<sub>4</sub> (ppm/g) From DMBZ-15 Resin at R = 50°C/min, ISO = 375 to 475°C, and in N<sub>2</sub>.

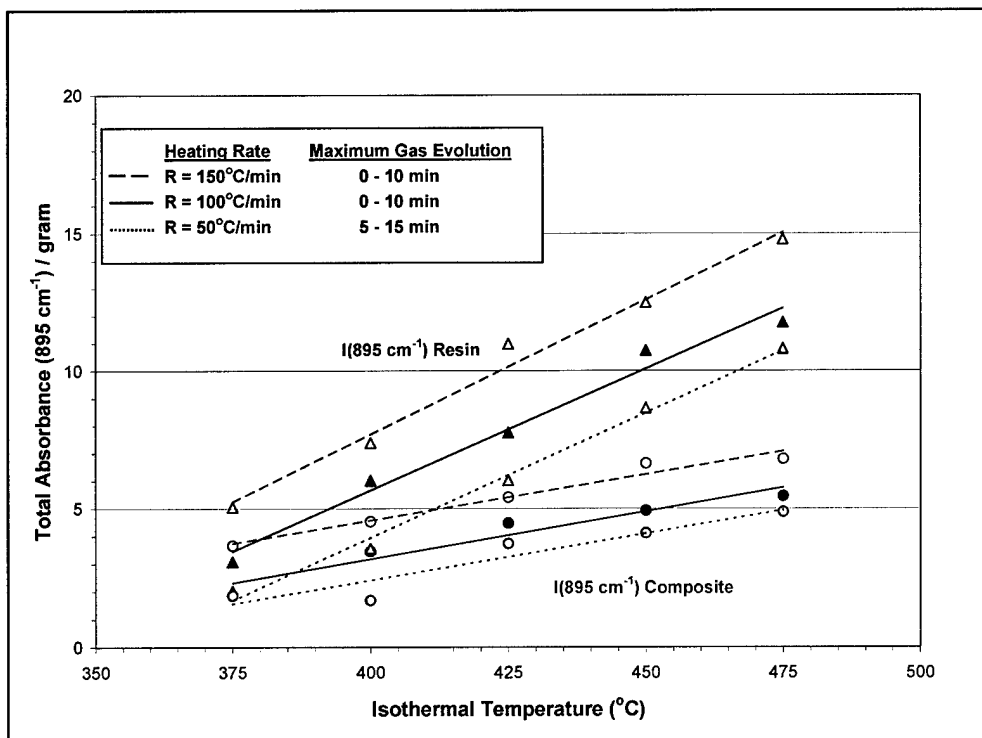


FIGURE 26. Total A(895 cm<sup>-1</sup>)/g During Maximum Gas Evolution Versus ISO and R for Composite and Resin in N<sub>2</sub>.

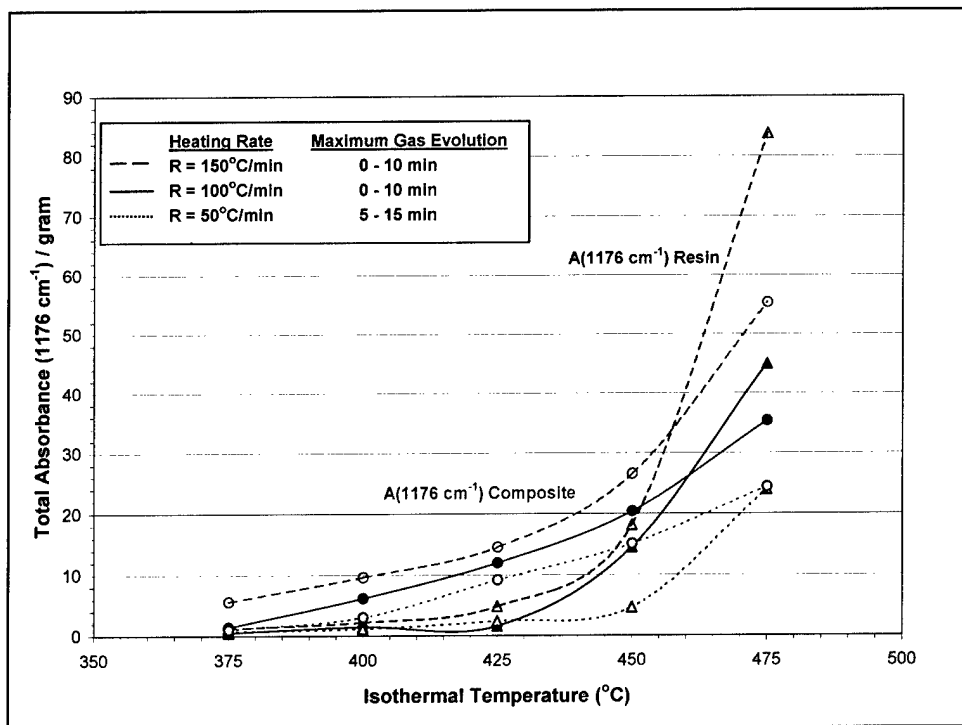


FIGURE 27. Total A(1,176 cm<sup>-1</sup>)/g During Maximum Gas Evolution Versus ISO and R for Composite and Resin in N<sub>2</sub>.

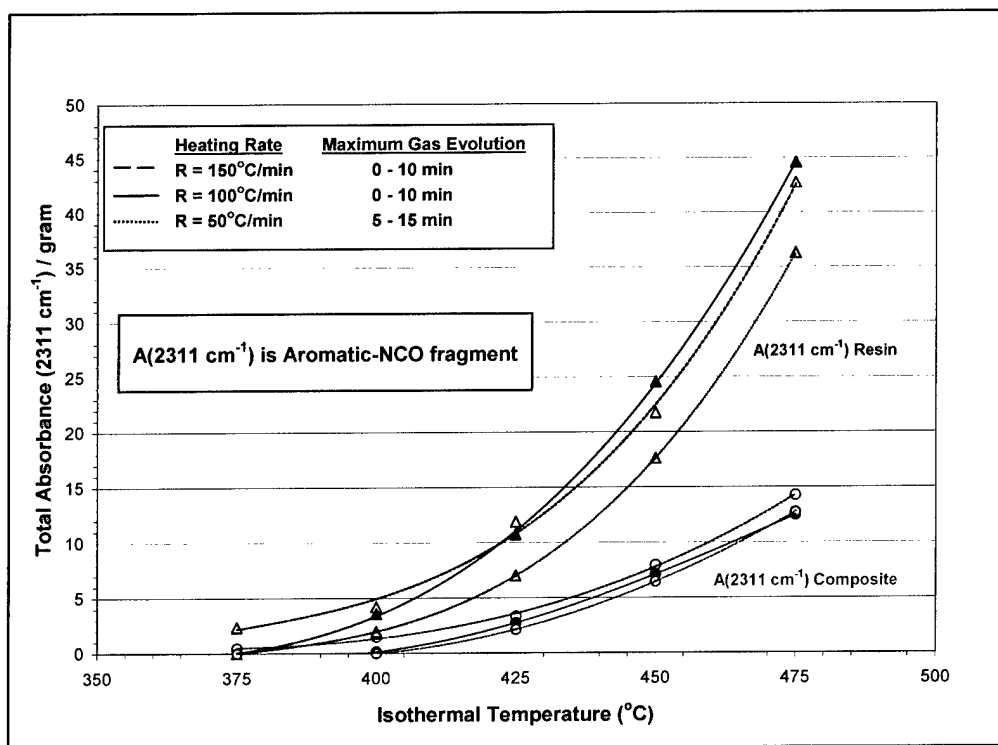


FIGURE 28. Total A(2,311 cm<sup>-1</sup>)/g During Maximum Gas Evolution Versus ISO and R for Composite and Resin in N<sub>2</sub>.

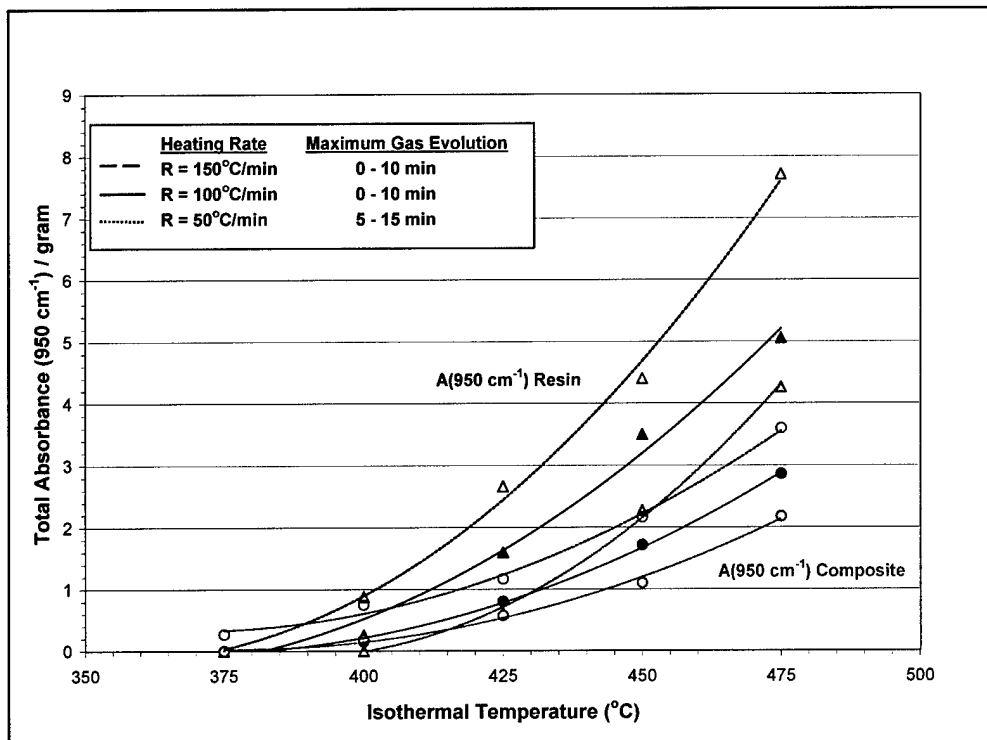


FIGURE 29. Total  $A(950\text{ cm}^{-1})/\text{g}$  During Maximum Gas Evolution Versus ISO and R for Composite and Resin in  $\text{N}_2$ .

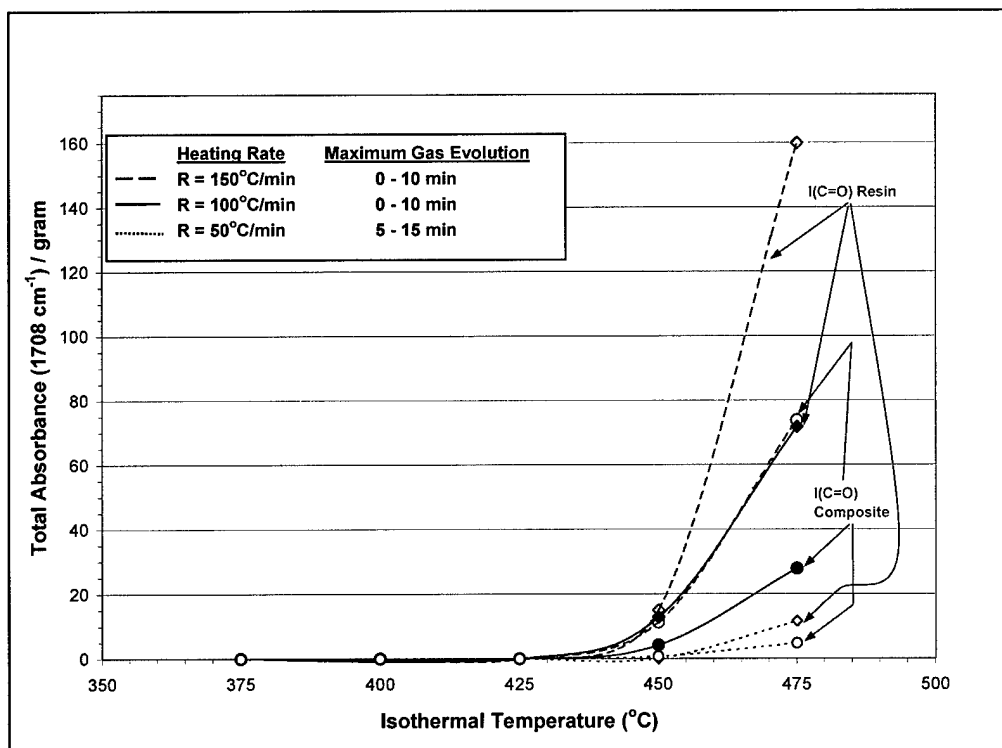


FIGURE 30. Total  $A(1,708\text{ cm}^{-1})/\text{g}$  During Maximum Gas Evolution Versus ISO and R for Composite and Resin in  $\text{N}_2$ .

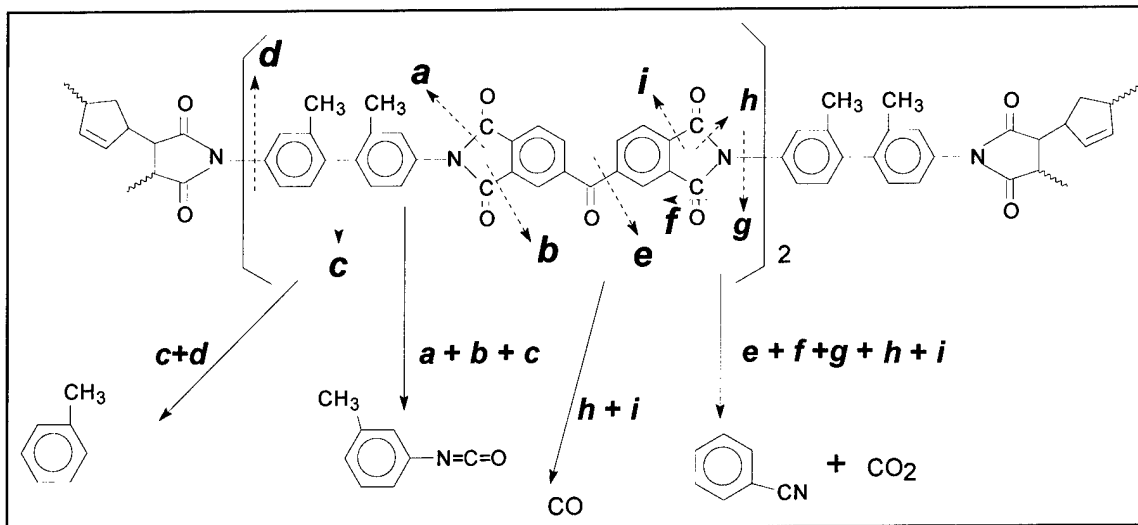


FIGURE 31. DMBZ-15 Resin Thermal Degradation Pathways and Potential Products (Reference 5).

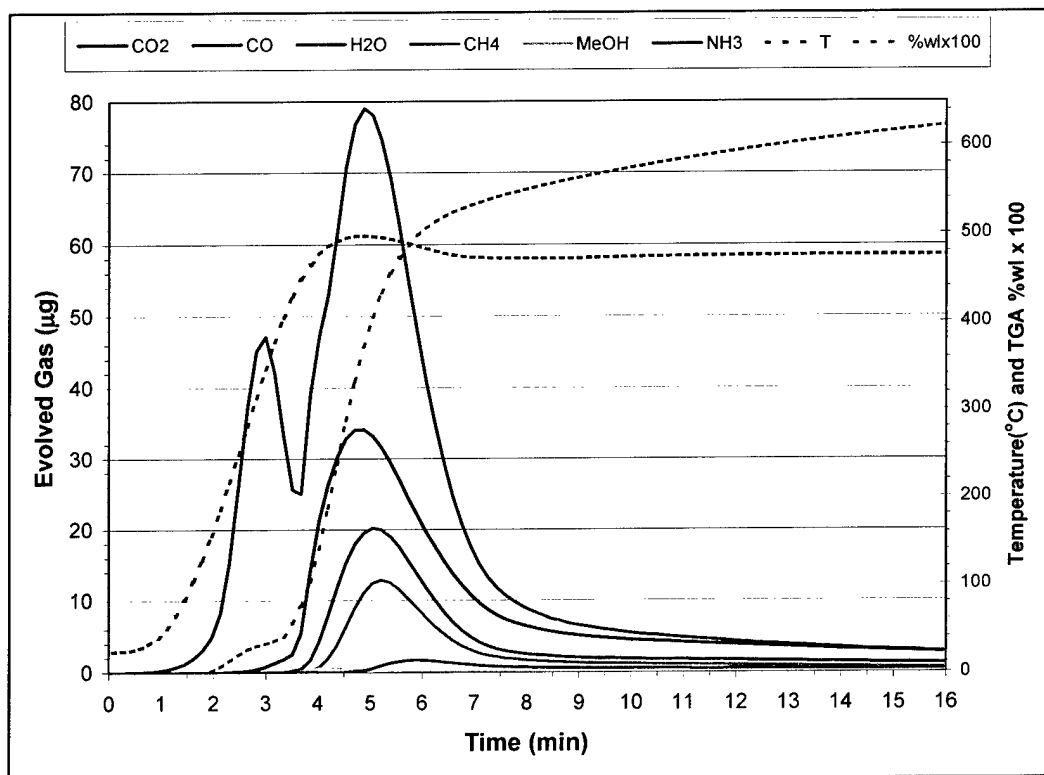


FIGURE 32. Quantified Species in µg, % Weight Loss, and T (°C) Versus Time; R = 150°C/min, ISO = 475°C in N<sub>2</sub> for IM7/DMBZ-15 Composite.

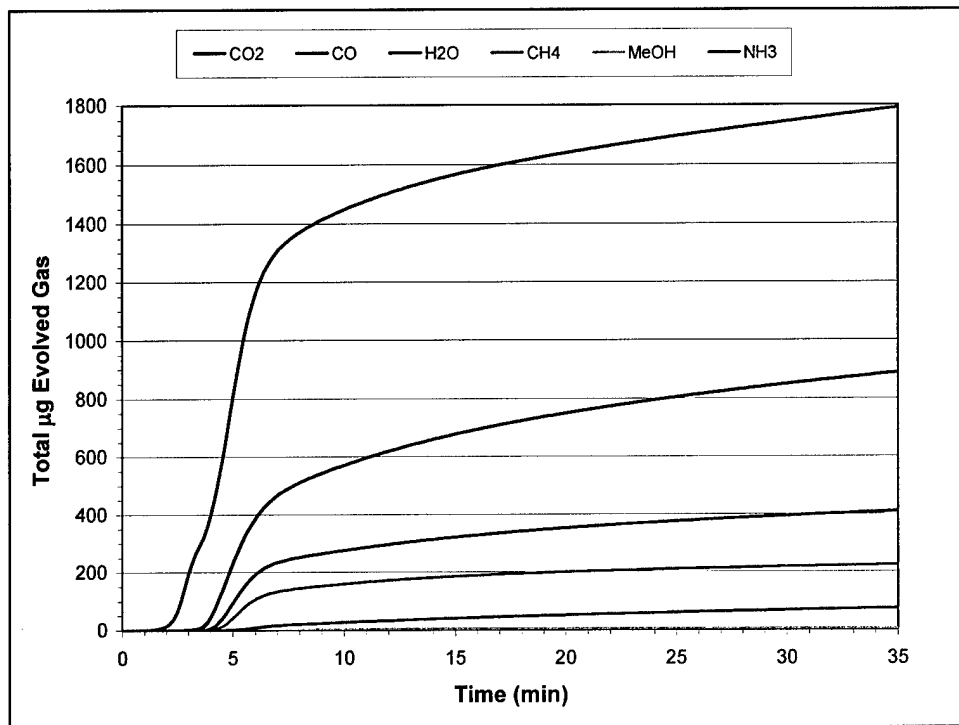


FIGURE 33. Total µg of Each Quantified Species; R = 150°C/min, ISO = 475°C in N<sub>2</sub> for IM7/DMBZ-15 Composite.

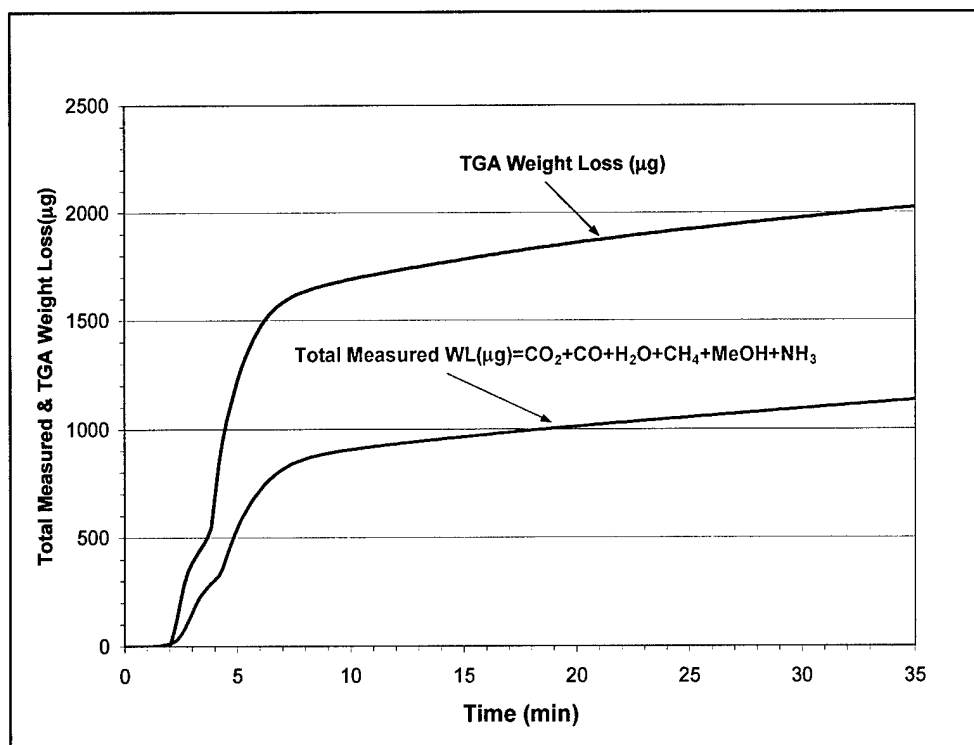


FIGURE 34. Composite TGA Weight Loss and Total Measured Weight Loss in µg; R = 150°C/min, ISO = 375°C, and in N<sub>2</sub>.

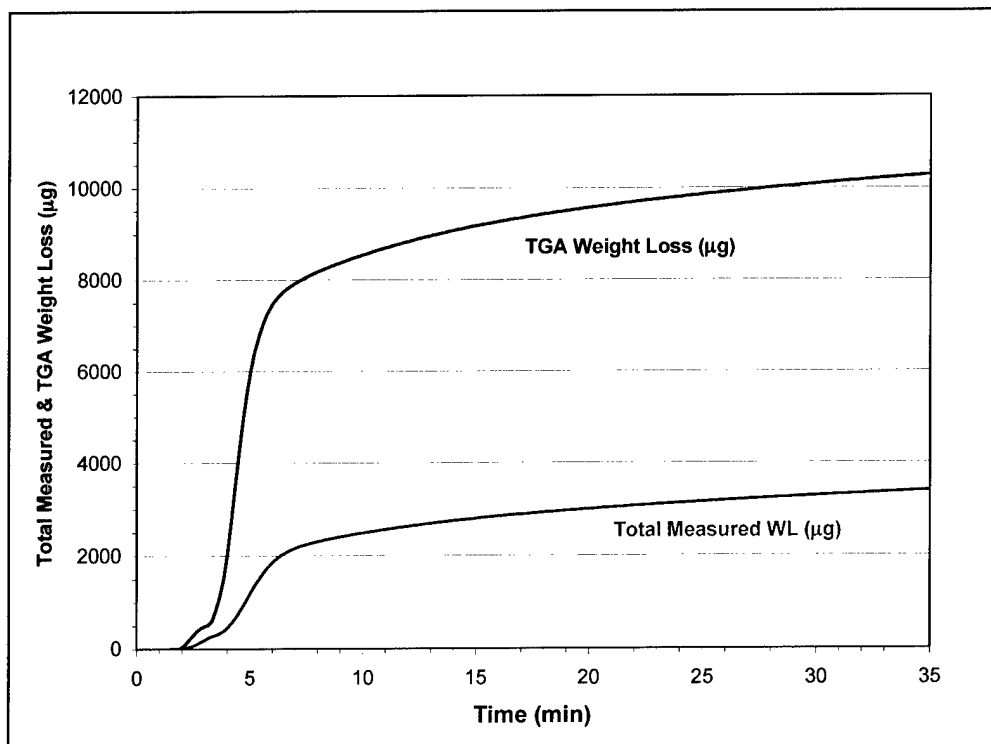


FIGURE 35. Composite TGA Weight Loss and Total Measured Weight Loss in  $\mu\text{g}$ ;  $R = 150^\circ\text{C}/\text{min}$ ,  $\text{ISO} = 475^\circ\text{C}$ , and in  $\text{N}_2$ .

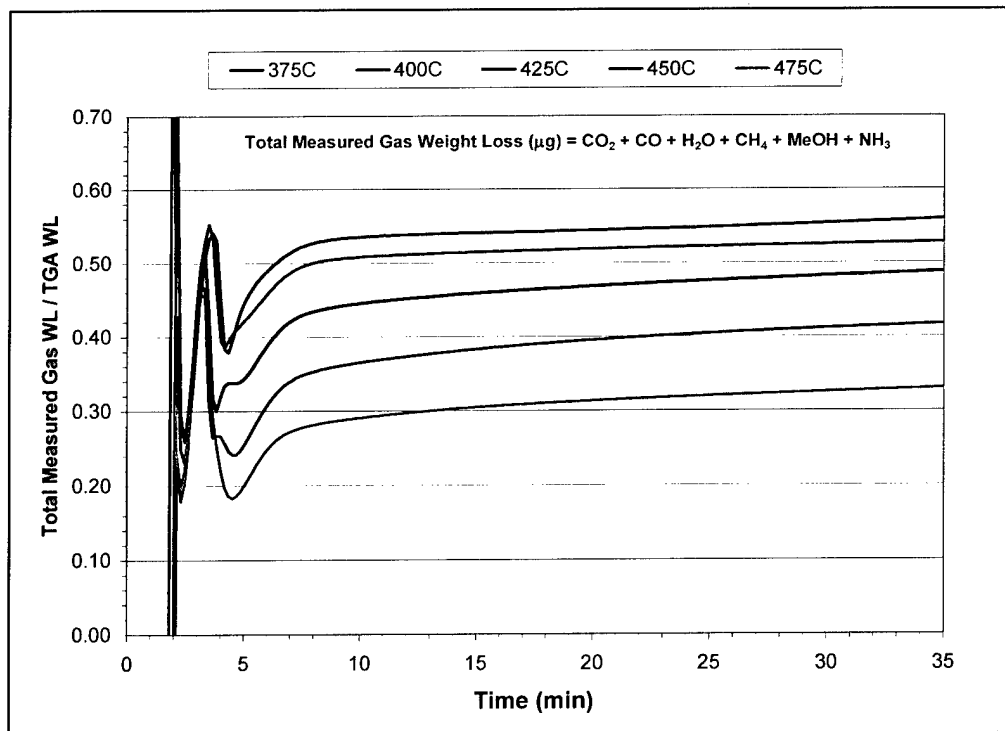


FIGURE 36. Composite Total Measured Weight Loss ( $\mu\text{g}$ ) / TGA Weight Loss ( $\mu\text{g}$ );  $R = 150^\circ\text{C}/\text{min}$  in  $\text{N}_2$  for  $\text{ISO} = 375$  to  $475^\circ\text{C}$ .



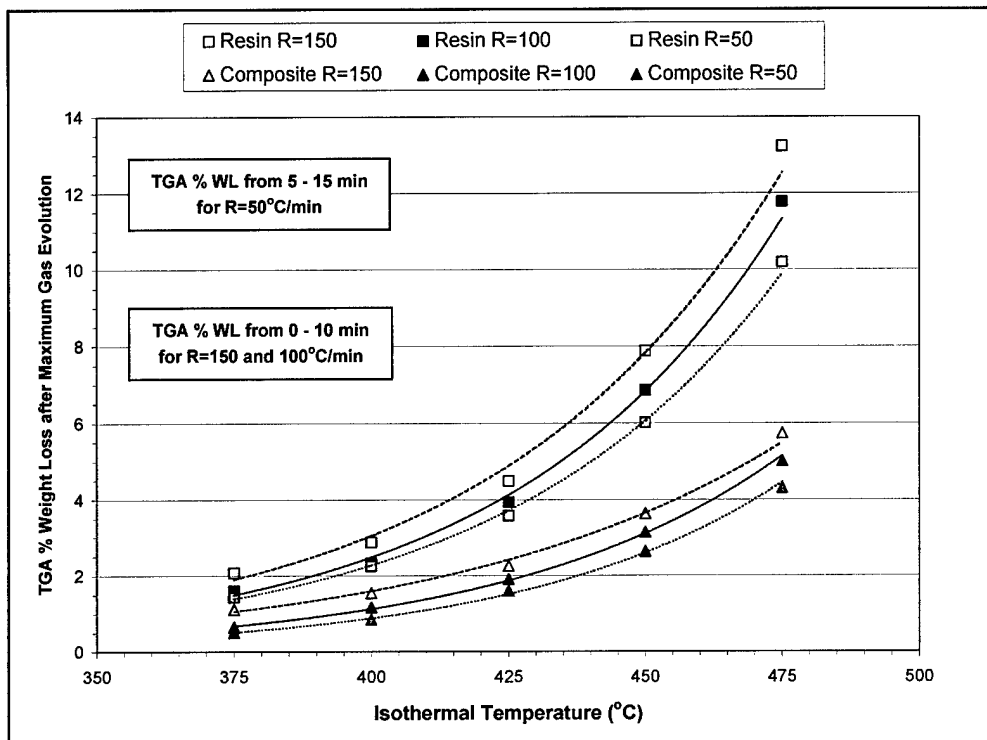


FIGURE 37. TGA % Weight Loss After Maximum Gas Evolution Versus Isothermal Temperature (ISO = 375 to 475°C).

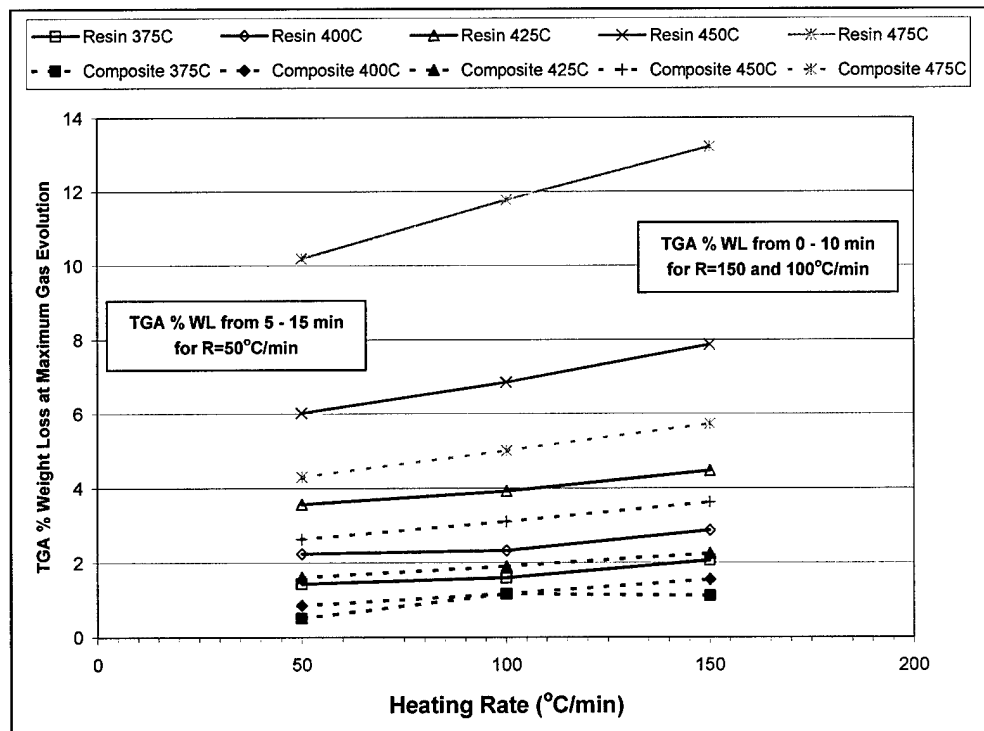


FIGURE 38. TGA % Weight Loss After Maximum Gas Evolution Versus Heating Rate (R = 50, 100, and 150°C/min).

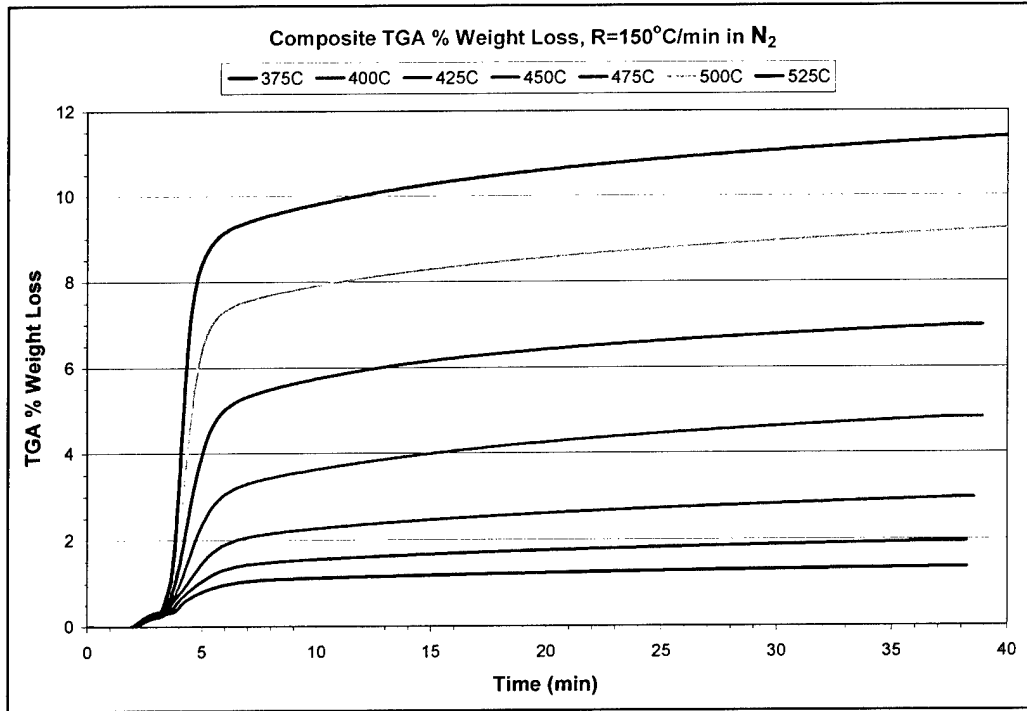


FIGURE 39. TGA % Weight Loss for Composite at R = 150°C/min From ISO = 375 to 525°C in N<sub>2</sub>.

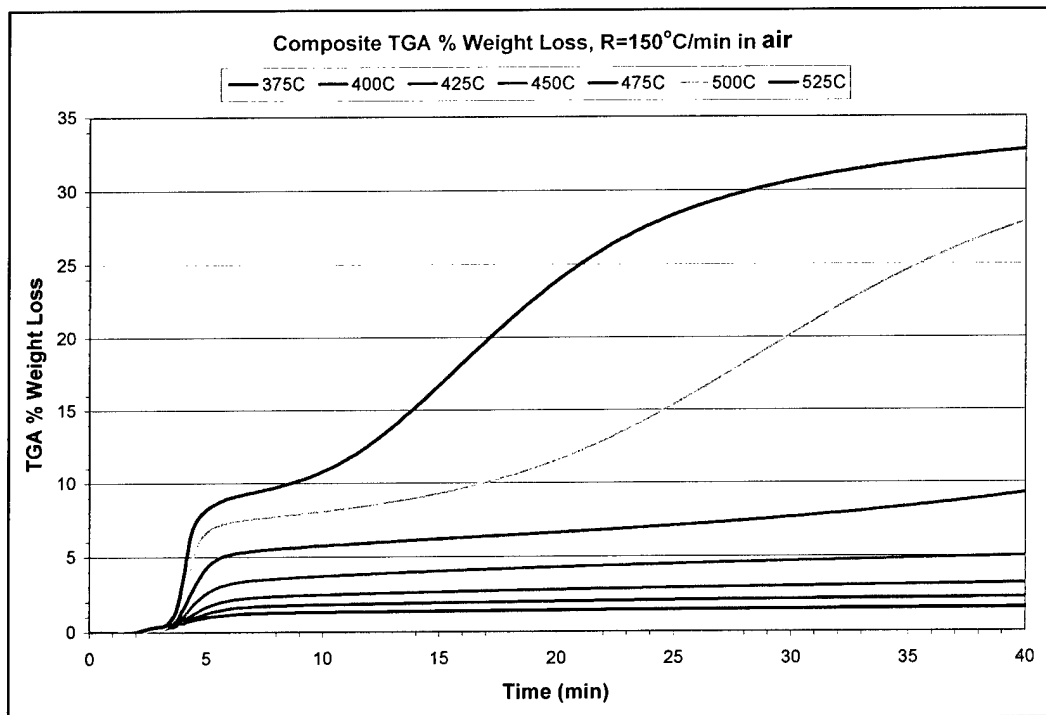


FIGURE 40. TGA % Weight Loss for Composite at R = 150°C/min From ISO = 375 to 525°C in Air.

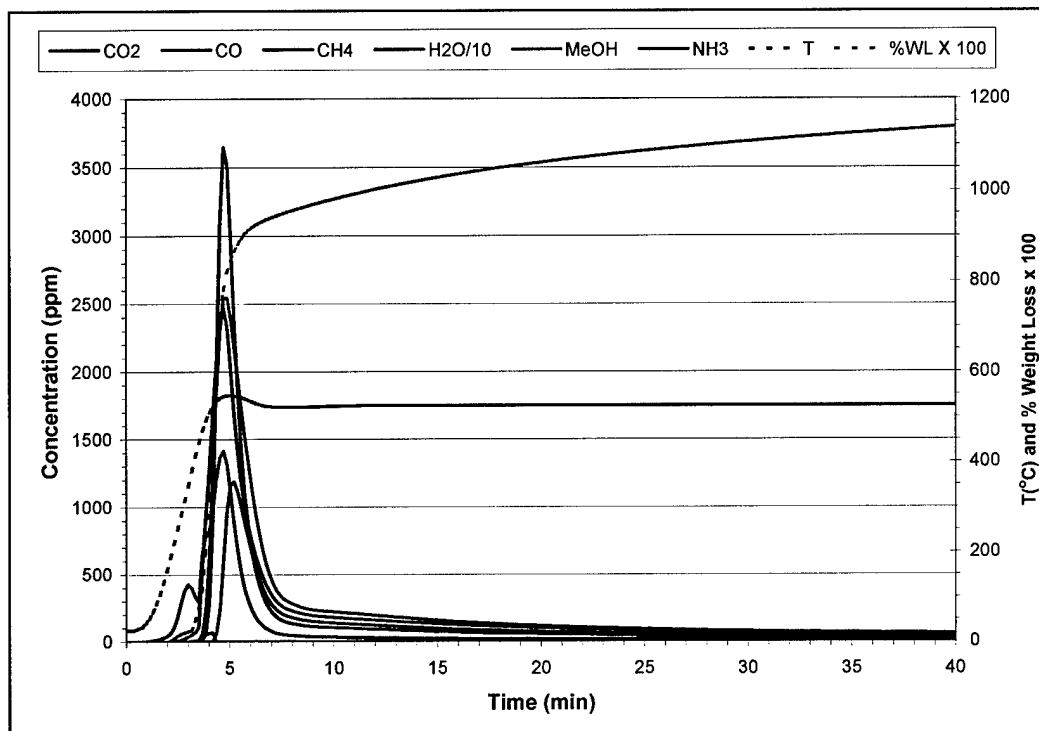


FIGURE 41. IM7/DMBZ-15 Composite Species Profiles at R = 150°C/min, ISO = 525°C in N<sub>2</sub>.

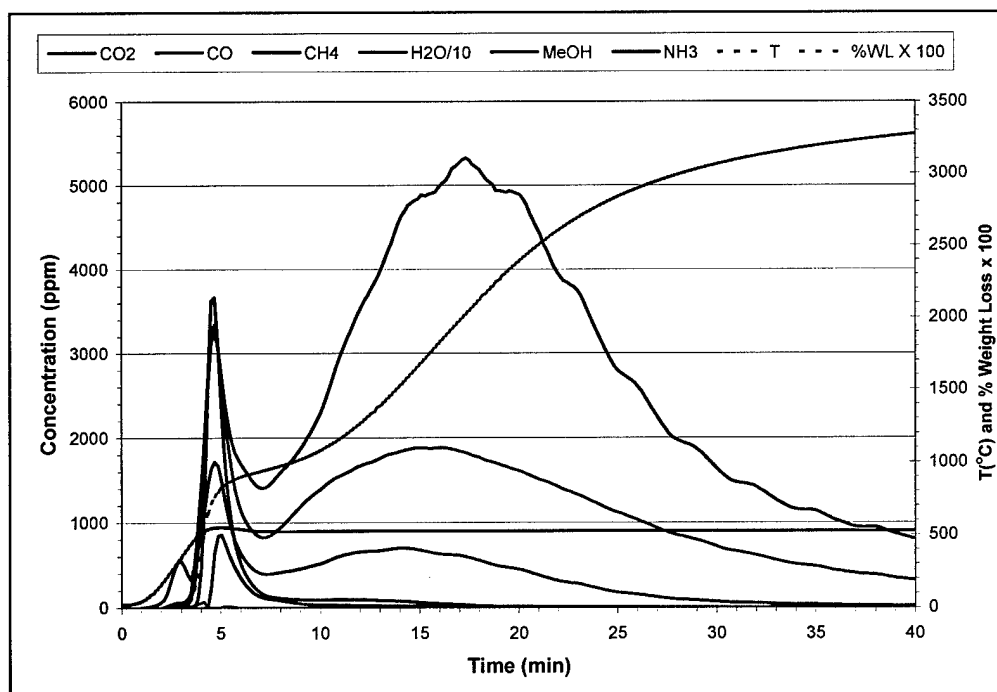


FIGURE 42. IM7/DMBZ-15 Composite Species Profiles at R = 150°C/min, ISO = 525°C in Air.

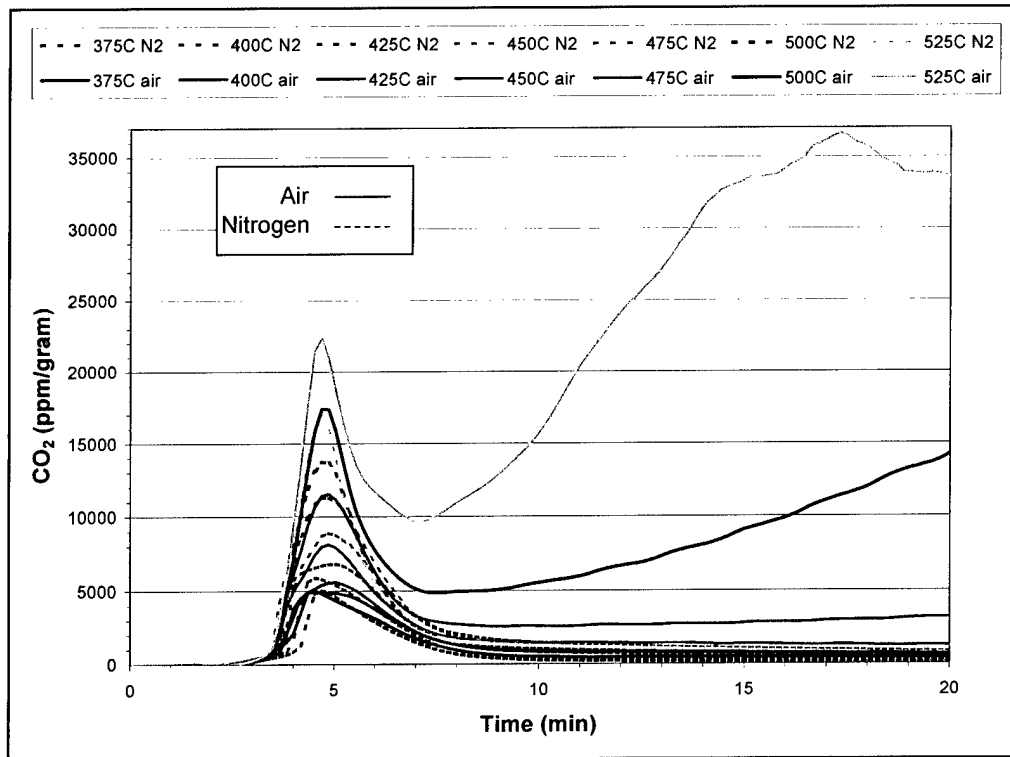


FIGURE 43. Composite CO<sub>2</sub> (ppm/g) at R = 150°C/min, ISO = 375 to 525°C in Air and N<sub>2</sub>.

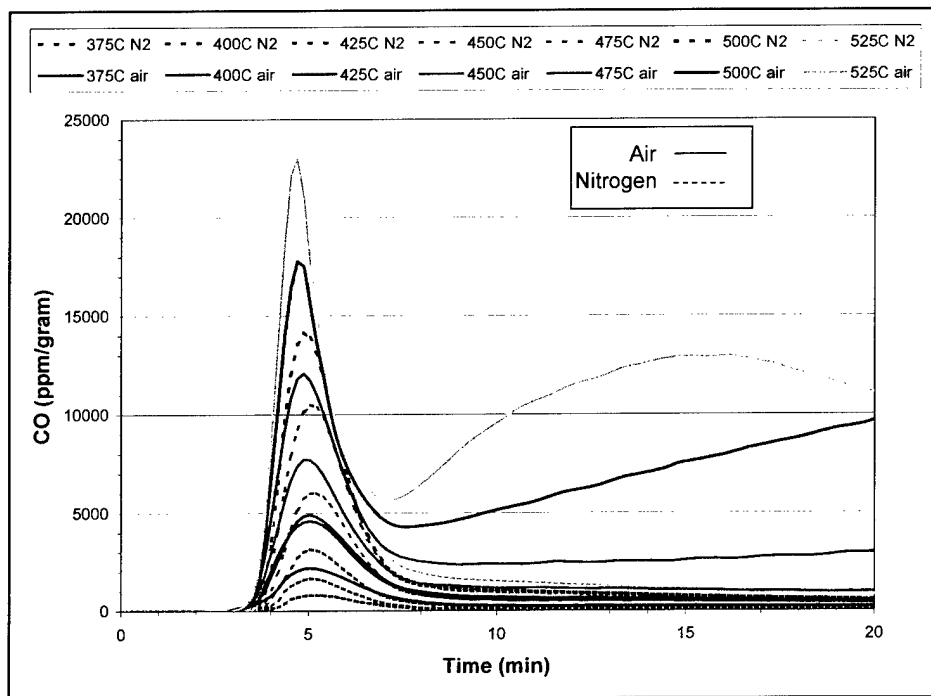


FIGURE 44. Composite CO (ppm/g) at R = 150°C/min, ISO = 375 to 525°C in Air and N<sub>2</sub>.

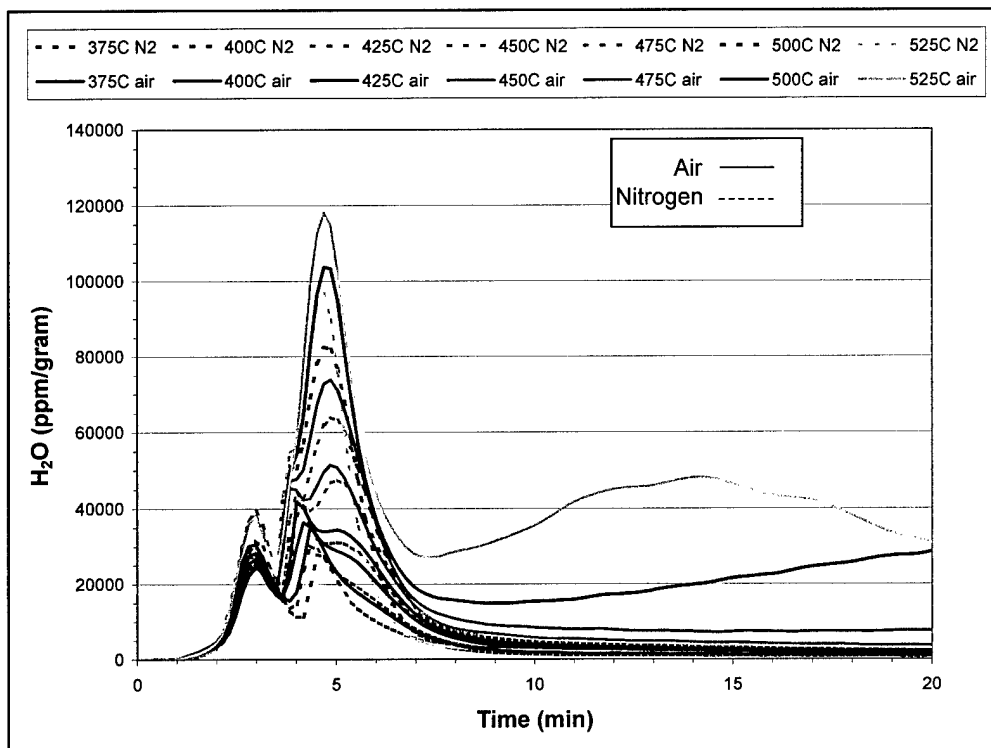


FIGURE 45. Composite H<sub>2</sub>O (ppm/g) at R = 150°C/min, ISO = 375 to 525°C in Air and N<sub>2</sub>.

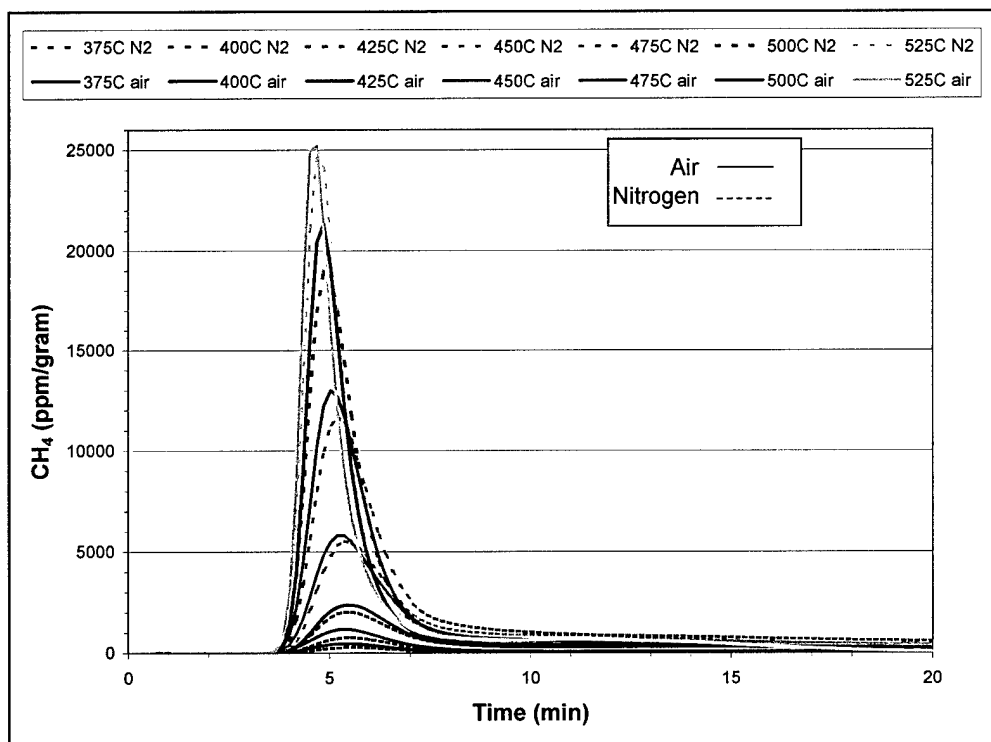


FIGURE 46. Composite CH<sub>4</sub> (ppm/g) at R = 150°C/min, ISO = 375 to 525°C in Air and N<sub>2</sub>.

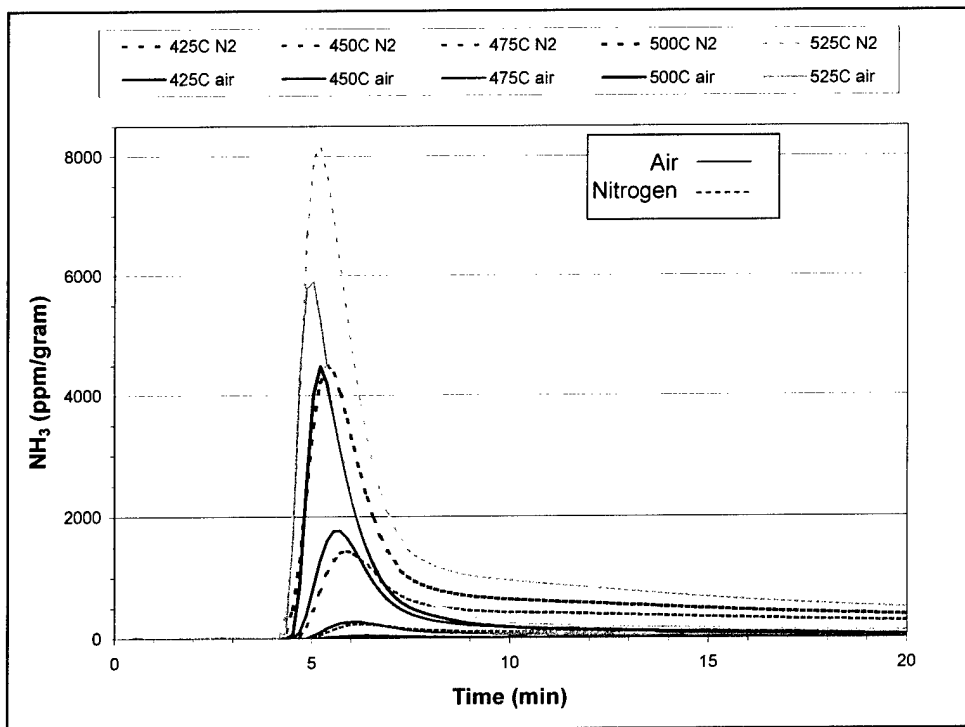


FIGURE 47. Composite  $\text{NH}_3$  (ppm/g) at  $R = 150^\circ\text{C}/\text{min}$ ,  $\text{ISO} = 375$  to  $525^\circ\text{C}$  in Air and  $\text{N}_2$ .

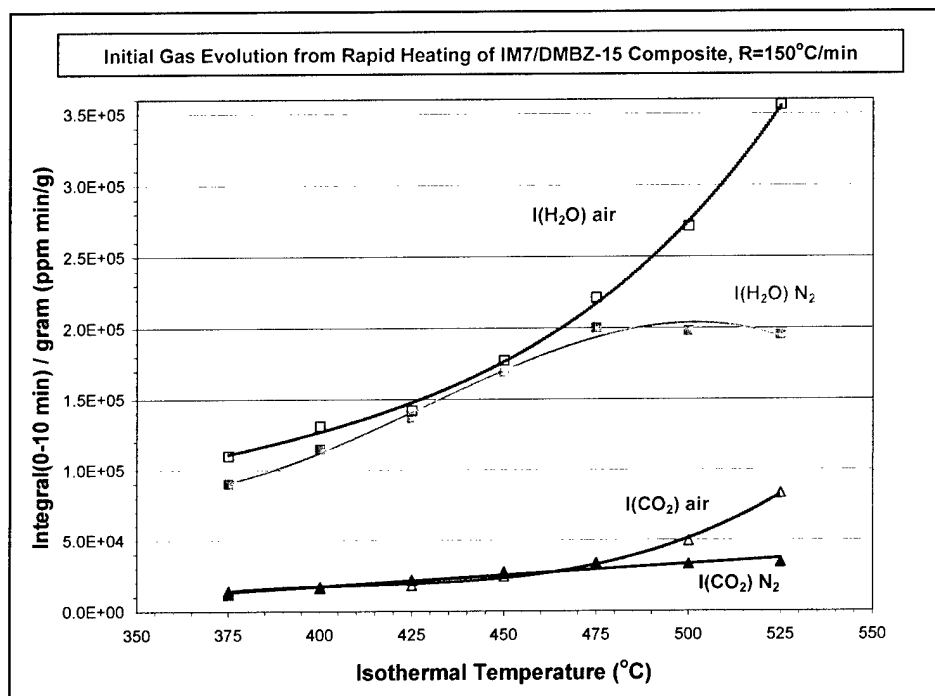


FIGURE 48. Integrated  $\text{H}_2\text{O}$  and  $\text{CO}_2$  (ppm min/g) During Maximum Gas Evolution (0 to 10 min) for Composite at  $R = 150^\circ\text{C}/\text{min}$ ,  $\text{ISO} = 375$  to  $525^\circ\text{C}$ , Air Versus  $\text{N}_2$ .

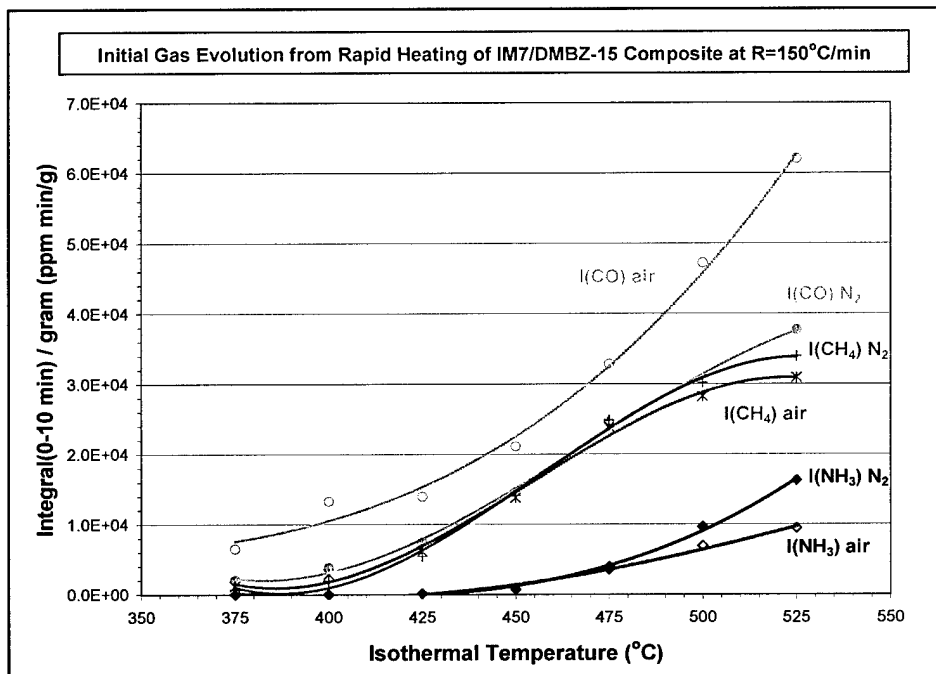


FIGURE 49. Integrated CO, CH<sub>4</sub>, and NH<sub>3</sub> (ppm min/g) During Maximum Gas Evolution (0 to 10 min) for Composite at R = 150°C/min, ISO = 375 to 525°C, Air Versus N<sub>2</sub>.

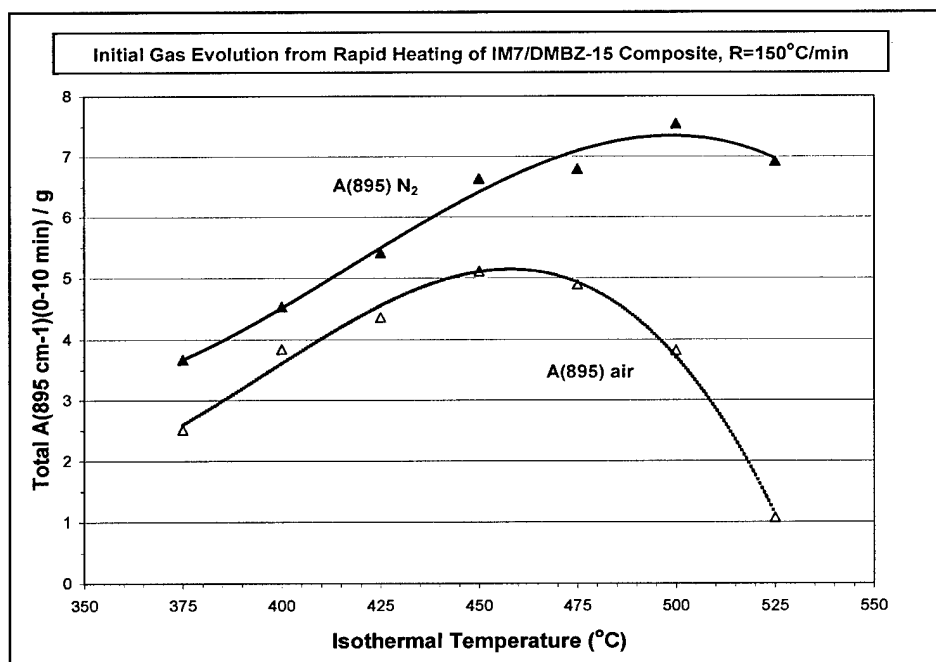


FIGURE 50. Total A(895 cm<sup>-1</sup>)/g During Maximum Gas Evolution (0 to 10 min) for Composite at R = 150°C/min, ISO = 375 to 525°C, Air Versus N<sub>2</sub>.

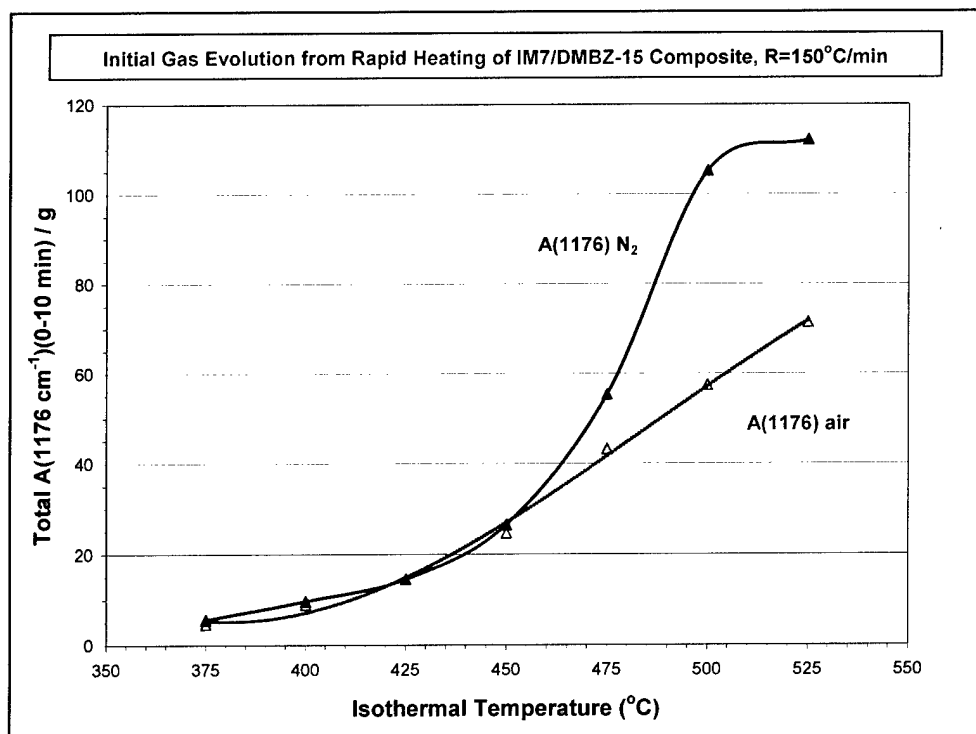


FIGURE 51. Total A(1,176 cm<sup>-1</sup>)/g During Maximum Gas Evolution (0 to 10 min) for Composite at R = 150°C/min, ISO = 375 to 525°C, Air Versus N<sub>2</sub>.

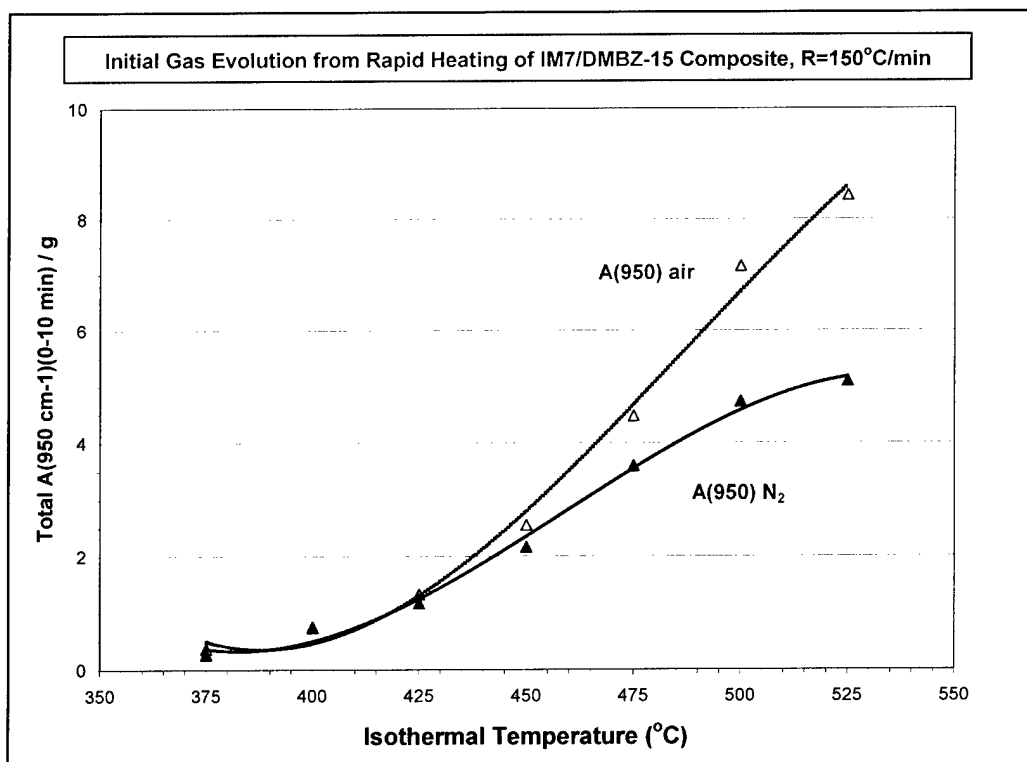


FIGURE 52. Total A(950 cm<sup>-1</sup>)/g During Maximum Gas Evolution (0 to 10 min) for Composite at R = 150°C/min, ISO = 375 to 525°C, Air Versus N<sub>2</sub>.



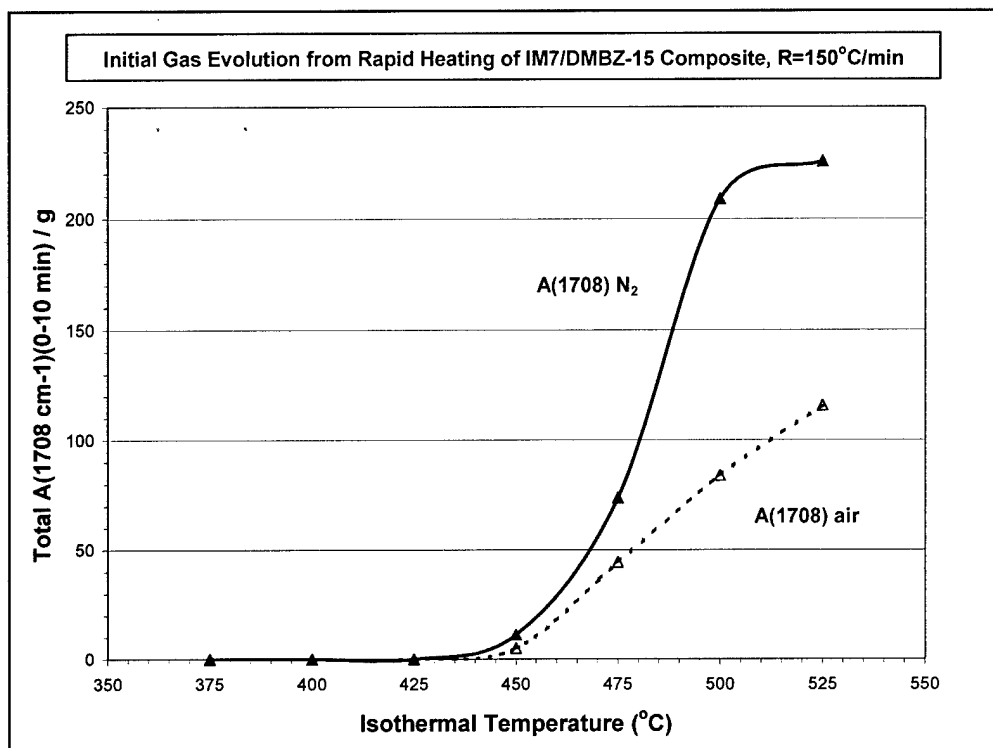


FIGURE 53. Total A(1,708  $\text{cm}^{-1}$ )/g During Maximum Gas Evolution (0 to 10 min) for Composite at R = 150°C/min, ISO = 375 to 525°C, Air Versus N<sub>2</sub>.

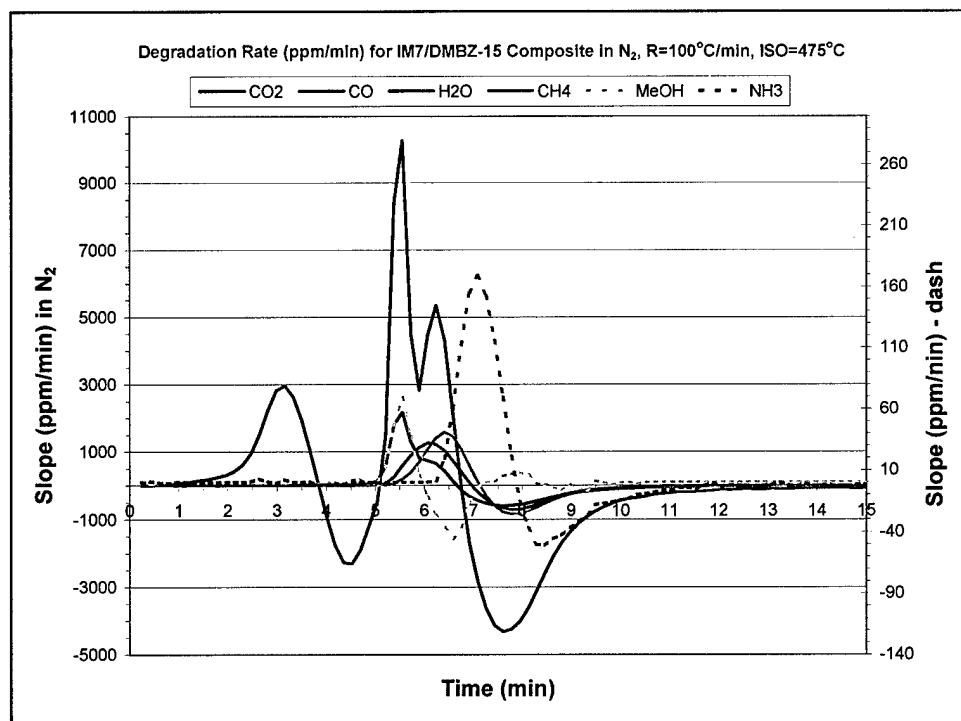


FIGURE 54. Degradation Rate for IM7/DMBZ-15 Composite in N<sub>2</sub>, R = 100°C/min, ISO = 475°C.

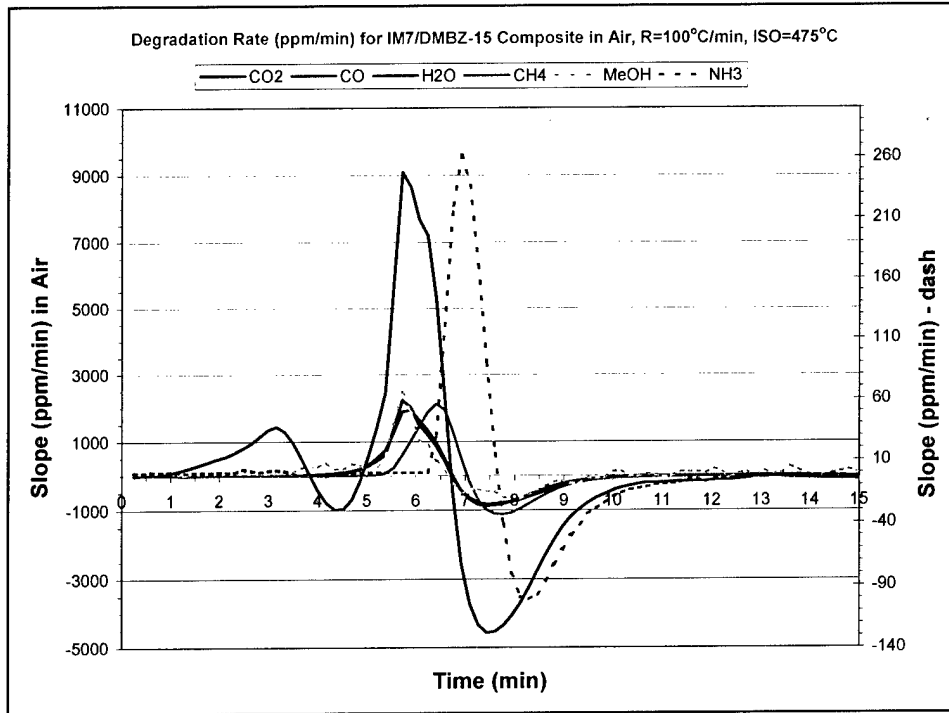


FIGURE 55. Degradation Rate for IM7/DMBZ-15 Composite in Air,  $R = 100^{\circ}\text{C/min}$ ,  $\text{ISO} = 475^{\circ}\text{C}$ .

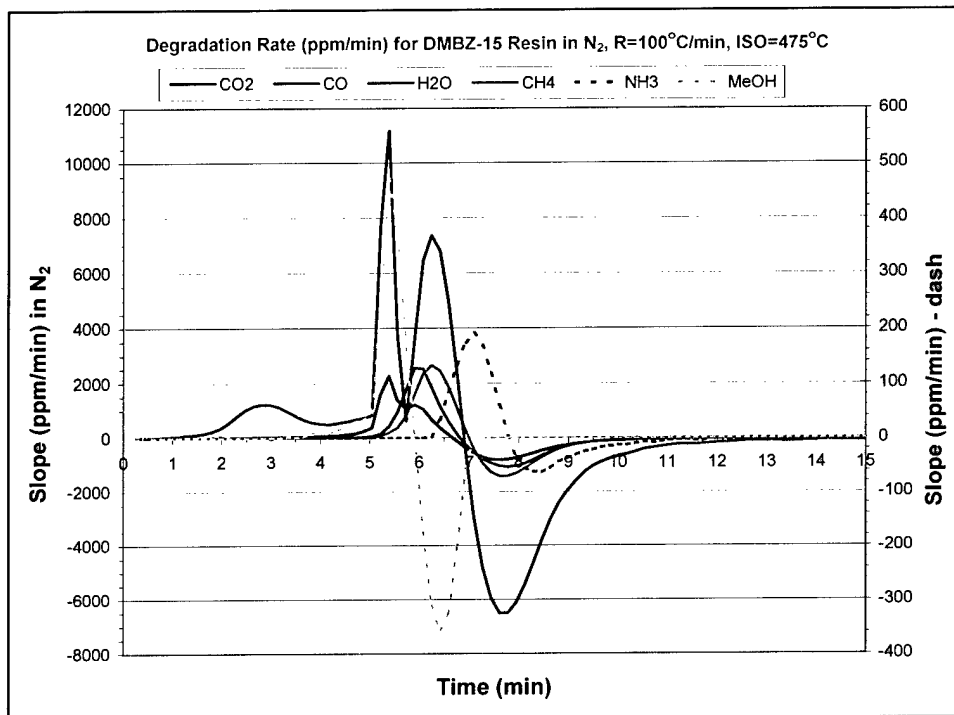


FIGURE 56. Degradation Rate for DMBZ-15 Resin in  $\text{N}_2$ ,  $R = 100^{\circ}\text{C/min}$ ,  $\text{ISO} = 475^{\circ}\text{C}$ .

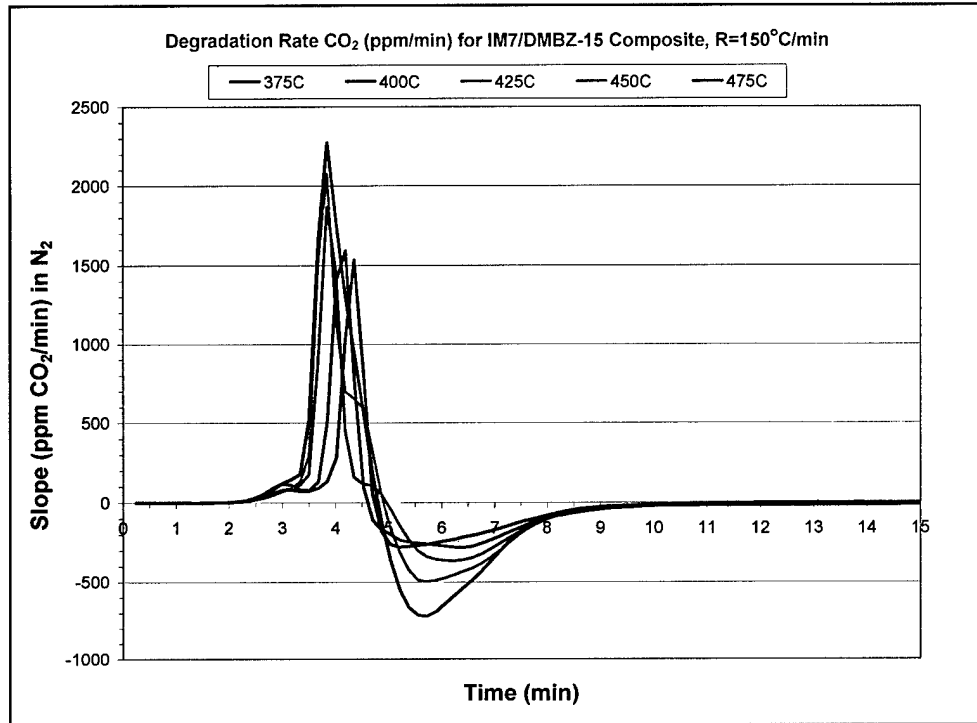


FIGURE 57. CO<sub>2</sub> Degradation Rate for Composite in N<sub>2</sub>, R = 150°C/min, ISO = 375 to 475°C.

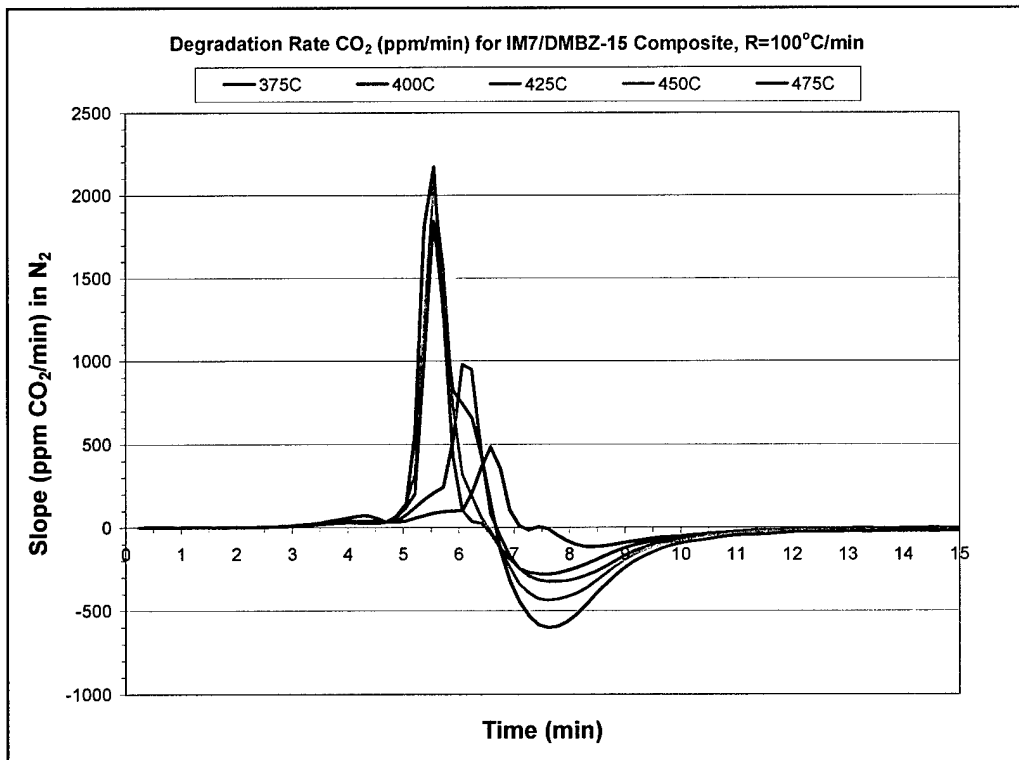


FIGURE 58. CO<sub>2</sub> Degradation Rate for Composite in N<sub>2</sub>, R = 100°C/min, ISO = 375 to 475°C.

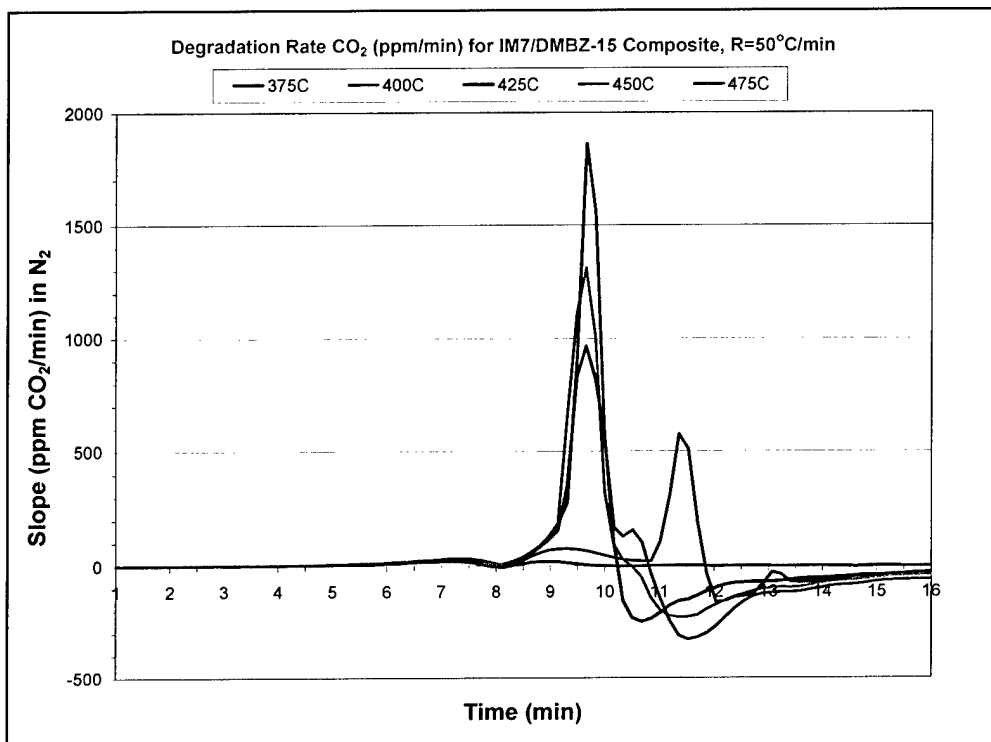


FIGURE 59. CO<sub>2</sub> Degradation Rate for Composite in N<sub>2</sub>, R = 50°C/min, ISO = 375 to 475°C.

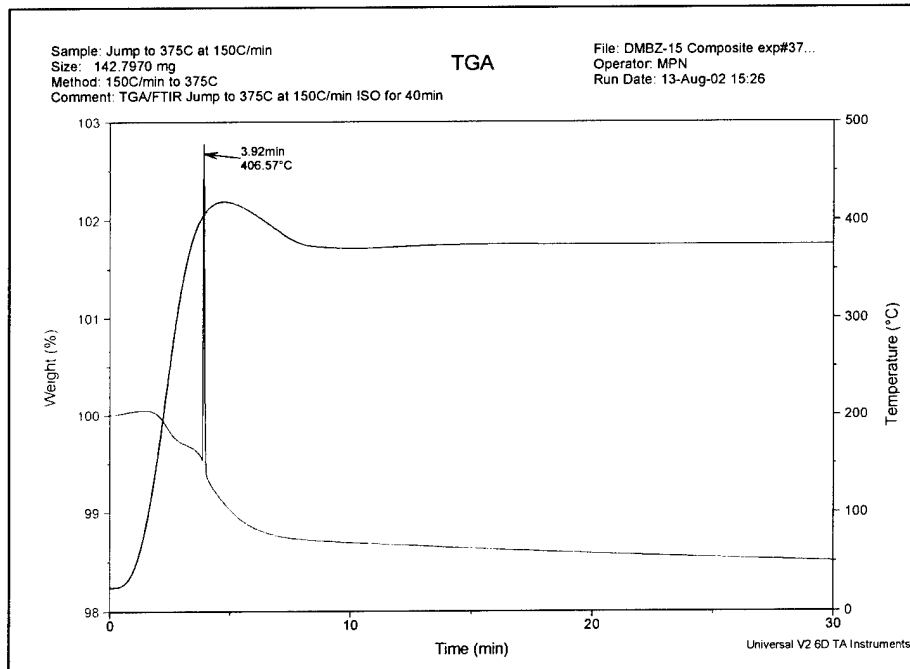


FIGURE 60. Spike in TGA Weight Loss From Rapid Gas Evolution at Onset of Catastrophic Delamination, Composite, R = 150°C/min, ISO = 375°C in Air.

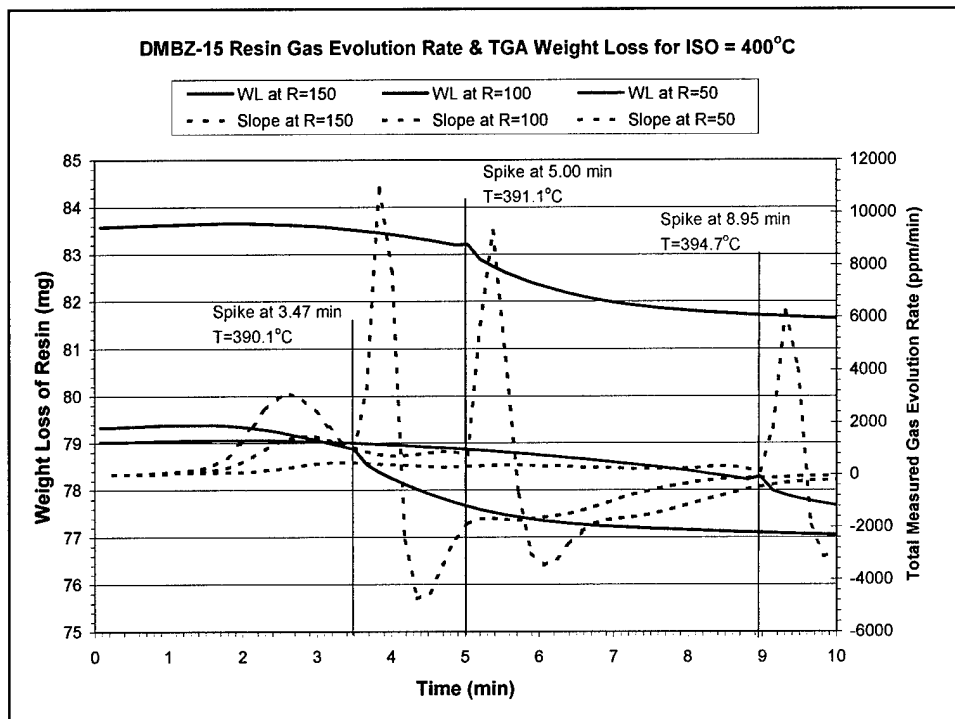


FIGURE 61. Correlation of TGA Weight Loss Spike Below-T<sub>g</sub> With Rapid Gas Evolution, Resin, ISO = 400°C in N<sub>2</sub>, R = 50, 100, and 150°C/min.

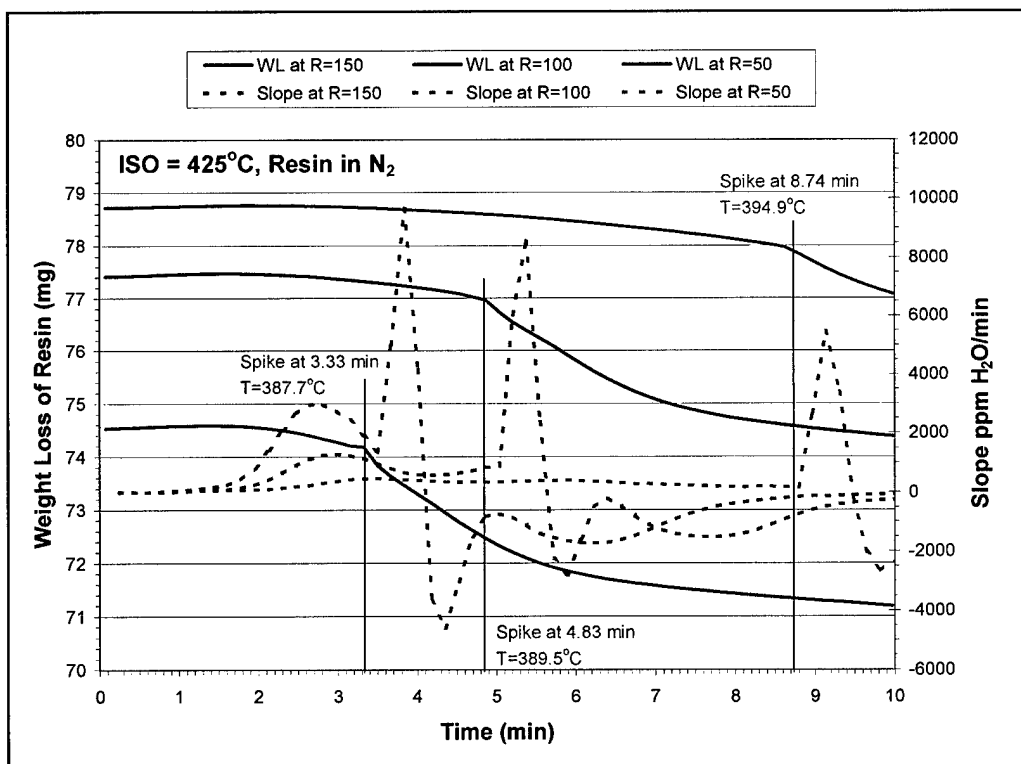


FIGURE 62. Correlation of TGA Weight Loss Spike Below-T<sub>g</sub> With Rapid Gas Evolution, Resin, ISO = 425°C in N<sub>2</sub>, R = 50, 100, and 150°C/min.

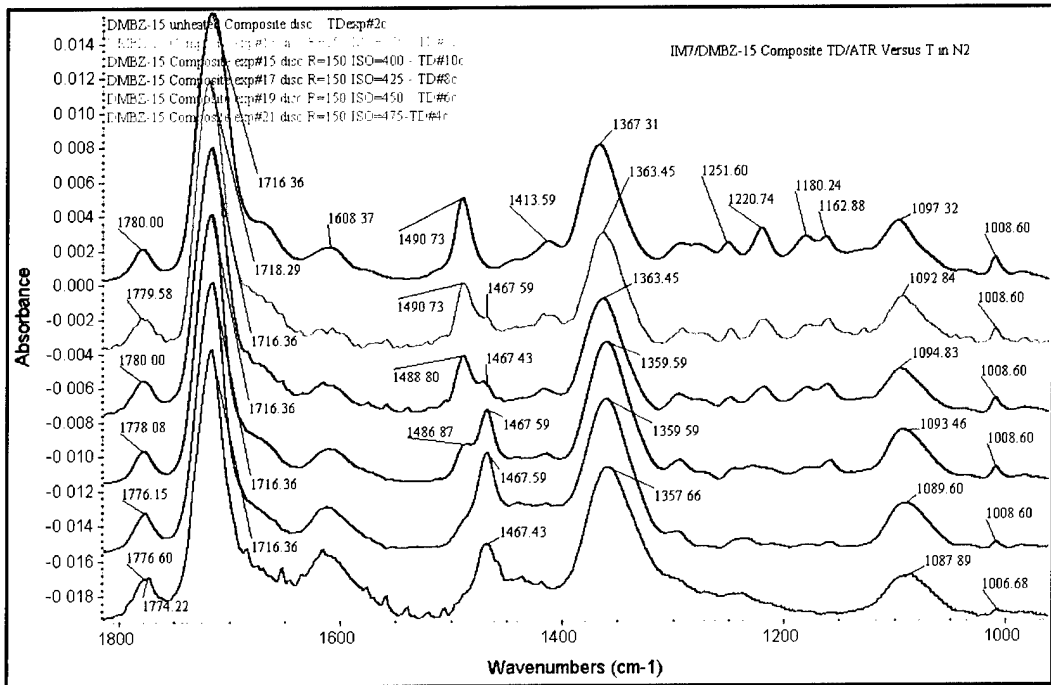


FIGURE 63. TD/ATR Top Surface Spectra of Unheated Versus Heated (ISO = 375 to 475°C) IM7/DMBZ-15 Composite at R = 150°C/min in N<sub>2</sub>.

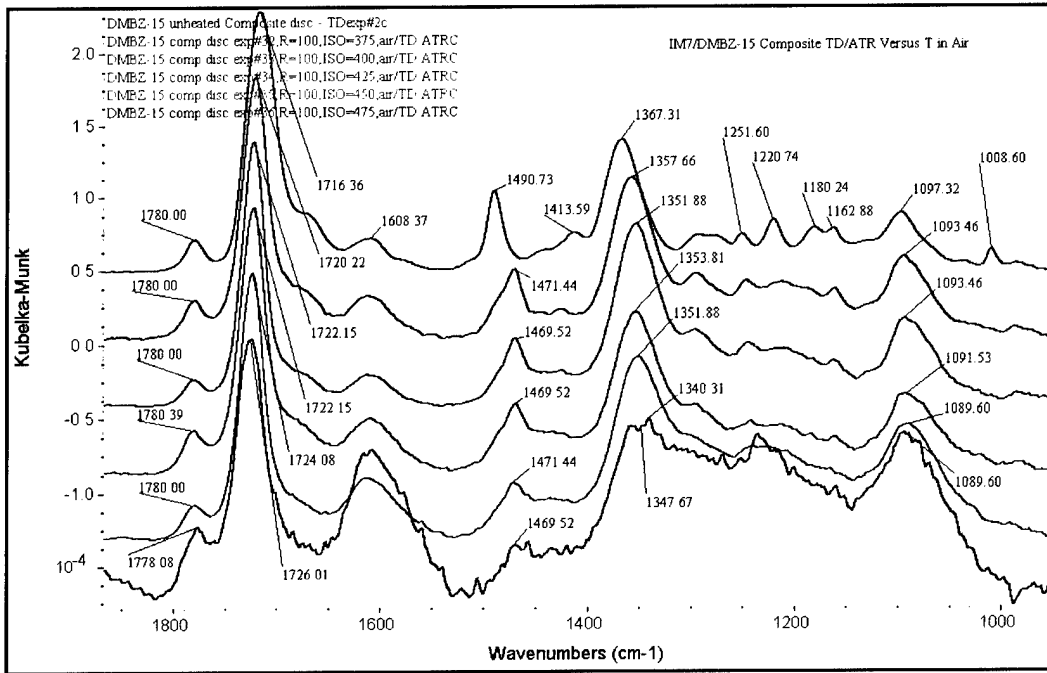


FIGURE 64. TD/ATR Top Surface Spectra of Unheated Versus Heated (ISO = 375 to 475°C) IM7/DMBZ-15 Composite at R = 100°C/min in Air.

## INITIAL DISTRIBUTION

- 2 Office of Naval Research, Arlington, VA
  - ONR-332
  - I. Perez
  - A. Perez
- 1 Naval Air Warfare Center Aircraft Division, Patuxent River (Library)
- 2 Naval Surface Warfare Center, Corona Division, Corona, (F. MacDonald)
- 2 Defense Technical Information Center, Fort Belvoir
- 1 Raytheon Electronic Systems, Tucson, AZ (S. Slocum)
- 2 NASA Research Center, Cleveland, OH
  - Kathy Chuang (1)
  - Technical Library (1)
- 1 Oak Ridge National Laboratory, Oak Ridge, TN (Technical Library)
- 1 Melvin Nadler,, Livingston, TX

---

## ON-SITE DISTRIBUTION

- 1 Code 4T0000D
- 1 Code 4T4100D
- 2 Code 4T4200D
  - Clark (1)
  - Nissan (1)
- 1 Code 4T42A0D
- 1 Code 4T4210D
- 2 Code 4T4220D
  - Lindsay (1)
  - Wright (1)
- 6 Code 4T4230D
  - Merwin (5)
  - Quintana (1)
- 2 Code 45T000D (1 plus Archives copy)
- 1 Code 476500D